# REMOVAL OF SILICA-BASED SCALES IN STEAM-ASSISTED GRAVITY DRAINAGE (SAGD) BOILERS

A Thesis

by

CANDAN UNAL

Submitted to the Office of Graduate and Professional Studies of
Texas A&M University
in partial fulfillment of the requirements for the degree of

MASTER OF SCIENCE

| | |
|---|---|
| Chair of Committee, | Hisham A. Nasr-El-Din |
| Committee Members, | Berna Hascakir |
| | Mahmoud M. El-Halwagi |
| Head of Department, | A. Daniel Hill |

May 2016

Major Subject: Petroleum Engineering

## ABSTRACT

Steam assisted gravity-drainage (SAGD) is a method to produce bitumen or extra-heavy oil by injecting steam into the reservoir. The steam lowers the viscosity and the mixture of oil and water are then able to flow through production well. After separating produced water and oil, the water is recycled to the steam generation system for economic and environmental reasons. The water then goes through treatment processes, and it is used in a once-through steam generator (OTSG) with additional water (makeup water) to produce steam for the SAGD injectors. At high pressure and temperature conditions, hard scales are formed on the inside surface of the boiler tubes. The fuel consumption increases as the scales decrease the thermal efficiency. The scale build-up might lead to plugging and boiler failure.

The objectives of this study are to 1) investigate the compositions of four different silica scales from SAGD boilers, 2) study the effect of different treatment solutions on the solubility of those silica scales, and 3) examine the effect of temperature on the working mechanisms of those solutions to find the most efficient formulation to dissolve the problematic scales.

Four different scale samples from SAGD boilers were analyzed to determine an effective and compatible solution to dissolve them. After removing organic matter by using xylene, the mineralogy of these samples was analyzed by using X-ray diffraction (XRD), X-ray fluorescence (XRF), scanning electron microscopy (SEM), and energy dispersive spectroscopy (EDS) before applying any treatment method.

The dissolution tests were conducted with four different chemical solutions: 1) preflush with 15 wt% HCl followed by main acid treatment with 9:1 wt% HCl-HF solution, 2) preflush with 10 wt% NaGLDA followed by main acid treatment with 10:1 wt% NaGLDA-HF solution, 3) preflush with 9 wt% formic acid followed by main acid treatment with 9:1 wt% formic acid-HF solution, and 4) 5 wt% KOH solution. Tests were run at 77 and 300ºF for three hours.

The ion concentrations in the filtrates were analyzed by using inductively coupled plasma (ICP) after all dissolution tests. Furthermore, solubility values also helped to draw a conclusion about compatibility of solution sets with scale samples by running dissolution tests. The HCl treatment set (preflush with 10 wt% HCl followed by main acid treatment with 9:1 wt% HCl-HF solution) was the most effective solution at 77 and 300ºF in terms of high total dissolved scale forming ions in solution and high solubility values.

# DEDICATION

I dedicate my thesis to my beloved family, to my beloved mother and father, Suna and Ilter Unal, to my little brothers, Okan and Gokhan Unal, and to my grandparents, Ilhan and Sahsenem Unal, for their endless love, support, and motivation.

Also, this thesis is dedicated to my fiancé, Ibrahim Kizilirmak, for all his love and patience.

ACKNOWLEDGEMENTS

Firstly, I would like to express my sincere gratitude to my advisor Prof. Dr. Hisham Nasr-El-Din for the support and guidance to my research, for his motivation and knowledge. He will be remembered all the time with his jokes and violin.

I would like also to thank Dr. Berna Hascakir and Dr. Mahmoud El-Halwagi for serving as committee members.

Thanks also go to Turkish Petroleum Corporation for the financial support of my education.

I also want to extend my gratitude to my friends and colleagues and the department faculty and staff for making my time at Texas A&M University a great experience.

## NOMENCLATURE

| | | |
|---|---|---|
| ABF | = | Ammonium bifluoride |
| EDS | = | Energy dispersive spectroscopy |
| HCl | = | Hydrochloric acid |
| HF | = | Hydrofluoric acid |
| ICP | = | Inductively coupled plasma |
| KOH | = | Potassium hydroxide |
| NaGLDA | = | Mono sodium L- glutamic acid-N, N diacetic acid |
| SAGD | = | Steam assisted gravity drainage |
| SEM | = | Scanning electron microscope |
| XRD | = | X-ray diffraction |
| XRF | = | X-ray fluorescence |

TABLE OF CONTENTS

Page

LIST OF FIGURES

Page

LIST OF TABLES

Page

# 1. INTRODUCTION

## 1.1 Silica Scales

Scale is one of the terms used in the petroleum industry to express the precipitation of solid minerals on the surfaces from inside the reservoir to topside production systems. Inorganic scales appear on the surfaces due to saturation of water with an inorganic salt. Scale starts appearing as the concentration of one or more component of a fluid is gone over the solubility limits (Crabtree et al. 1999). According to Frenier and Ziauddin (2008), the main inorganic scale types are: carbonates, sulfates, oxides and hydroxides, sulfides, and silicates.

Different scale problems are dependent on the degree of supersaturation (or scale-forming tendency), temperature, pressure, time, and in-situ brine chemistry. Frenier and Ziauddin (2008) suggest simple analysis to find out the mineral composition of scales. These simple analyses might be started by checking whether the scale sample floats in water or not. If the sample floats in water, it is most probably organic scale. If the sample does not float in water and it is soluble in water, it is most probably sodium chloride. Researchers can continue analysis by using chemicals. For example, the samples which are soluble in hot HCl-HF solutions are silica-based scales. Furthermore, if a scale sample with odor of rotten eggs is not soluble in both hot HCl-HF and hot HCl solution but soluble in HCl, it might be iron sulfide. The samples soluble in hot HCl but not in hot HCl-HF solution can be iron oxide. These methods should be justified by other methods including X-ray diffraction (XRD), X-ray fluorescence (XRF), scanning electron microscopy (SEM), and energy dispersive spectroscopy (EDS).

Scales might occur in several locations from the reservoir to production facilities (at pressure drops, water mixing points, outgassing points, shear points, and gravel pack). Determination of scale intensity and location requires more elaborate investigation.

Crabtree et al. (1999) introduced an approach for the concept of inorganic scales development. Despite the fact that the formation of many scales result from temperature or/and pressure shift, outgassing, change in pH, or contact with incompatible water, most of the oversaturated produced waters, which have tendency to form scales do not always develop scale. A scale must grow from the solution.

**Fig. 1** illustrates the procedure from supersaturation to the development of ion pairs. Homogenous nucleation as the first stage within a saturated fluid indicates the development of unstable clusters of atoms. The last process, heterogeneous nucleation, involves the growth of scale crystals on a preexisting fluid-boundary surface.

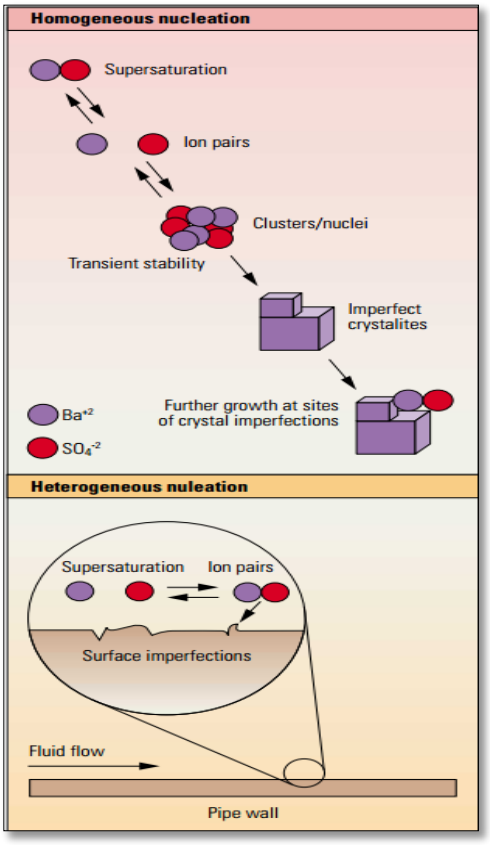


**Fig. 1—Scale growth mechanism (Crabtree et al. 1999).**

Silica is the one of the main components of the earth's crust. Naturally existing minerals (feldspars, chert, opal, micas, ferromagnesian, and clay minerals,) are the main sources of silica (Todd 1980). Groundwater usually contains dissolved silica ($SiO_2$) owing to erosion of those minerals. The chemistry of silica is very complex, and its concentration is contingent on the solubility of quartz and the geochemical environment. The solid-solution interface undergoes hydrolysis stage that initiates the dissolution process (**Fig. 2**). The incomplete bonds with oxygen atoms form Si-OH groups, which makes the structure appropriate for the dissolution and hydrolysis mechanism (Iler 1979).

The tetrahedral arrangement of four oxygen atoms around one silicon atom is the common structure for both silica and silicates (Wahl 1977). Silica can be present in various types, namely, dissolved or monomeric, molecular, colloidal, and particulate. Silica scale formation may contain any of those structures or mixtures of those forms with acid, alkali, and multivalent ions (Milne et al. 2014).

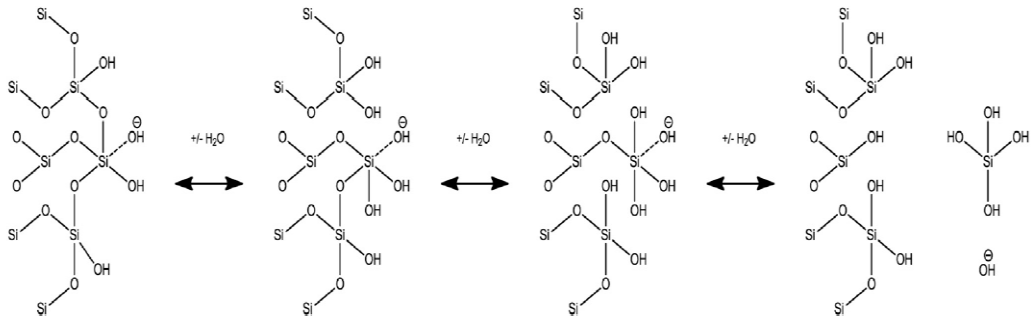


**Fig. 2—Dissolution mechanism of silica to silicic acid (Milne et al. 2014).**

At pH levels close to 7, monosilicic acid ($H_4SiO_4$) which is also known as silicic acid, ortosilicic acid (fully hydrated) or reactive (ionized) silica, exists in solution. Dissolution of $SiO_2$ in water (Eq. 1.1) creates monosilicic acid (means not polymerized):

$$SiO_2 + 2H_2O \Leftrightarrow H_4SiO_4 \quad . \quad \ldots\ldots\ldots\ldots\ldots\ldots\ldots\ldots\ldots\ldots\ldots\ldots\ldots\ldots \quad (1.1)$$

Monomeric silica (**Fig. 3**) is present when the silica concentrations do not exceed the saturation concentration of amorphous silica. If the monovalent ions, such as $Na^+$ and

$K^+$, are available, the deposition rate of monomeric silica is accelerated. Reactive silica forms colloidal silica.

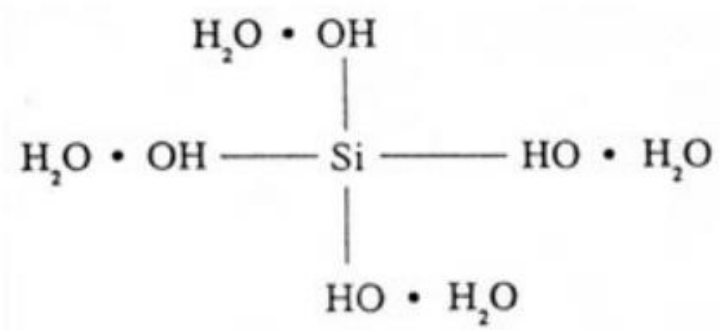


**Fig. 3—Monosilicic acid structure (Iler 1979).**

Polymeric silica is a term used to describe the dimers, trimers and oligomers of silicic acid. Due to the small number of silanol groups, monosilicic acid is more reactive than polymeric silica in terms of solubility. The scale built from molecular deposition, which takes place at a pH range of 7 to 11, has no porosity (Ning 2003; Ning et al. 2010). Low pH values (less than 7) trigger the silicic acid polymerization (**Fig. 4**).

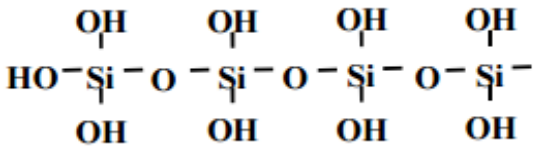


**Fig. 4—Polymeric silica, $(H_2SiO_3)_n$ (Meyers 1999).**

If the level of supersaturation is too high, polymerization leads to the deposition of colloidal particles. Silica starts to polymerize and yield colloidal silica at pH levels less than 10.5 (Amjad and Zuhl 2008). The colloidal silica particles have small diameters ranging from 0.01 to 0.5 micron (Iler 1979). Colloidal silica is a form of silicon that is formed by the combination of multiple SiOH species by losing a bond with other inorganic structures, such as aluminum and calcium oxide (Milne et al. 2014). The colloidal silica is composed of $SiO_2(OH)_n$ groups, where $n \geq 8$.

**Fig. 5** summarizes the silica polymerization mechanism briefly by demonstrating the polymerization pathway of silicates to produce silicate dimers and finally colloidal silica and amorphous silica particles.

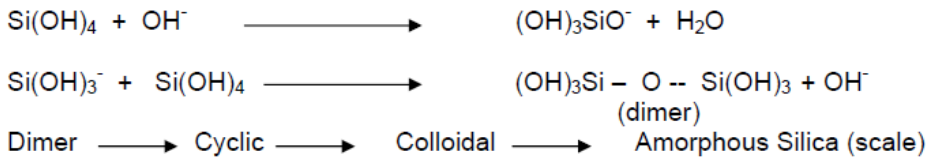


**Fig. 5—Silica polymerization mechanism (Amjad and Zuhl 2008).**

Briefly, different kinds of silica species specify the kind of silica deposition. Consolidated, hard scales are the product of monomeric silica. At the higher saturation levels, scale formed from colloidal deposition is a kind of a gel in suspension (Sahachaiyunta et al. 2002). Temperature, pH, multivalent cations, ionic strength, and anions are the primary factors affecting the solubility of silica.

Higher pH values cause an increase in the solubility of silica. Ionic and polymeric species promote the precipitation of silica from the solution. An alkaline, pH greater than 10, causes silicate ionization, which increases the solubility of the silica. Amorphous silica scaling is more likely to occur at pH values less than 8.5, resulting in polymerization, which means loss of solubility of silica (Demadis et al. 2007). The presence of hydroxide ions in the fluid catalyzes the polymerization process (Amjad and Zuhl 2008) (Fig. 5).

It is difficult to correlate behavior of silica with pH change. Researchers disagree on the behavior of silica at different pH values. Gill (1998) indicates that silica scale is more likely to form in the systems with pH above 8.5 and high temperatures. On the other hand, amorphous silica is more prone to deposit in systems with pH less than 10.5 and decreasing temperature. According to Demadis (2010), amorphous silica scale is very likely to form below pH 8.5. The formation of magnesium silicate scale is triggered at pH larger than 8.5 and precipitation starts at lower pH values when temperature is high enough. Thus, the presence of magnesium or other scaling ions should be taken into consideration before setting pH for the solution.

As the temperature increases, the solubility of silica increases. According to Sheikholeslami and Bright (2002), increase in temperature also affects the kinetics of polymerization in a positive way. Increase in polymerization kinetics might cause a further shift in solubility of silica and bring about a decrease in the solubility values. On the other hand, this temperature effect is inverse for various metal-silicate types, in such a way that increase in temperature leads to a decrease in their solubility, even at concentrations below silica saturation (Clark 1948).

Because of their interaction with silicate anions, multivalent cations have an effect on the solubility of silica. Hardness increases the polymerization rate of silica that results in decrease in solubility of silica (Ueda et al. 2003). Bremere et al. (2000) reported that amorphous silica has a solubility ten times higher than iron silicates. Metal silicates with different solubility values can be present at higher pH ranges. The order of cations on decreasing silica solubility from least effective to most effective is K, Na, Li, Sr, Ca, Mg, Ag, Ni, Pb, Cd, Mn, Zn, and Cu (Chan 1989; Sheikholeslami et al. 2001; Ning 2003). In general, silica solubility shows a decreasing trend with increasing divalent ion concentration, such as Ca and Mg. The presence of Mg exacerbates silica scale deposition and increases the rate of precipitation by supplying a hydroxide ion. When pH value exceeds 8.5, magnesium silicate precipitation tends to form (Demadis et al. 2007; Amjad and Zuhl 2008).

## 1.2 Silica Scale in SAGD Boiler Water

Steam-assisted gravity drainage (SAGD) is an enhanced oil recovery method to produce extra-heavy oil or bitumen by thermally reducing its viscosity (Butler 1981; Butler et al. 1981). As illustrated in **Fig. 6** , the concept of the method consists of two horizontal wells, an upper injection well and a lower production well, which are placed in the formation, generally 4-10 m apart. The upper well heats the target reservoir by injecting steam that decreases the viscosity of the oil. As the viscosity of oil decreases, its mobility increases, and it starts flowing through the lower wellbore under the effect of gravity. The bottom well, the production well, produces this mobile oil via injected steam.

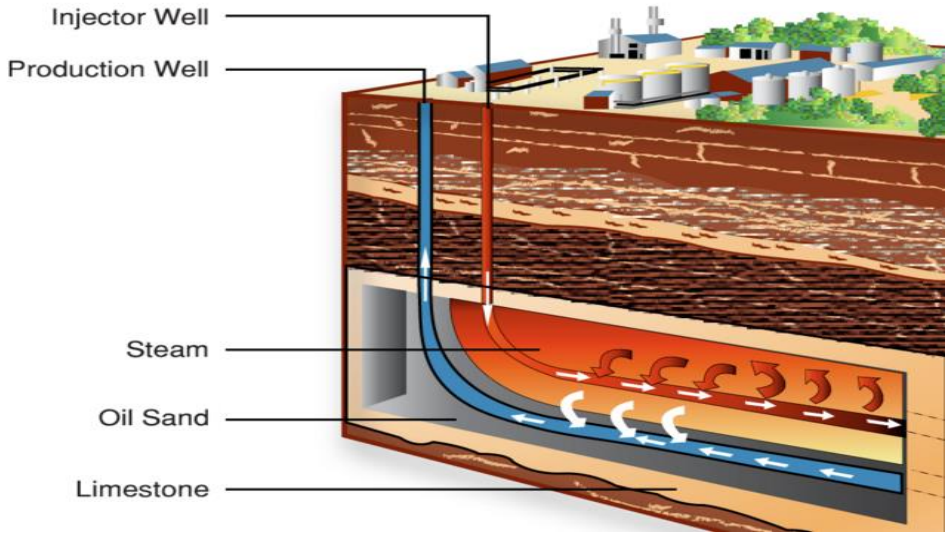


**Fig. 6—Schematics of SAGD process (Canadian Center for Energy Information, 2013).**

Almost 75% of the produced mixture is water, and the rest is heavy oil. De-oiled water goes through several processes for reuse. This recycled hot water is called as produced water. The amount of steam needed to produce a barrel of oil is referred as the steam-to-oil ratio (SOR). The SOR value for the extraction of bitumen or heavy oil by SAGD ranges from 2 to 4. Typically, a significant amount of steam is required for SAGD. Considering its cost-effectiveness and environmental regulations, produced water should be recycled as much as possible (80 to 90%) in SAGD methods (Pedenaud et al. 2004).

All the water has to go through additional treatments before it can be reused in the system. Almost 90 percent of the water used can be recycled, so only a small amount of new water (make-up water) is required to be added to the process for each barrel of oil produced. The produced water contains silica and residual hydrocarbon, and make-up

water involves dissolved salts. The scale caused by dissolved salts and silica reduces the thermal efficiency and might result in plugging and failure.

Once-through steam generators (OTSGs) and conventional drum boilers are two main systems for steam generation. They produce low pressure, low quality (80% vapor, 20% liquid) steam.

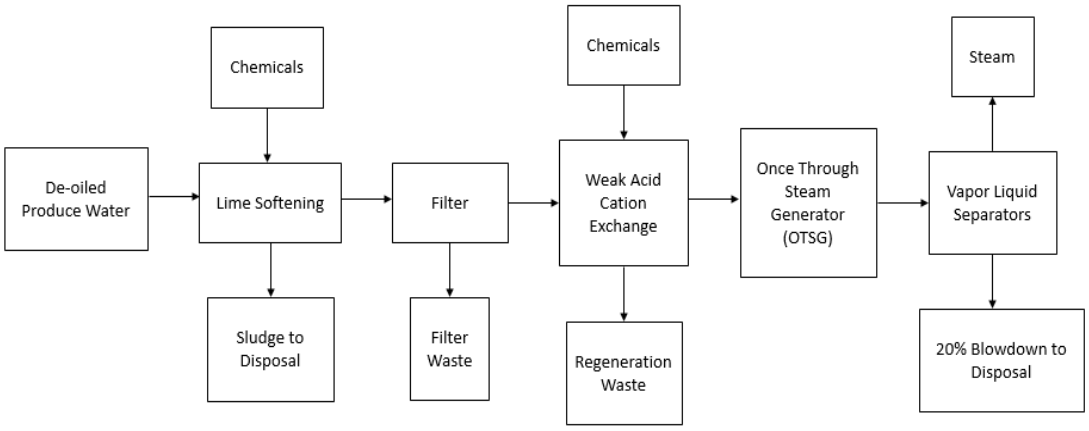


**Fig. 7—SAGD water treatment stages and steam generation system (Heins 2010).**

**Fig. 7** shows a typical produced water treatment process after separation of oil from produced water (by free-water knockout, skim tank, induced gas flotation, and oil removal filters such as walnut shell filters). An OTSG system uses warm lime softening (WLS) or hot lime softening (HLS) to partially decrease the level of silica concentration and hardness. In this process, the amounts of calcium and magnesium are also lowered. In either WLS or HLS, lime ($Ca(OH)_2$) and magnesium oxide (MgO) are present in the system at a pH of 9.5-9.8. Hardness as precipitated calcium carbonate and magnesium oxide is removed with sludge solids, and silica is removed by adsorption onto the

precipitating magnesium oxide. Filters dispose of the sludge coming from the lime-softening process. Finally, remaining hardness removal requires weak acid cation exchange (WAC). The exchange process minimizes the concentration of metals such as calcium, magnesium and iron.

Increasing the OTSG specifications for silica (more than 100 mg/L) might cause silica-salt precipitation that leads to the tube failure as a result of increasing local thermal resistance.

**Table 1** lists the boiler feed water specification for OTSG boilers.

| | |
|---|---|
| Total hardness | < 1 mg/l $CaCO_3$<br>(0.5 mg/l recommended) |
| Barium | < 0.1 mg/l |
| Iron | < 0.25 mg/l |
| Free chlorine | < 0.1 mg/l |
| Oxygen | < 0.02 mg/l |
| pH | 7.0 – 9.5 |
| Silica | < 100 mg/l |
| Total dissolved solids | < 12,000 mg/l<br>(600 mg/l recommended) |
| Oil | < 0.5 mg/l |

**Table 1—OTSG boiler specification (Pedenaud 2005).**

The silica scale is tenacious and hard to remove. In addition to amorphous silica, as mentioned before, SAGD plants remove various sorts of silica scale, such as tremolite

(a calcium and magnesium chain structure silicate), talc (a magnesium silicate), and acmite (a sodium and iron silicate, best avoided in steam generator boiler tubes) (Thimm 2008). In an OTSG system, 75 to 95% of the scale contains forms of some or all of the following: acmite, iron silicates, magnesium silicates, calcium silicates, and iron oxides; 25 to 5% of the scale is usually carbon (Myszczyszyn 2010). Colloidal silica sticks into the tube, causing silica scale, and amorphous silica is more likely to polymerize into colloidal silica when water in OTSG boilers evaporates (Pedenaud et al. 2006). Gill (1998) investigated silicate scales, their deposition, polymerization, co-precipitation with other minerals, and precipitation with other multivalent ions in the water. It is hard to predict solubility for silica, as many of those processes occur at the same time. The presence of calcium carbonate or other mineral precipitates promotes the formation of tenacious silica scale by entrapping the silica into a crystalline matrix (Demadis, 2010).

The most common methods for controlling silica scale in OTSG are hot-lime softening, filters, ion exchange softeners, reverse osmosis, adsorption or co-precipitation of treatments by aluminum and iron salts (Sheikholeslami and Bright 2002; Tokoro et al. 2014), and silica scale inhibitors (Gill 1993; Pedenaud 2006; Amjad and Zuhl 2008). Removal of silica by chemical methods is based on coagulation, according to the literature. Metal oxide or metal hydroxide (ferric, ferrous, aluminum and calcium) is used to adsorb or coagulate silica in this method (Iler 1979). According to Zeng et al. (2007), silica removal by zinc sulfate has higher efficiency values in the Xinjiang heavy oil field than regular coagulants such as $AlCI_3$ and $FeCl_3$. Most of the inhibitors used in geothermal applications could be put into practice in OTSG boiler systems if they are thermally stable

(Pedenaud 2006). The main focuses of these previous studies are the removal of silica and the inhibition of silica scale to prevent any operational problems. The study explained in this proposal, however, is a case study with scale samples from SAGD boilers. While the removal of silica scales in SAGD boilers has been investigated with a different process that was not mentioned in the literature before, no previous studies describe silica removal after scaling.

The aims of this research are to: 1) analyze the compositions of silica scales from SAGD boilers, 2) study the effect of different treatment solutions on the solubility of those silica scales, and 3) examine the effect of temperature on the working mechanisms of those solutions to find the most efficient formulation to dissolve them.

# 2. REMOVAL OF SILICA SCALE IN SAGD BOILERS

Experimental work and procedure, which were carried out to remove four scale samples from SAGD boilers, will be explained in this chapter. As the evaluation of chemical, physical and compositional properties of scales is fundamental step to design an effective removal process, scale analysis was conducted before applying any treatment method. Composition of each scale helped to determine which chemical treatment was applied.

## 2.1 Methods Used for Scale Analysis

Four different scale samples from SAGD boilers were analyzed to determine an effective solution to dissolve them. In this research, scale samples were named as Scale #1, #2, #3, and #4. Four grams of each scale sample was soaked into 40 g of xylene for 24 hours at room temperature to remove organic material. After the filtration process, 40 g of acetone was used to eliminate the remaining xylene from the xylene-preflushed samples. Then, the samples were dried in the oven at least 3 hours at 300ºF before the application of further analyses listed below:

### 2.1.1 Scanning Electron Microscopy (SEM) and Energy Dispersive X-Ray Spectroscopy (EDS)

Scanning electron microscopy (SEM) is a type of electron microscope that generates images in microscopic scale by using high-energy electrons instead of light to scan the sample surface. Energy Dispersive X-Ray Spectroscopy (EDS) produces elemental analysis when combined with SEM. EDS provides elemental analysis that is

more helpful when combined with SEM. The atomic number of an element is directly related with intensity of the backscattered electrons, which is reflected from atoms in the sample. The samples were coated with gold using a special sputter prior to the analysis to enhance the electron-sample interactions.

SEM has allowed researchers to analyze their samples with higher resolution and magnification levels. For detailed description of each samples, 2-dimensional SEM images and EDS results were generated before acid solubility tests to identify elements within the samples. These analyses give information about the samples' chemical composition, crystalline structure, and texture.

### 2.1.2 X-ray Fluorescence Spectrometry (XRF)

X-ray fluorescence (XRF) spectrometry is an x-ray process run to obtain data about chemical composition of minerals, sediments, scale, and rock samples. The interaction between x-ray fluorescence and the atoms result in the elemental analysis. Each of elements exist in the sample generates distinctive fluorescent x-rays that are unique for that specific element.

### 2.1.3 X-ray Diffraction (XRD)

The atomic and molecular structure of a crystalline materials is characterized by using X-ray Diffraction (XRD) process based on the diffraction patterns. This method uses x-rays and their diffractions. When the incident beam of x-ray interact with the crystalline material, the x-ray is scattered that is called as diffraction. The diffraction process is explained by Bragg's Law. The directions of diffractions are contingent upon the shape and size of crystalline structure. The density of electrons in the crystalline material, which

is directly related with the positions of atoms and chemical bonds in the crystalline structure, can be obtained by evaluating the angles and distances between crystal faces.

## 2.2 Scale Analysis Before Acid Treatments

SEM, EDS, XRF, and XRD analyses were used to define the composition of scale samples before starting any treatment.

### 2.2.1 Scale #1

#### *2.2.1.1 SEM and EDS Analysis*

Scale #1 (**Fig. 8**) does not seem homogenous in appearance in terms of its color. It has grey, brown, and white parts.

**Fig. 8—Scale #1 - as received.**

There is no significance change in the color of both xylene and Scale #1 after the soaking stage (**Fig. 9**).

**Fig. 9—Scale #1 – in xylene (left) and dried sample after acetone wash (right).**

Scale #1 was divided into three different color parts, grey, brown, and white (**Fig. 10**). Samples were in chip size to be analyzed in SEM and EDS.

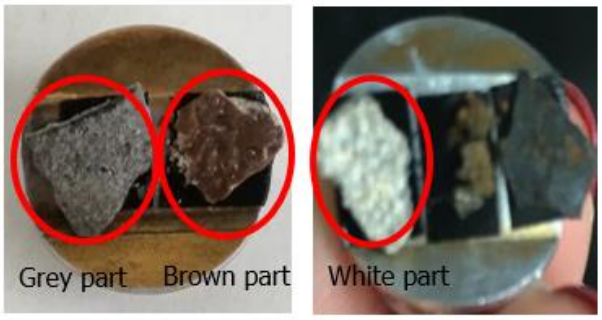


**Fig. 10—Sample #1 - parts for SEM-EDS analysis.**

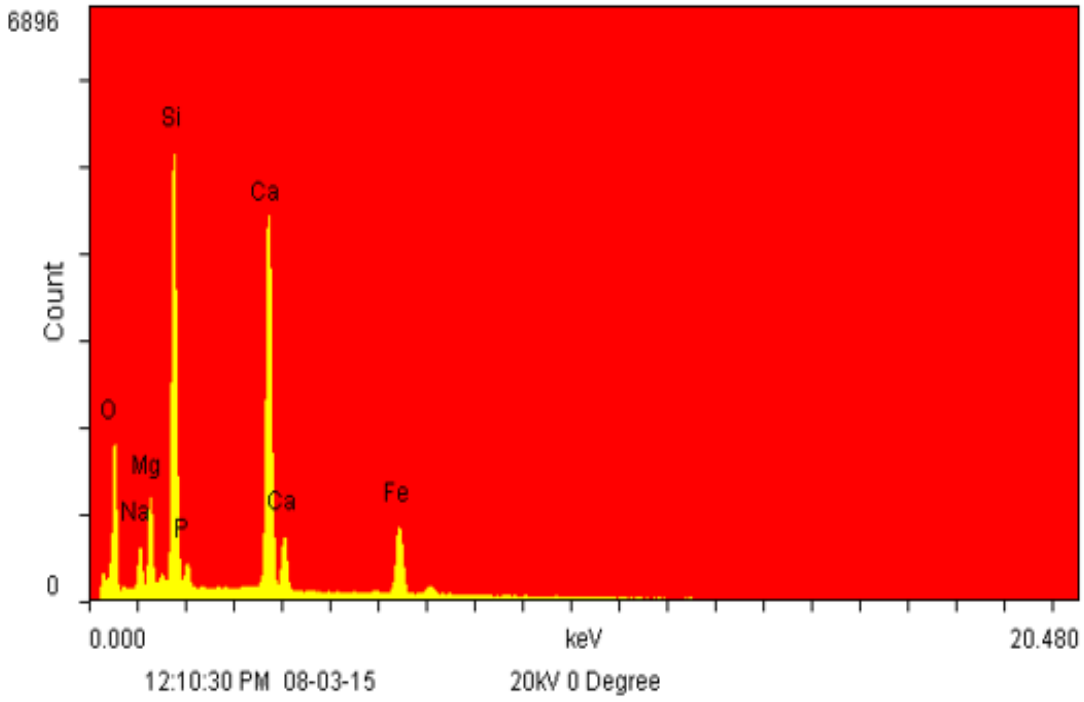


| Elements: | WT% | AT% | K_A | K_F | K_Z | Intensity | P/pkg |
|---|---|---|---|---|---|---|---|
| O K | 55 | 70.49 | 0.181 | 1 | 1.028 | 50.754 | 9.9 |
| NaK | 4.23 | 3.77 | 0.199 | 1.002 | 0.962 | 12.906 | 1.3 |
| MgK | 5.58 | 4.71 | 0.257 | 1.003 | 0.986 | 30.261 | 2.8 |
| SiK | 16.27 | 11.87 | 0.442 | 1.002 | 0.985 | 180.749 | 17.6 |
| P K | 1.28 | 0.85 | 0.393 | 1.002 | 0.949 | 9.818 | 1.1 |
| CaK | 12.71 | 6.5 | 0.885 | 1.002 | 0.956 | 188.304 | 21.7 |
| FeK | 4.92 | 1.81 | 0.986 | 1 | 0.869 | 41.352 | 6.7 |

**Fig. 11—EDS data for Scale #1 - grey part.**

**Fig. 11** shows the quantitative data about the chemical composition of Scale #1 – grey part. EDS result for this part of sample indicates that the sample is mostly composed of Si and Ca. This composition strongly points out that the grey part of scale #1 has metal

silicates, particularly calcium silicate. Mg, Fe, and Na exist in small quantities, and trace amount of phosphorus is present in this part of the sample.

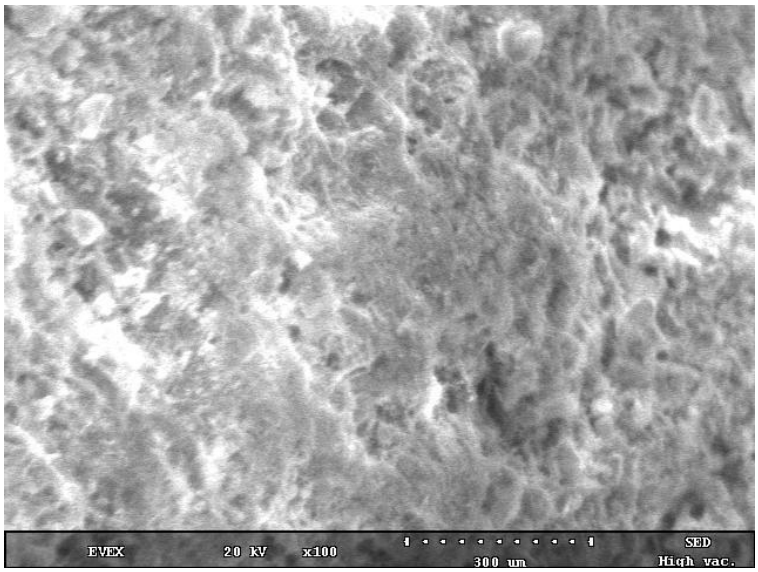


**Fig. 12—Scale #1 – grey part- SEM image (magnification: 100X).**

**Fig. 12** shows the electron microscope image of Scale #1-grey part with magnification of 100X. The grey part of Scale #1 shows high aggregation on the surface of sample. The particles with sharp edges might be indication for the presence of quartz based on EDS results which show high Si concentration (16.27 wt%). Scale #1-grey part has an amorphous phase with some porosities. There is no specific morphological shapes for this part of the scale.

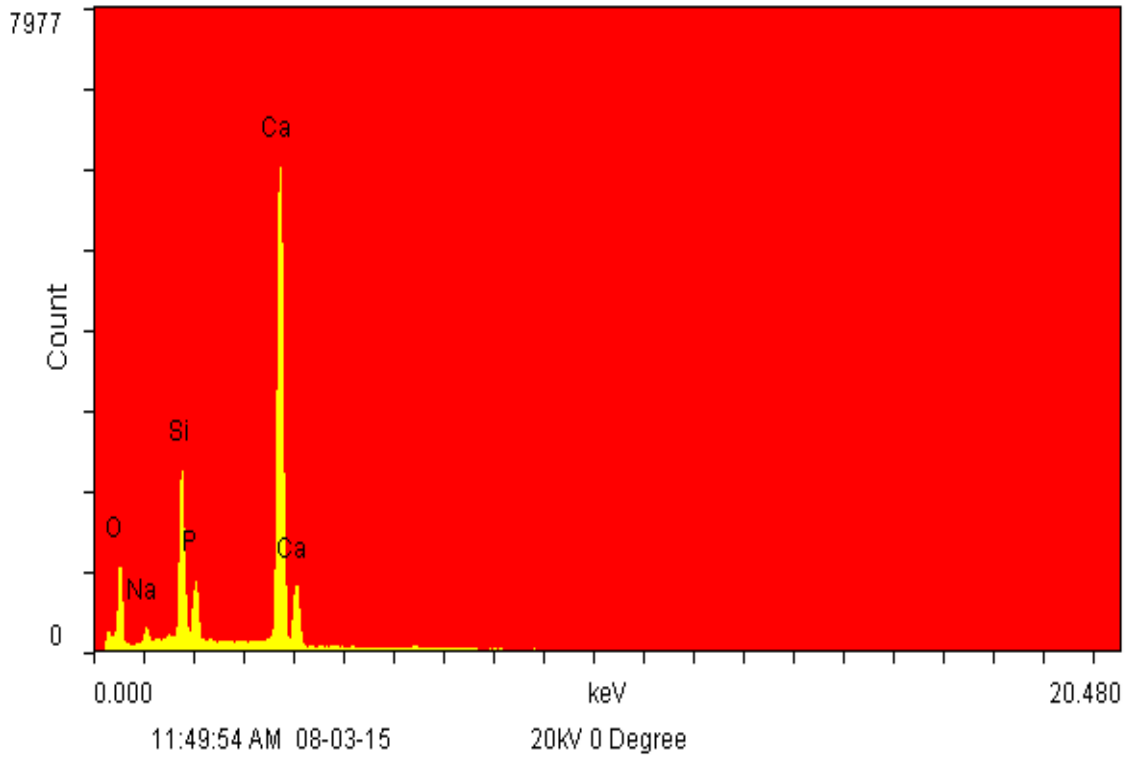


| Elements: | WT% | AT% | K_A | K_F | K_Z | Intensity | P/bkg |
|---|---|---|---|---|---|---|---|
| O K | 60.79 | 76.77 | 0.137 | 1 | 1.024 | 55.344 | 8.9 |
| NaK | 2.72 | 2.39 | 0.194 | 1.001 | 0.958 | 10.498 | 1 |
| SiK | 8.57 | 6.17 | 0.51 | 1.004 | 0.981 | 142.942 | 10.2 |
| P K | 4.01 | 2.62 | 0.519 | 1.004 | 0.945 | 52.886 | 3.8 |
| CaK | 23.91 | 12.05 | 0.94 | 1 | 0.952 | 486.664 | 37.8 |

**Fig. 13—EDS data for Scale #1 - brown part.**

**Fig. 13** demonstrates the quantitative data about the chemical composition of Scale #1 – brown part (Fig. 10). EDS result for this part of sample shows that the sample is mostly composed of Ca and Si. P and Na are present in small quantities. This composition

strongly indicates that the brown part of Scale #1 has large amounts of metal silicates, particularly calcium silicate as well as the grey part.

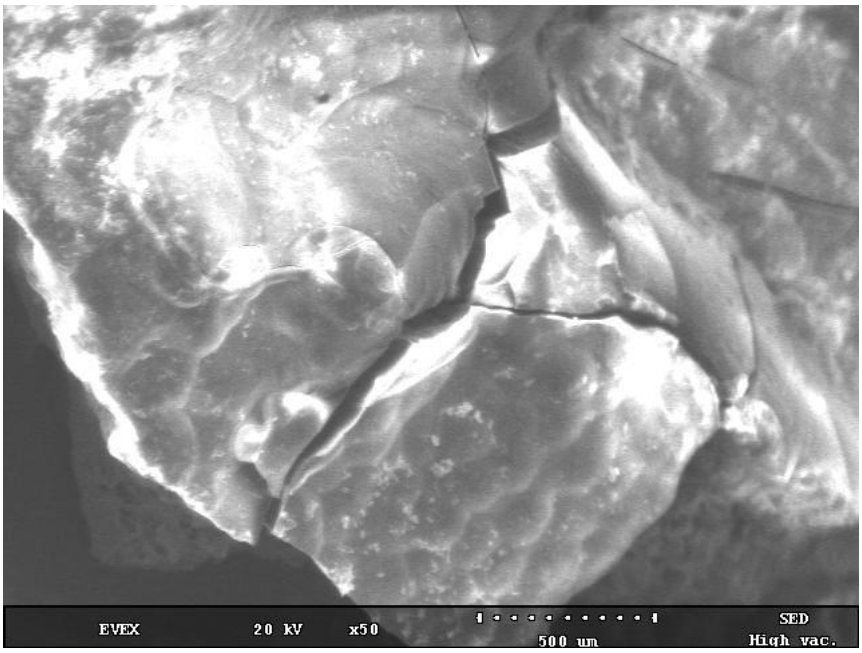


**Fig. 14—Scale #1 – brown part- SEM image (magnification: 50X).**

**Fig. 14** and **Fig. 15** show the electron microscope images of Scale #1-brown part with magnifications of 50 and 500X. This part of scale sample has a more specific morphology of particles with sharp corners. The base area is most probably quartz and the scattered particles on it might be because of the presence of calcium silicate.

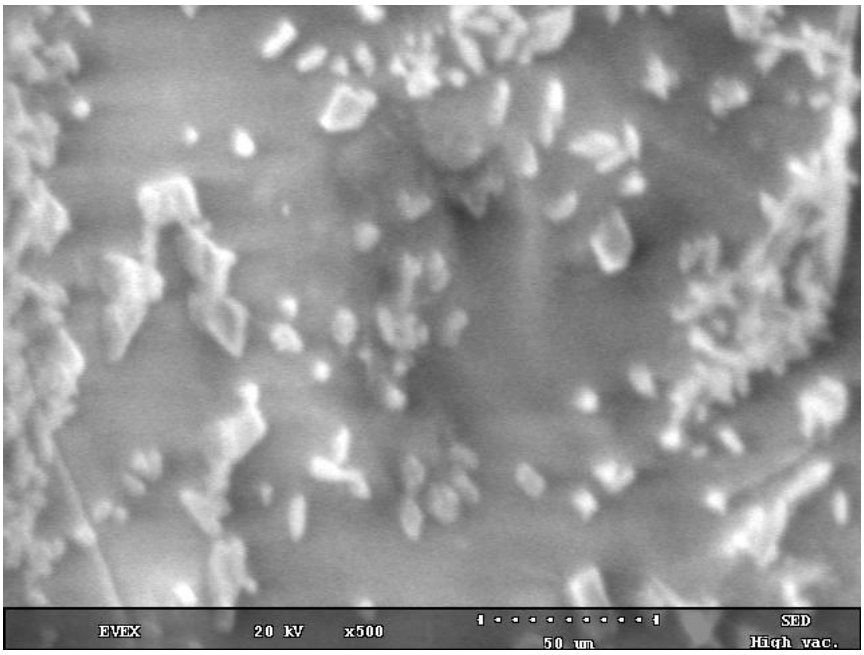


**Fig. 15—Scale #1 – brown part- SEM image (magnification: 500X).**

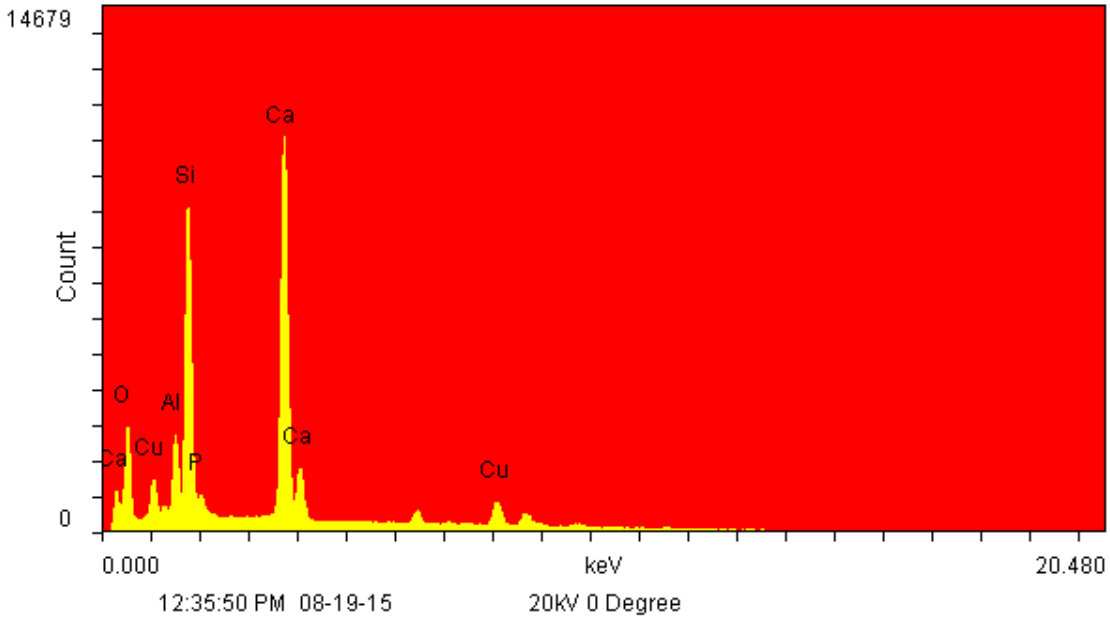


| Elements: | WT% | AT% | K_A | K_F | K_Z | Intensity | P/bkg |
|---|---|---|---|---|---|---|---|
| CaL | 40.14 | 23.8 | 1.169 | 1 | 0.969 | 140.045 | 2.1 |
| O K | 43.86 | 65.14 | 0.084 | 1 | 1.037 | 456.51 | 7 |
| AlK | 1.79 | 1.58 | 0.354 | 1.004 | 0.966 | 353.937 | 1.8 |
| SiK | 5.68 | 4.81 | 0.455 | 1.005 | 0.994 | 1577.83 | 7.5 |
| P K | 0.11 | 0.09 | 0.516 | 1.008 | 0.96 | 27.852 | 0.1 |
| CaK | 6.57 | 3.89 | 0.968 | 1 | 0.967 | 2573.557 | 24.1 |
| CuK | 1.85 | 0.69 | 0.962 | 1 | 0.849 | 214.474 | 2.9 |

**Fig. 16—EDS data for Scale #1 - white part.**

**Fig**. **16** shows the quantitative data about the chemical composition of Scale #1 – white part (Fig. 10). EDS results for this part of sample indicate that the sample is mostly composed of Ca and Si. Ca concentration of this part is much higher when compared to other color parts, grey and brown. Three different points in Scale #1 – white part were analyzed by EDS.

**Fig. 17** and **Fig. 18** show the electron microscope images of Scale #1-white part with magnifications of 100 and 500X. The morphology of this part of scale is flakier and highly amorphous.

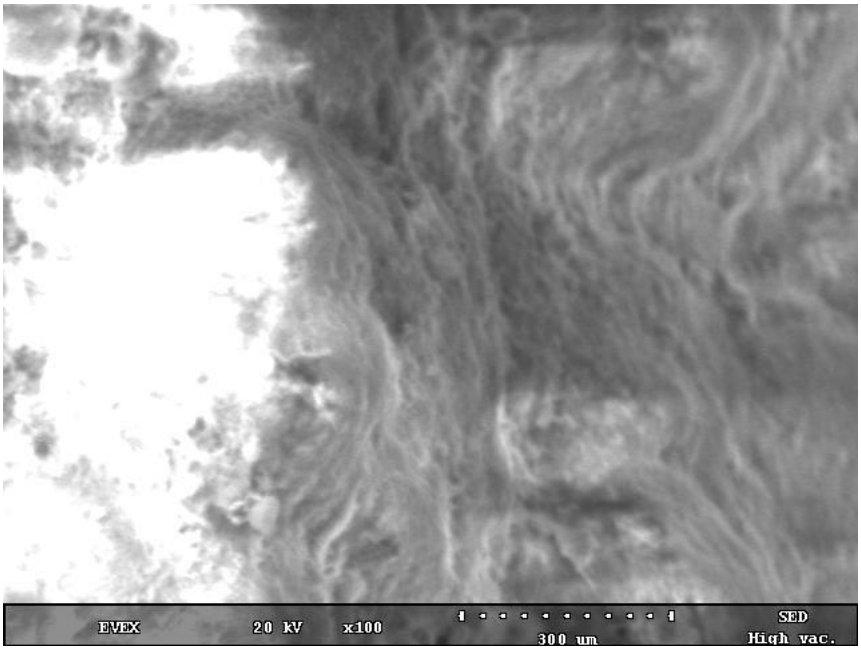


**Fig. 17—Scale #1 – white part- SEM image (magnification: 100X).**

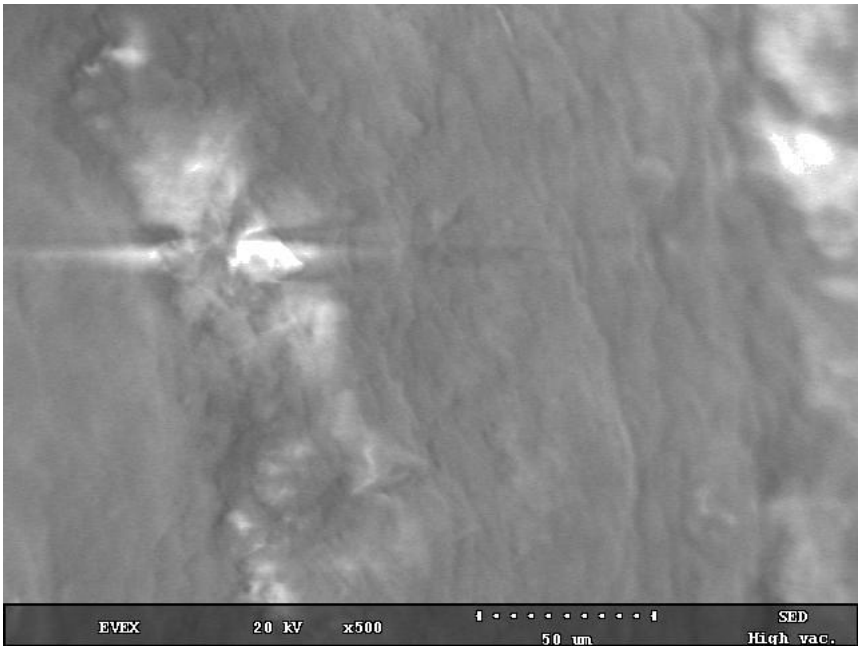


**Fig. 18 —Scale #1 – white part- SEM image (magnification: 500X).**

*2.2.1.2 XRF Analysis*

The whole sample was ground by the help of mortar and pestle without damaging the crystal structure (**Fig. 19**)**.**

**Fig. 19—Scale #1 for XRF analysis.**

**Table 2** indicates that Scale #1 mostly consists of sodium dioxide, calcium oxide and silicon dioxide. The concentration values below 1 wt% are removed from the table.

| Formula | Concentration (wt%) |
|---|---|
| $Na_2O$ | 67.0 |
| CaO | 14.7 |
| $SiO_2$ | 13.2 |
| $Fe_2O_3$ | 2.0 |

**Table 2—XRF results for Scale #1.**

By combining all the results, it can be concluded that the grains of quartz are consolidated by Fe, Ca, and Na oxides. In other words, Scale #1 is mostly composed of Na and Ca silicates. Ca appears on the surface of scales samples according to EDS results.

*2.2.1.3 XRD Analysis*

XRD qualitative analysis for Scale #1 (**Fig. 20**) is consistent with XRF and EDS results that the Scale #1 is composed of minerals with Na, Ca, Si, and Fe ions. Scale #1 has pectolite and anorthite which are slightly soluble in HCl solution. Tremolite, which is not soluble in HCl, also exists in Scale #1. The minerals present in scale #1 are silica-based minerals with metal cations.

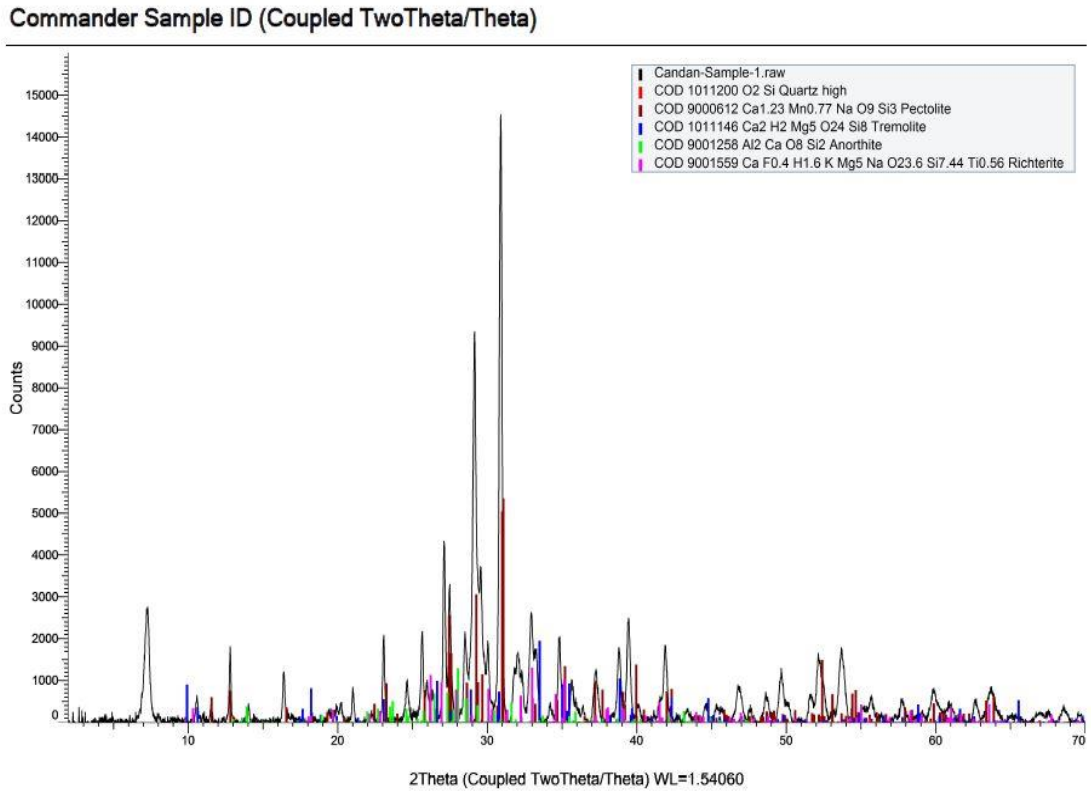


**Fig. 20—XRD qualitative results for Scale #1.**

2.2.2 Scale #2

*2.2.2.1 SEM and EDS Analysis*

Scale #2 (**Fig. 21**) does not seem homogenous in appearance in terms of its color.

**Fig. 21— Scale #2 - as received.**

It has both grey and black sides and SEM-EDS analysis were run for those sides separately after washed with xylene and acetone (**Fig. 22**)**.**

**Fig. 22—Scale #2 – in xylene (left) and dried sample after acetone wash (right).**

The xylene did not show any significant color change after the soaking stage of Scale #2 and xylene that is an indication for low content of organic matter.

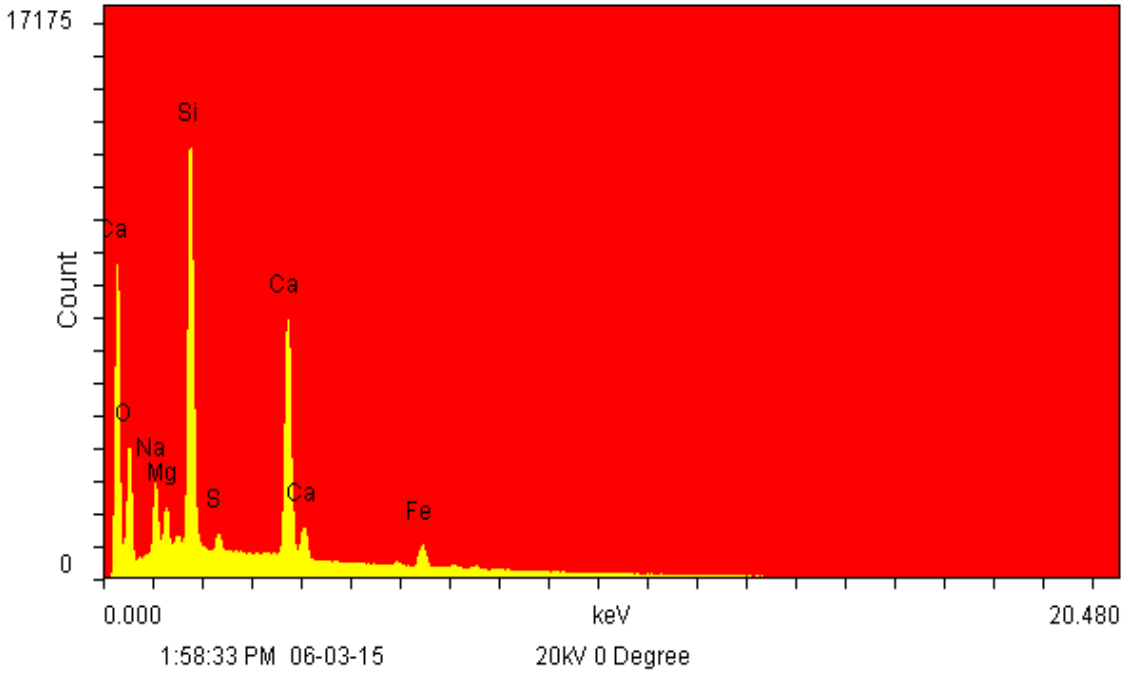


| Elements: | WT% | AT% | K_A | K_F | K_Z | Intensity | P/bkg |
|---|---|---|---|---|---|---|---|
| O K | 52.91 | 67.14 | 0.191 | 1 | 1.026 | 219.814 | 4.3 |
| NaK | 9.43 | 8.33 | 0.224 | 1.002 | 0.96 | 137.895 | 1.6 |
| MgK | 4.05 | 3.39 | 0.253 | 1.003 | 0.985 | 92.054 | 1 |
| SiK | 19.88 | 14.37 | 0.452 | 1.001 | 0.984 | 961.882 | 8.7 |
| S K | 0.86 | 0.54 | 0.483 | 1.003 | 0.968 | 37.448 | 0.4 |
| CaK | 10.87 | 5.51 | 0.869 | 1.001 | 0.955 | 673.498 | 8.6 |
| FeK | 2 | 0.73 | 0.989 | 1 | 0.867 | 71.747 | 1.3 |

**Figure 23—EDS data for Scale #2 - black side.**

**Fig. 23** shows the quantitative data about the chemical composition of Scale #2 – black side. EDS results for this part of sample reveals that the sample is mostly composed

of Ca, Si, and Na. This composition strongly indicates that the black part of Scale #2 is mostly metal silicates, particularly Ca and Na silicates. There is a trace of S and Fe in this part of the scale with 0.86 and 2 wt%, respectively.

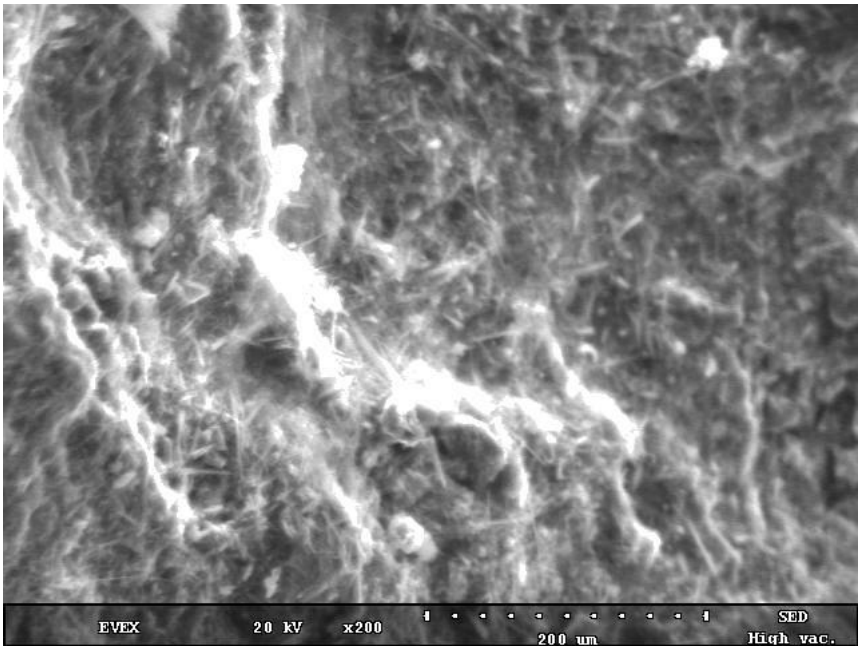


**Fig. 24—Scale #2 – black side - SEM image (magnification: 200X).**

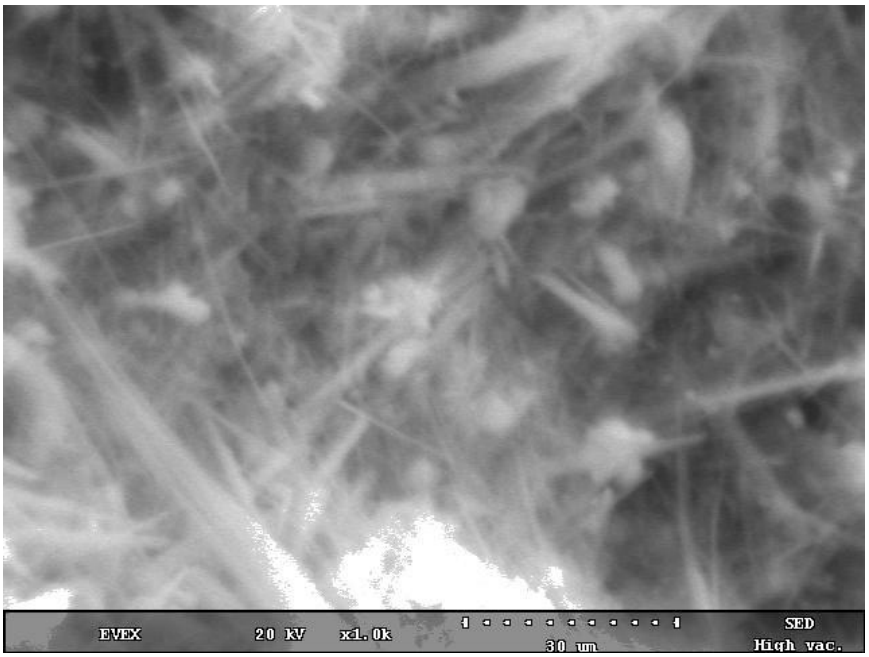


**Fig. 25—Scale #2 – black side - SEM image (magnification: 1000X).**

Needle like structures are easy to be observed in SEM images for Scale #2- black side in **Fig. 24** and **Fig. 25** with magnifications of 200 and 1000X. These structures are in different sizes (small, medium, and large).

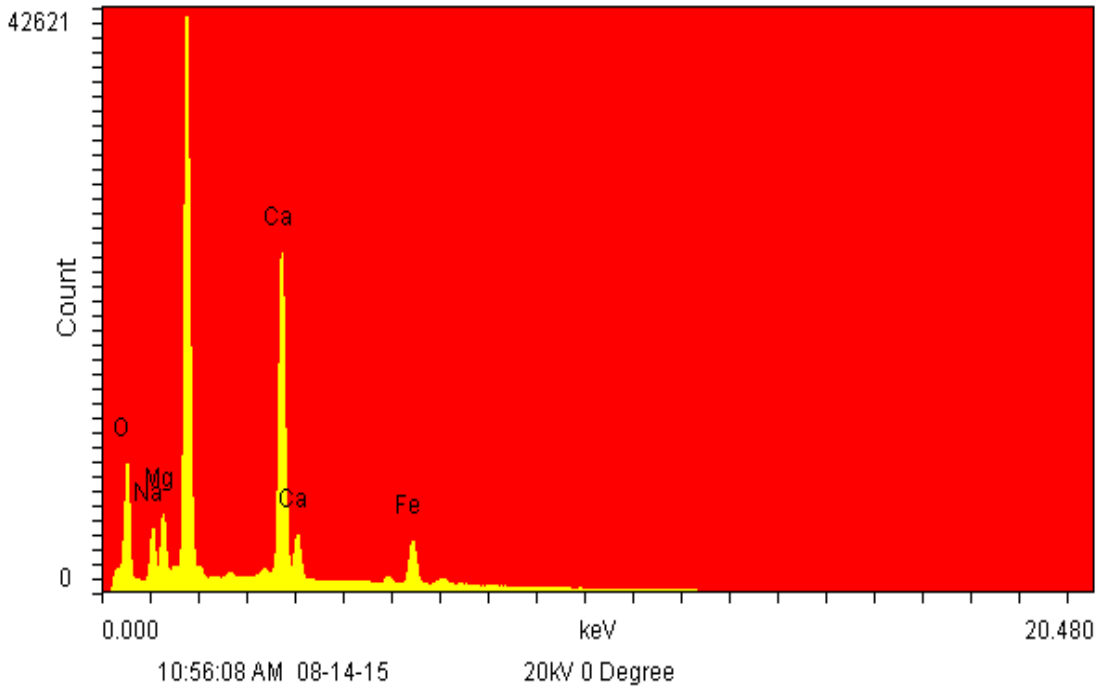


| Elements: | WT% | AT% | K_A | K_F | K_Z | Intensity | P/bkg |
|---|---|---|---|---|---|---|---|
| O K | 51.87 | 66.99 | 0.179 | 1 | 1.027 | 546.457 | 7.7 |
| NaK | 6.17 | 5.54 | 0.214 | 1.002 | 0.961 | 234.027 | 2 |
| MgK | 4.43 | 3.77 | 0.263 | 1.004 | 0.986 | 283.515 | 2 |
| SiK | 21.95 | 16.15 | 0.461 | 1.001 | 0.985 | 2939.635 | 21.7 |
| CaK | 12.29 | 6.34 | 0.868 | 1.001 | 0.956 | 2060.885 | 17.9 |
| FeK | 3.28 | 1.21 | 0.984 | 1 | 0.868 | 317.864 | 3.3 |

**Fig. 26—EDS data for Scale #2 - grey side.**

**Fig. 26** shows the quantitative data about the chemical composition of Scale #2 – grey side. EDS result for this part of sample reveals that the sample comprises mostly Si and Ca. Na, Mg, and Fe are also present in the grey side of the scale as well as black side.

Needle like shapes in SEM image (**Fig. 27**) were detected once again in this side of the scale sample. Both SEM image and EDS results indicate that both sides of Scale #2 is similar in terms of their compositions.

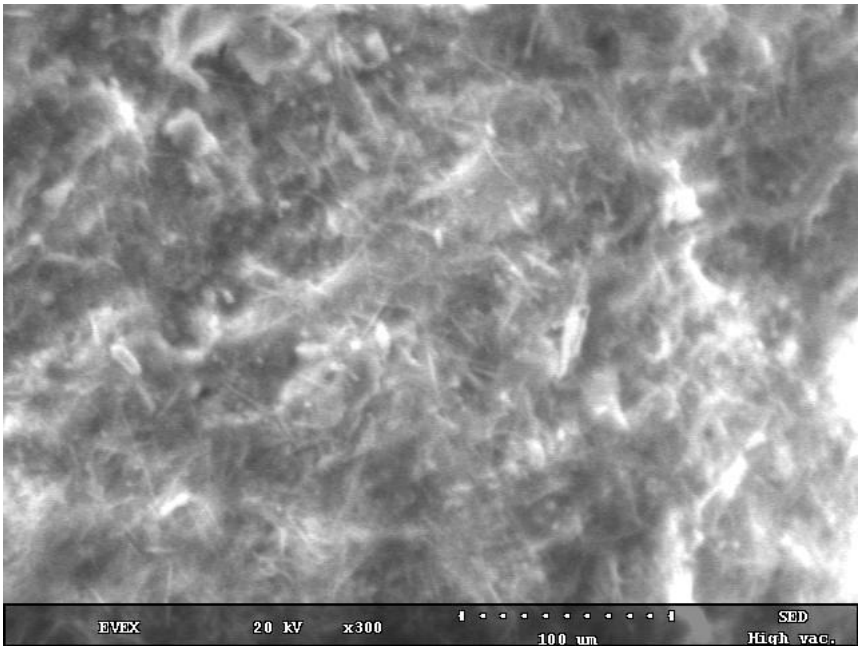


**Fig. 27—Scale #2 – grey side - SEM image (magnification: 300X).**

*2.2.2.2 XRF Analysis*

The whole sample was ground by the help of mortar and pestle without damaging the crystal structure (**Fig. 28**)**.**

**Fig. 28—Scale #2 for XRF analysis.**

**Table 3** indicates that this sample mostly consists of silicon dioxide and iron (3) oxide. The concentration values below 1 wt% are removed from the table.

| Formula | Concentration (wt%) |
|---|---|
| $SiO_2$ | 31.2 |
| MgO | 25.9 |
| $Fe_2O_3$ | 24.3 |
| CaO | 3.21 |

**Table 3—XRF results for Scale #2.**

*2.2.2.3 XRD Analysis*

XRD qualitative analysis for Scale #2 (**Fig. 29**) is consistent with XRF and EDS results that the Scale #2 is composed of minerals with Si, Mg, Fe, and Ca ions. The minerals present in Scale #2 are pectolite, fayalite, tremolite, and anorthite. Needle-like

shapes in SEM pictures can be explained by the presence of tremolite mineral in Scale #2 (Campopiano et al. 2015).

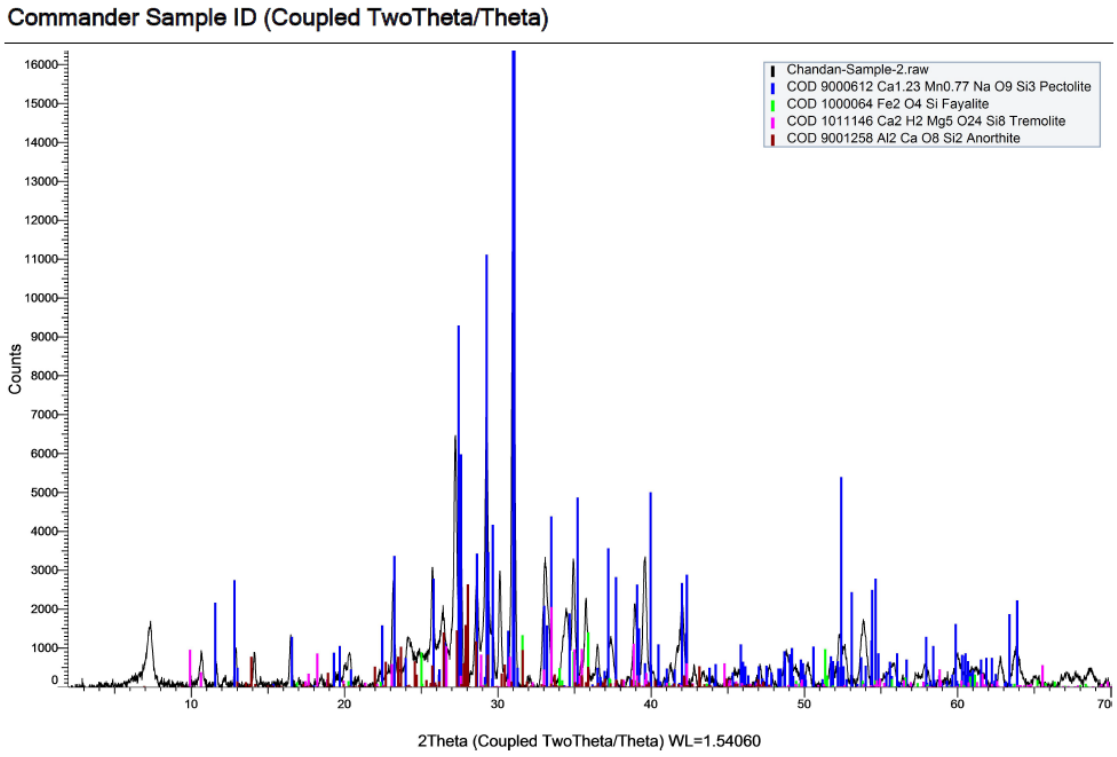


**Fig. 29—XRD qualitative results for scale #2.**

## 2.2.3 Scale #3

### *2.2.3.1 SEM and EDS Analysis*

Scale #3 (**Fig. 30**) was wet at first when it was received. After preheated in the oven, it went through the same procedure as well as other scale samples (**Fig. 31**).

**Fig. 30—Scale #3 - as received (left), after preheated in the oven (right).**

The xylene did not show any significant color change after the soaking stage of Scale #3 (Fig. 31) and xylene that is an indication for low content of organic matter.

**Fig. 31—Scale #3 – in xylene (left) and dried sample after acetone wash (right).**

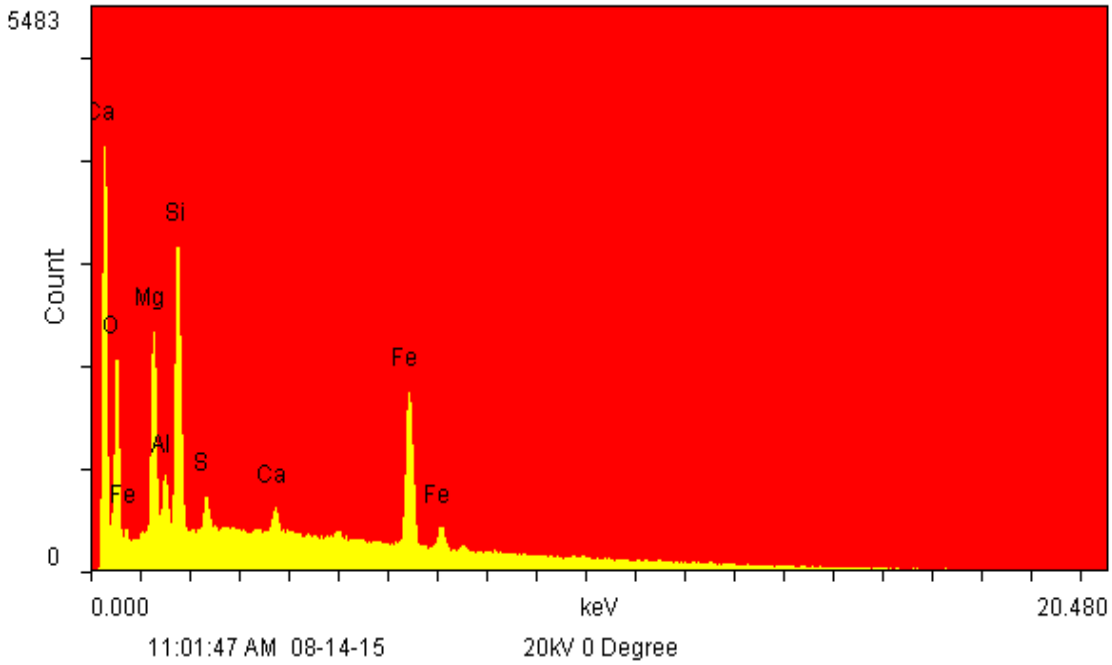


| Elements: | WT% | AT% | K_A | K_F | K_Z | Intensity | P/bkg |
|---|---|---|---|---|---|---|---|
| O K | 46.28 | 63.31 | 0.253 | 1 | 1.041 | 133.737 | 5 |
| FeL | 6.78 | 2.66 | 0.515 | 1.001 | 0.892 | 12.783 | 0.5 |
| MgK | 14.75 | 13.28 | 0.248 | 1.003 | 0.998 | 172.635 | 4 |
| AlK | 3.99 | 3.24 | 0.257 | 1.004 | 0.969 | 53.046 | 1.2 |
| SiK | 15.08 | 11.75 | 0.325 | 1.001 | 0.997 | 276.027 | 5.4 |
| S K | 1.66 | 1.13 | 0.434 | 1.001 | 0.984 | 34.16 | 0.6 |
| CaK | 0.94 | 0.51 | 0.825 | 1.006 | 0.969 | 29.165 | 0.5 |
| FeK | 10.52 | 4.12 | 1.015 | 1 | 0.881 | 203.946 | 4.3 |

**Fig. 32—EDS data for Scale #3.**

**Fig. 32** shows the quantitative data about the chemical composition of Scale #3. EDS results for this sample show that the sample is mostly composed of silicon, magnesium and iron. This composition strongly reveals that Scale #3 is mostly metal silicates, especially iron and magnesium silicates. There is a trace of calcium and sulphur in Scale #3. SEM images with magnification of 50 and 200X (**Fig. 33** and **Fig. 34**,

respectively) show various scattered particles on the surface of the sample. SEM images might show that the base area is quartz and the small particles on it is most probably iron(III) oxide ($Fe_2O_3$) and magnesium oxide (MgO).

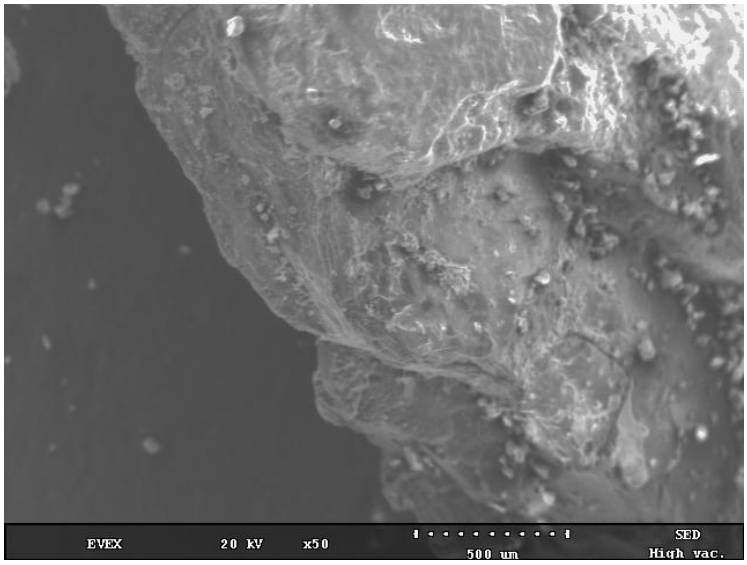


**Fig. 33—Scale #3 - SEM image (magnification: 50X).**


**Fig. 34— Scale #3 - SEM image (magnification: 200X).**

One of the scattered particles on the surface Scale #3 was analyzed once again by focusing this exact part of the sample with SEM and EDS. This part was showed with a red circle in Fig. 34**.**

EDS result for this part of sample (**Fig. 35**) shows that the sample comprises mostly Fe, Mg, and Si. This composition is similar to the one in Fig. 32**.**

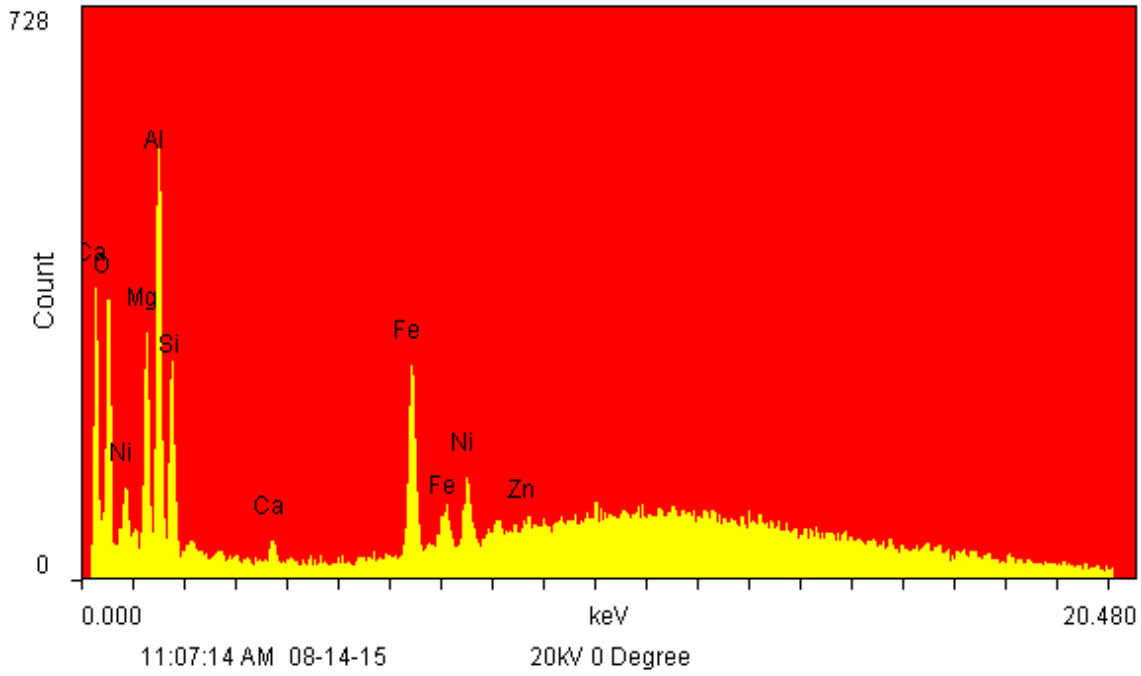


| Elements: | WT% | AT% | K_A | K_F | K_Z | Intensity | P/bkg |
|---|---|---|---|---|---|---|---|
| O K | 45.65 | 63.47 | 0.252 | 1 | 1.045 | 20.849 | 10.4 |
| NiL | 9.75 | 3.7 | 0.501 | 1.001 | 0.914 | 4.499 | 1 |
| MgK | 9.82 | 8.98 | 0.219 | 1.003 | 1.002 | 16.139 | 4 |
| AlK | 16.4 | 13.52 | 0.258 | 1.002 | 0.973 | 34.62 | 10.1 |
| SiK | 7.61 | 6.03 | 0.257 | 1 | 1.001 | 17.42 | 5.5 |
| CaK | 0.46 | 0.26 | 0.823 | 1.004 | 0.973 | 2.277 | 1 |
| FeK | 7.38 | 2.94 | 1.016 | 1.036 | 0.885 | 23.546 | 4.5 |
| NiK | 2.94 | 1.12 | 0.991 | 1 | 0.898 | 6.703 | 0.8 |
| ZnK | 0 | 0 | 0.966 | 1 | 0.855 | 0 | 0 |

**Fig. 35— EDS data for Scale #3 - focused particle.**

*2.2.3.2 XRF Analysis*

The whole sample was ground by the help of mortar and pestle without damaging the crystal structure (**Fig. 36**).

**Fig. 36—Scale #3 for XRF analysis.**

XRF result of the ground mixture for Scale #3 (**Table 4**) indicates that this sample mostly consists of silicon dioxide and magnesium oxide. The concentration values below 1 wt% are removed from the table.

| Formula | Concentration (wt%) |
|---|---|
| $Fe_2O_3$ | 50.9 |
| $SiO_2$ | 15.7 |
| MgO | 9.88 |
| CaO | 3.95 |
| $K_2O$ | 3.45 |

**Table 4—XRF results for Scale #3.**

*2.2.3.3 XRD Analysis*

XRD qualitative analysis for Scale #3 (**Fig. 37**) is consistent with XRF and EDS results that the Scale #3 is composed of minerals with Fe, Si, Mg, and Ca ions. The minerals present in Scale #3 are quartz, tremolite, pectolite, greenalite, and fayalite.

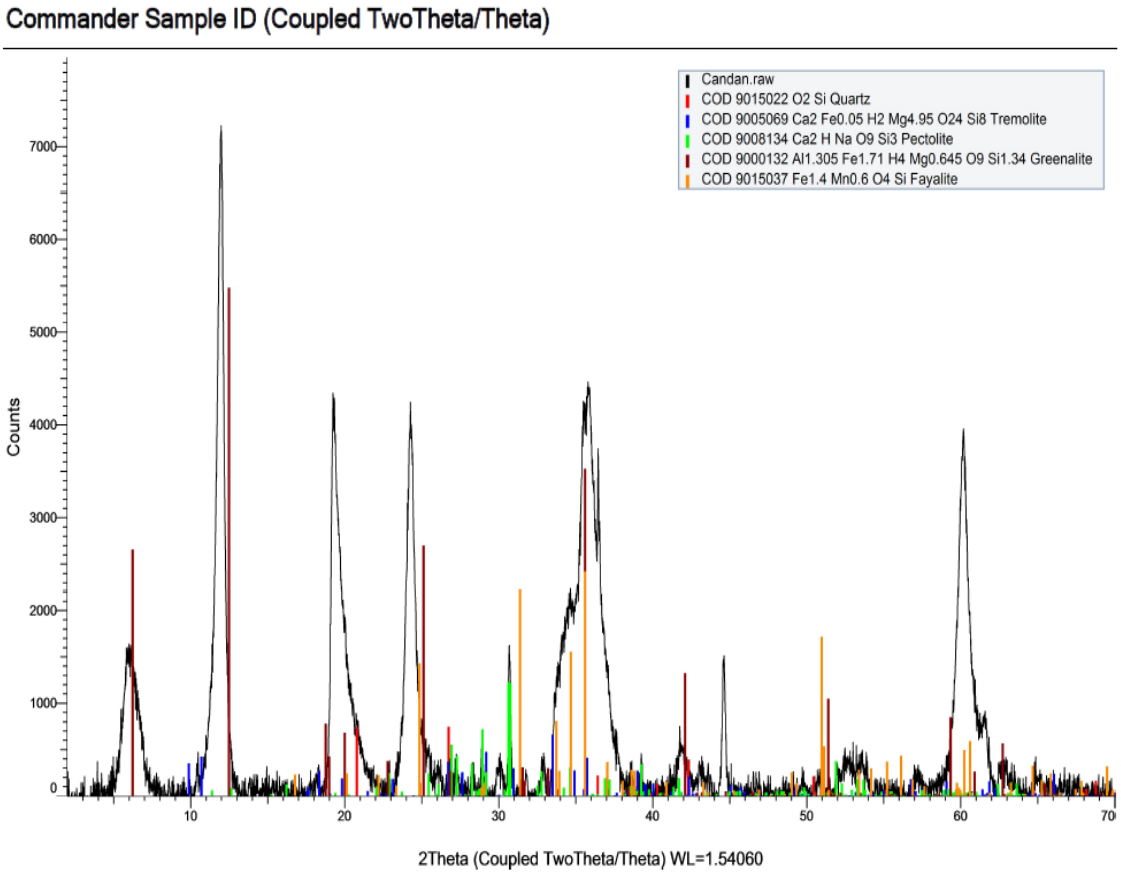


**Fig. 37—XRD qualitative results for Scale #3.**

2.2.4 Scale #4

*2.2.4.1 SEM and EDS Analysis*

Scale #4 (**Fig. 38**) was wet and a kind of slurry according to its appearance. After filtration of Scale #4, liquid part of sample was analyze at first when it was received.


**Fig. 38—Scale #4 - as received (left), after preheated in the oven (right).**

After preheated in the oven, Scale #4 went through the same procedure as well as other scale samples (**Fig. 39**).

**Fig. 39—Scale #4 – in xylene (left) and dried sample after acetone wash (right).**

**Fig. 40** shows the quantitative data about the chemical composition of Scale #4. EDS results for this sample show that the sample is mostly composed of Fe and Si by almost 37 and 9 wt%, respectively. This composition strongly reveals that Scale #4 is iron silicate with some other metals which are present in small quantities, such as, Ca, Mg, and Na.

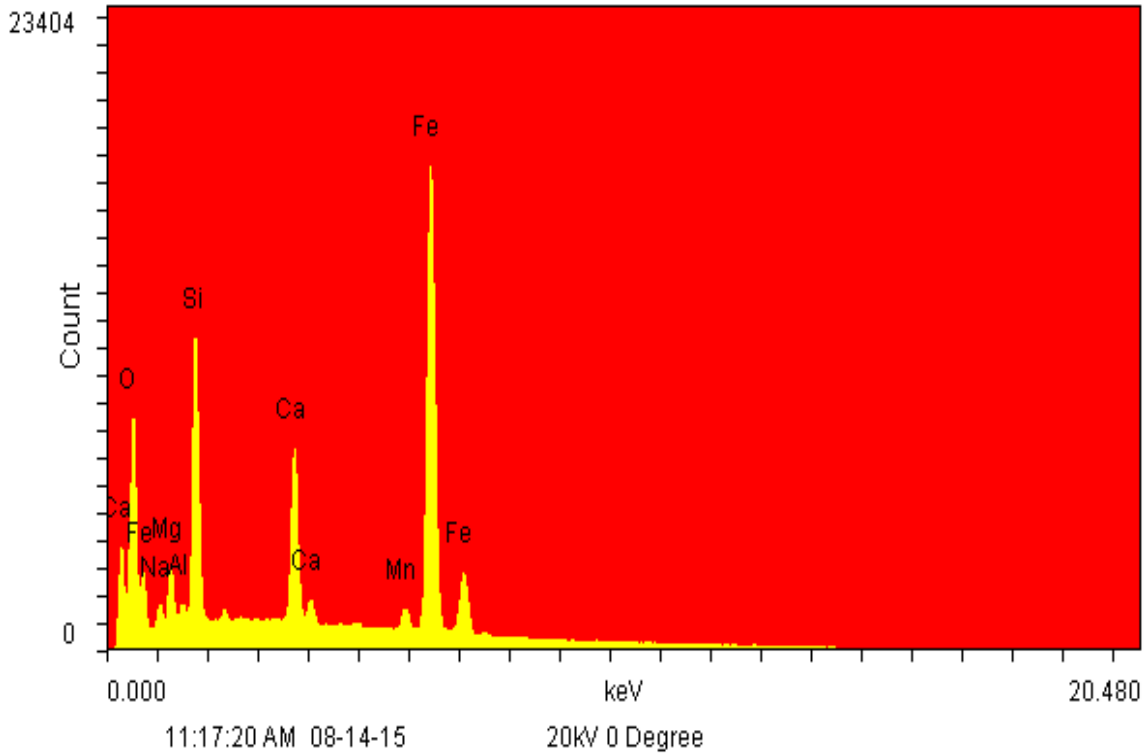


| Elements: | WT% | AT% | K_A | K_F | K_Z | Intensity | P/bkg |
|---|---|---|---|---|---|---|---|
| O K | 44.64 | 67.99 | 0.219 | 1 | 1.062 | 505.409 | 8.3 |
| FeL | 16.43 | 7.17 | 0.496 | 1 | 0.91 | 135.294 | 2.2 |
| NaK | 1.98 | 2.09 | 0.12 | 1.001 | 0.994 | 36.928 | 0.4 |
| MgK | 3.28 | 3.29 | 0.167 | 1.001 | 1.018 | 116.552 | 1.2 |
| AlK | 0.55 | 0.49 | 0.228 | 1.002 | 0.988 | 29.216 | 0.3 |
| SiK | 9.03 | 7.84 | 0.312 | 1.001 | 1.017 | 718.734 | 6.4 |
| CaK | 3.53 | 2.15 | 0.862 | 1.013 | 0.99 | 523.603 | 5.1 |
| MnK | 0.77 | 0.34 | 1.006 | 1 | 0.885 | 73.75 | 0.7 |
| FeK | 19.79 | 8.64 | 1.014 | 1 | 0.901 | 1740.18 | 16.7 |

**Fig. 40—EDS data for Scale #4.**

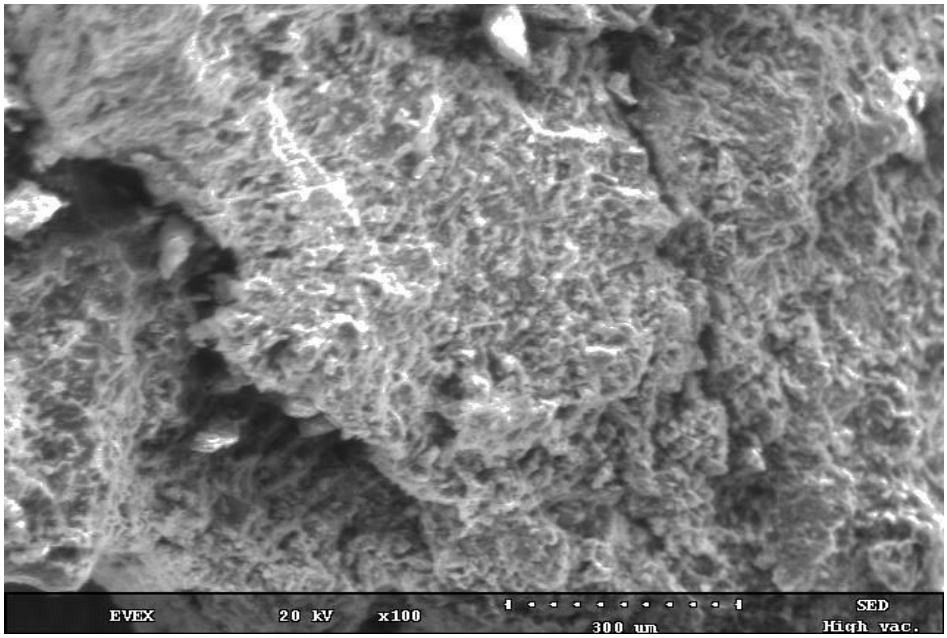


**Fig. 41—Scale #4 - SEM image (magnification: 100X).**

**Fig. 41** shows the electron microscope image of Scale #4 with magnification of 100X. Scale #4 is not amorphous with a lot of porosities.

*2.2.4.2 XRF Analysis*

The whole sample was ground by the help of mortar and pestle without damaging the crystal structure (**Fig. 42**).

**Fig. 42—Scale #4 for XRF analysis.**

XRF result of the ground mixture for scale #4 (**Table 5**) indicates that this sample mostly consists of oxides of Ca, Si, and Fe. The concentration values below 1 wt% are removed from the table.

| Formula | Concentration (wt%) |
|---|---|
| CaO | 38.0 |
| $SiO_2$ | 34.6 |
| $Fe_2O_3$ | 11.4 |
| $P_2O_5$ | 5.8 |
| $K_2O$ | 3.3 |
| MgO | 2.5 |

**Table 5—XRF results for Scale #4.**

*2.2.4.3 XRD Analysis*

XRD qualitative analysis for Scale #4 (**Fig. 43**) is consistent with XRF and EDS results that the Scale #4 is composed of quartz, pectolite, chlorite, and tremolite.

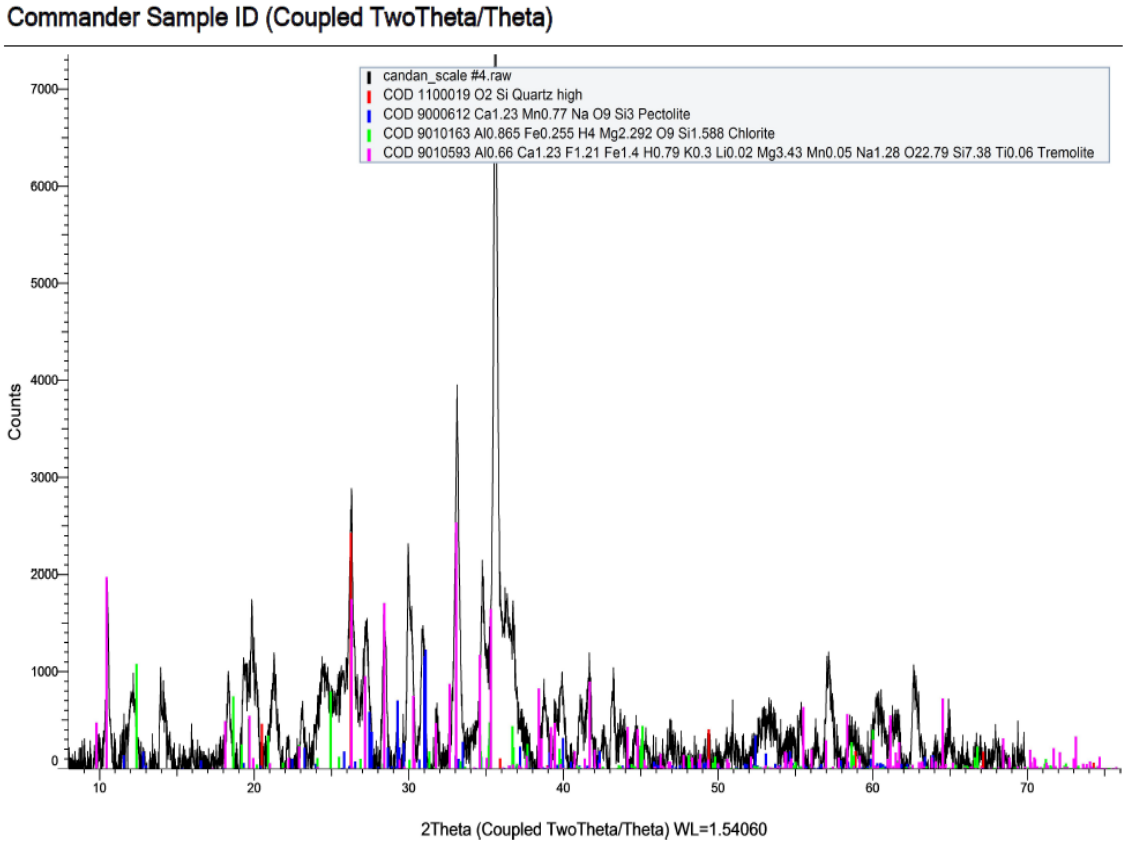


**Fig. 43—XRD qualitative results for Scale #4.**

## 2.3 Dissolution Tests

After analysis by SEM-EDS and XRF, scale samples went through several dissolution tests to figure out the best solution for their removal. For this purpose, solubility tests were performed with preflush stages by using hydrochloric acid (HCl), formic acid, and a chelating agent, mono- sodium GLDA (NaGLDA). Then, the main acid solutions were formed by mixing hydrofluoric acid (HF) and those preflush fluids. Dissolution tests were performed at 77 and 300ºF. The materials used in the dissolution tests and the methodology will be explained in this section.

### 2.3.1 Materials

The chemicals used in this project are hydrochloric acid (HCl), formic acid ($CH_2O_2$), mono-sodium GLDA (NaGLDA), potassium hydroxide (KOH), and ammonium bifluoride ($NH_4.HF_2$) (**Table 6**).

| Chemical | Density ($g/cm^3$) | Concentration (%) | Molecular Weight (g/mol) |
|---|---|---|---|
| HCl | 1.18 | 36.5 | 36.5 |
| Formic Acid | 1.20 | 96.0 | 46.0 |
| NaGLDA | 1.41 | 40.0 | 350.0 |

**Table 6—Physical properties of fluids used in tests.**

Solutions used in main acid treatments were prepared by hydrofluoric acid (HF), other fluids listed in (**Table 6**) and de-ionized water with a resistivity of 18.2 MΩ.cm at

room temperature. HCl (with 36.5 wt% concentration) and crystalized ammonium bifluoride were mixed according to Eq. 2.1 shown below:

$$NH_4.HF_2 + HCl \leftrightarrow 2HF + NH_4Cl \quad . \quad \ldots\ldots\ldots\ldots\ldots\ldots\ldots\ldots\ldots\ldots \quad (2.1)$$

| DISSOLUTION TESTS | | | | |
|---|---|---|---|---|
| Preflush | 15 wt% HCl | 10 wt% NaGLDA | 9 wt% Formic Acid | - |
| Main Treatment | 9 wt% HCl<br>1 wt% HF | 10 wt% NaGLDA<br>1 wt% HF | 9 wt% Formic Acid<br>1 wt% HF | 5 wt% KOH |

**Table 7—Concentrations of chemicals used in the tests.**

HCl, NaGLDA, and formic acid preflush treatments were applied to each scale sample separately. The preflush stages were followed by the main acid treatment stages with HCl-HF, NaGLDA-HF, and formic-HF, respectively (**Table 7** for concentrations). 5 wt% KOH solution was prepared with deionized water for dissolution tests to see the effect of alkaline solutions. All the treatment stages are summarized in **Fig. 44**.

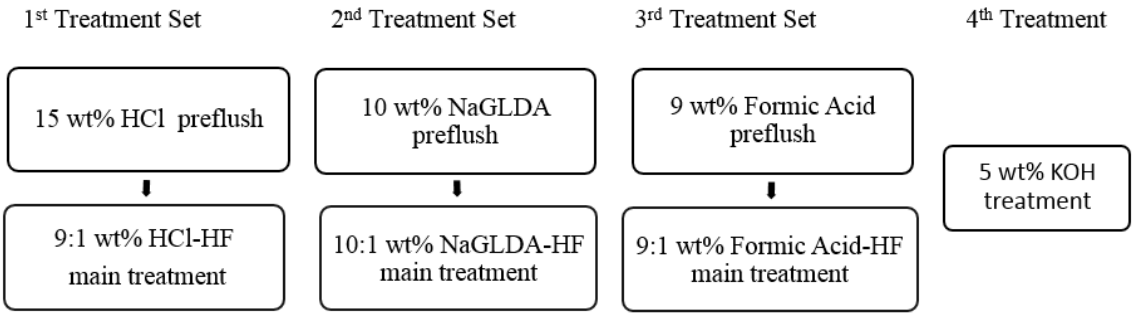


**Fig. 44—Treatment sets.**

As Ning et al. (2010) states, anions (OH- and F-) take active roles in decreasing the Si-O bond strength by causing an increase in the coordination number of silicon atom to more than four. Therefore, using HF and HF-based solutions are effective in silica scale dissolution.

### 2.3.2 Equipment and Experimental Procedure

#### *2.3.2.1 Tests at Room Temperature*

Dissolution tests at room temperature were performed by using a magnetic stirrer. The ratio between chemical mixtures and the scale samples was 10:1 (10 g of chemical mixture for each gram of scale sample). Test duration was three hours per run.

The medium size filter paper with 5 to 10 micron particle retention (60 mL/min) was then used with a funnel to separate the supernatant from the filtrate part. After obtaining enough of filtrate for analysis, the supernatant washed with DI water to stop further reactions and prevent formation of any other salt deposition. The supernatant with filter paper was dried in the oven for at least 3 hours at 300°F before the main treatment processes. The procedure

for main treatment was same with preflush stage. The only change in the process was the fluid used in the main treatment process. All the tests with HF were conducted in plastic tubes to avoid an HF reaction with glass and prevent silica leeching from glassware.

All the filtrates collected after filtering process were diluted to a factor of 500 by using deionized water. Diluted samples were analyzed by the use of Optima 7000 DV Inductively coupled plasma optical emission spectrometer (ICP-OES) system and Winlab $32^{TM}$ software.

ICP is an analytical technique for analysis of metals in liquid solutions. It counts the number of ions at a certain mass of the element to detect the elemental content. Samples are most commonly introduced as liquids. The ions detected by ICP are typically positive ions, therefore, elements with negative ions, such as CI, I, F, etc., are very hard to determine by ICP. Detection limits of elements range from parts per million (ppm) to parts per billion (ppb).

The solubility of scale samples after each treatment were determined in percent by using Eq. 2.2 given in below:

$$\text{Solubility} = \left(1 - \frac{M_{\text{supernatant}}}{M_{\text{initial}}}\right) * 100 \quad . \quad \ldots\ldots\ldots\ldots\ldots\ldots\ldots\ldots\ldots \quad (2.2)$$

where $M_{\text{supernatant}}$ is the dry mass of the scale after the reaction with fluids by filtering through medium size filter paper, and $M_{\text{initial}}$ is the mass of the scale, which will be used in the reaction.

*2.3.2.1 Tests at High Temperature*

A hastelloy aging cell, a Teflon liner, and a roller oven were used in the tests at 300ºF. The samples can be exposed to the temperature levels much higher than the boiling point of water and still sustain their liquid phase by the help of the OFITE aging cell (**Fig. 45**), which is a pressure cylinder.

**Fig. 45—OFITE aging cell.**

The aging cells might be subjected to static temperature conditions or used dynamically within roller oven. They are made by stainless steel (grade 303 or grade 316) and hastelloy (grade C-276) which enable to run the tests at high temperatures (max 600°F).

**Fig. 46—OFITE teflon liner with a t-screw.**

A Teflon liner **(Fig. 46)** is used for testing highly corrosive fluids at high temperature and pressure to prevent any damage to aging cells. Besides its common properties with regular aging cell, the OFITE Teflon Liner is used to avoid the damage caused by high corrosive fluids. The floating piston is placed and removed by the help of a t-screw and used to pressurize the fluid sample. Any possible leakage is avoided by providing seal with a plug. In our tests, the model of #175-60 was used with hastelloy aging cell.

For the solubility tests conducted at 300ºF, the steps listed below were followed:

- The mixture (1:10 mass ratio of scale sample and treatment fluid, respectively) was put in the Teflon liner and closed with a piston plug. The difference of mixture from the one used at room temperature was corrosion inhibitors. 7 gram per thousand gram (gpt) of CI-31 (corrosion inhibitor) was chosen for the tests run with HCl-HF mixture at high temperature. CI-27 (corrosion inhibitor) was used for the tests run with NaGLDA-HF, and formic acid-HF mixtures at high temperature. As KOH is not

corrosive at high temperature, tests with KOH solutions were conducted without corrosion inhibitor.

- The Teflon liner was placed in the hastelloy aging cell (Fig. 45), which was pressurized to 300 psi by a nitrogen source.

**Fig. 47—Roller oven with aging cells for dynamic testing.**

- Pressurized aging cell was placed into roller oven (**Fig. 47**) and rotated for three hours at 300ºF to meet the dynamic testing requirements.
- After the cooling of aging cell, the mixture was filtered by the medium size filter paper with 5 to 10 micron particle retention (60 mL/min), and a plastic funnel.
- After enough of filtrate was obtained for analysis, the supernatant was washed with deionized water to stop further reactions and prevent formation of any other salt deposition. The supernatant with filter paper was dried in the oven before the main treatment process. The procedure for the main treatment was the same as the preflush

stage. All tests with HF were conducted in plastic tubes to avoid an HF reaction with glass and prevent silica leeching from glassware.

- All the filtrates collected after the filtering process were diluted with a dilution factor of 500 by using deionized water. Diluted samples went through the same stages within the case of room temperature.
- Solubility values in percent were calculated by using Eq. 2.2.

# 3. RESULTS AND DISCUSSION

The aims of this research are to: 1) analyze the compositions of silica scales from SAGD boilers, 2) study the effect of different treatment solutions on the solubility of those silica scales, and 3) examine the effect of temperature on the working mechanisms of those solutions to find the most efficient formulation to dissolve the scales.

In the performed tests, NaGLDA was used as a chelating agent. Chelating agents (chelants) are capable of forming stable complexes with metal ions. They are used for solving and inactivating metal ions and preventing the possible deposition of scales by complexing with di-valent and tri-valent cations. Formic acid and HCl were used at both preflush stages to dissolve carbonates in the scales. The reason behind the use of HF and HF-based solutions was that they cause an increase in coordinating number of silicon atom to more than four by decreasing Si-O bond strength (Ning et al. 2010). Hence, they are remarkably effective to remediate the silica scale precipitations. KOH was chosen as a solution to investigate the effect of strong alkaline medium on the dissolution mechanism of the scale samples.

In this chapter, the solubility and ICP results of the applied dissolution tests will be discussed and evaluated one by one for each sample.

## 3.1 Scale #1

### 3.1.1 Results for Scale #1

Dissolution tests for Scale #1 consist of four different treatment sets: HCl preflush followed by HCl-HF main acid, NaGLDA preflush followed by NaGLDA-HF main acid, formic acid preflush followed by formic acid-HF main acid, and use of KOH solution. These tests were performed dynamically at 77 and 300°F for three hours.

Si is dissolved slightly after all the preflush stages with NaGLDA, HCl, and formic acid (**Fig. 48 (a)**). The main acid treatment is the most significant stage in terms of dissolving considerable amounts of Si for all treatment sets (**Fig. 48 (b)**). The increase in temperature from 77 to 300ºF causes a decrease in silica concentrations for all main acid treatments except for formic acid-HF main acid treatment. The decrease in Si concentration is almost 55% for the NaGLDA-HF and 60% for the HCl-HF main acid treatments. Dissolved Si concentration is the highest after HCl-HF main acid treatment with the concentration values of 7,695 and 2,970 mg/l at 77 and 300ºF, respectively. KOH is the least effective solution with the lowest dissolved Si concentration at 77 and 300ºF (595 and 295 mg/l).

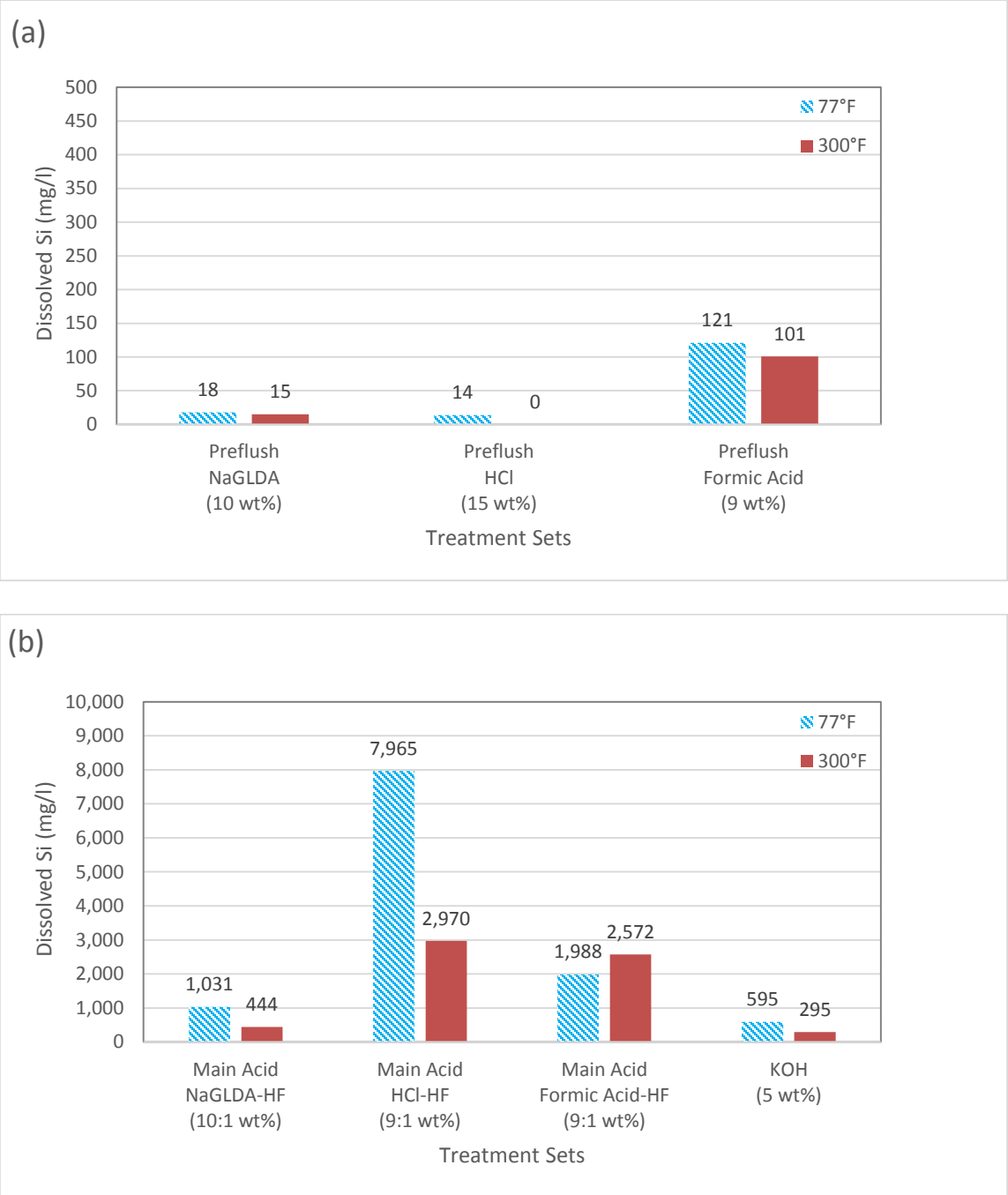


**Fig. 48—(a) Dissolved Si concentration after preflush treatments for Scale #1. (b) Dissolved Si concentration after after main treatments for Scale #1.**

The preflush stage is the most significant one in terms of dissolving considerable amounts of Ca for all treatment sets (**Fig. 49 (a))**. The increase in temperature from 77 to 300ºF causes an increase in Ca concentrations for all preflush stages. The increase in Ca concentration is almost 70% for the NaGLDA preflush, 20% for the HCl preflush, and 60% for the formic acid preflush. The preflush stages with HCl at 77 and 300ºF are the most successful treatments in terms of dissolving Ca at preflush stage. Dissolved Ca concentration is the highest after 15 wt% HCl preflush with the concentration values of 27,125 and 31,990 mg/l at 77 and 300ºF, respectively.

The dissolved Ca concentrations for the NaGLDA and HCl main acid treatments (**Fig. 49 (b)**) are not as high as the ones after the preflush stages. The low Ca concentration after main acid treatments is desired because the purpose of preflush is to dissolve as much as Ca before the main acid stage to prevent precipitations with HF. KOH solution does not dissolve Ca at any test temperature.

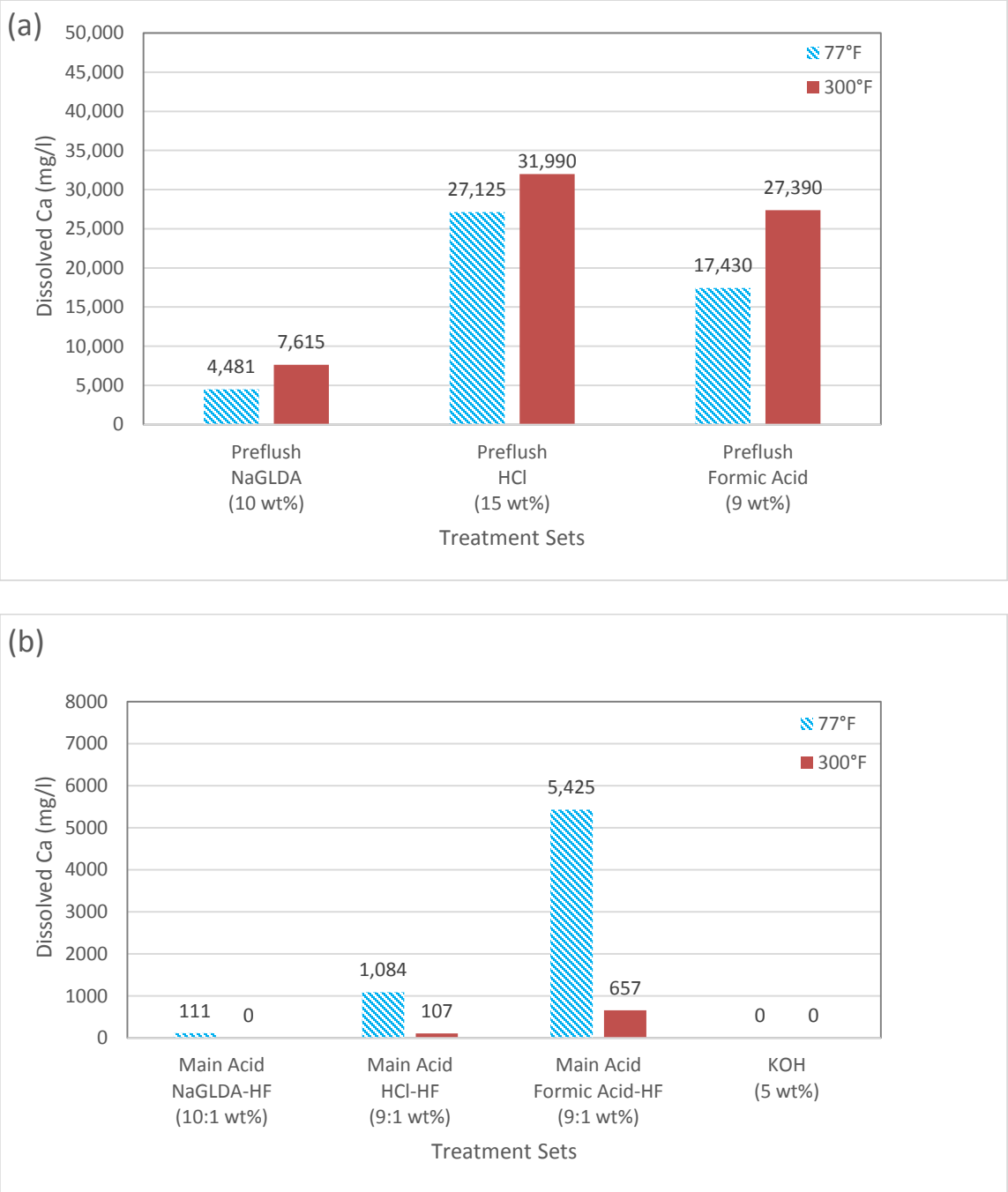


**Fig. 49—(a) Dissolved Ca concentration after preflush treatments for Scale #1. (b) Dissolved Ca concentration after main treatments for Scale #1.**

Dissolved Na concentration is the highest after the preflush and main acid treatment stages with NaGLDA (**Fig. 50 (a)** and **(b)**). These results can be explained by the Na content of NaGLDA itself; therefore, Na concentration obtained by ICP is misleading. Na concentrations in the filtrate solutions after the dissolution tests include Na coming from the scale and NaGLDA itself. Na concentration is almost 15,000 mg/l for 10 wt% NaGLDA solution and 12,000 mg/l for 10:1 wt% NaGLDA-HF solution. In the light of this information, it can be inferred from the results that dissolved Na concentration (almost 7,000 mg/l) is similar in the case of the NaGLDA and HCl preflush stages at room temperature.

Although the increase in temperature from 77 to 300ºF causes a decrease in Na concentrations for all treatment sets, formic acid-HF and KOH solutions are still able to dissolve Na at 300ºF. Increase in temperature results in negative Na concentration values (after subtraction of Na concentration which comes from NaGLDA solution itself) for preflush and main acid treatments with NaGLDA. Dissolved Na concentration is the highest after the HCl and formic acid preflush stages at 77 and 300ºF, respectively. Dissolved Na concentration is the highest after 9:1 wt% formic acid-HF main acid treatment with the concentration values of 6,860 and 1,817 mg/l at 77 and 300ºF, respectively.

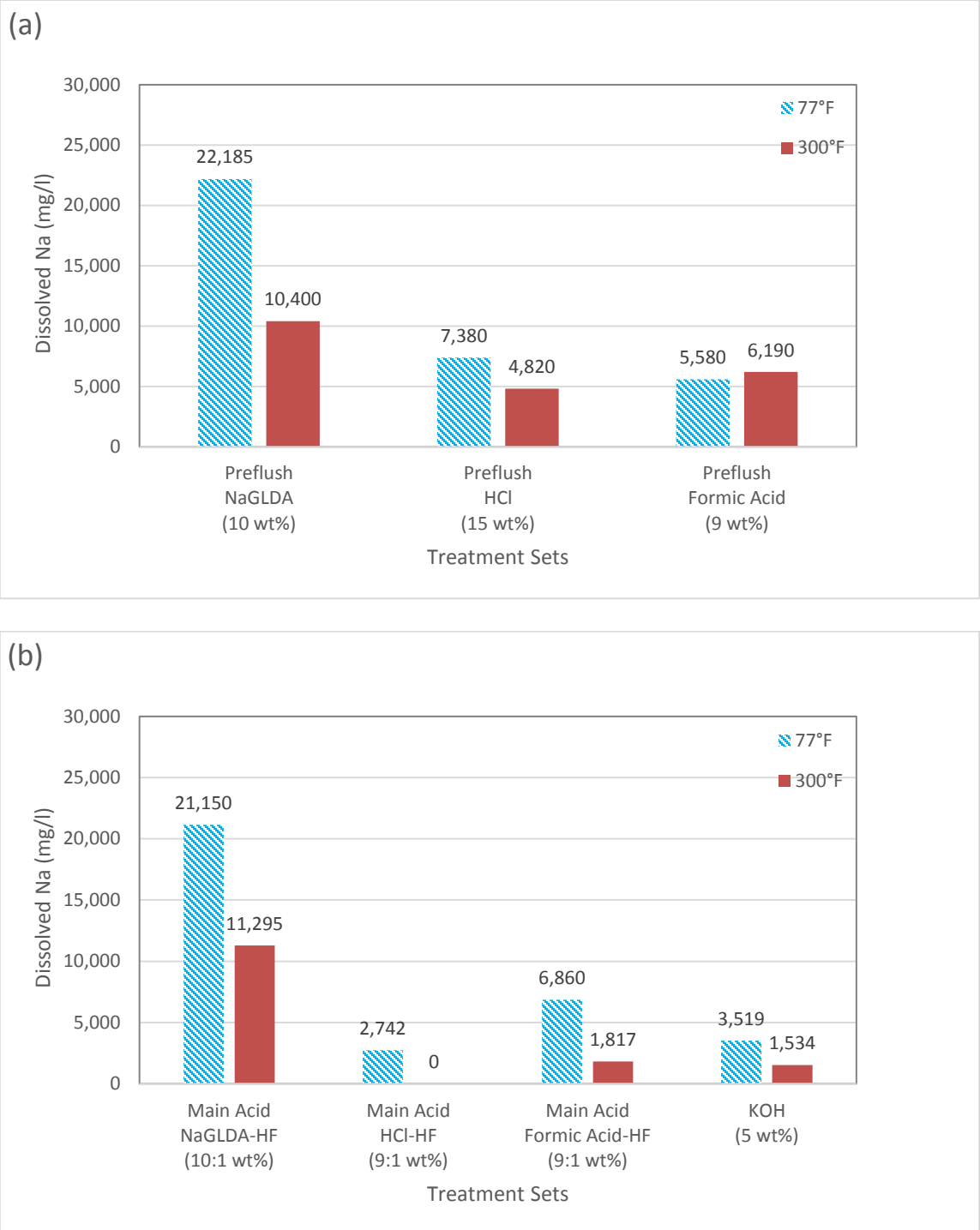


**Fig. 50—(a) Dissolved Na concentration after preflush treatments for Scale #1. (b) Dissolved Na concentration after main treatments for Scale #1.**

Dissolved Fe concentration is the highest after the preflush with 15 wt% HCl at 77 and 300ºF (**Fig. 51 (a)**).The preflush with 10 wt% NaGLDA is not capable of dissolving Fe at any test temperature. The increase in temperature from 77 to 300ºF causes increase in Fe concentrations for all preflush stages. The increase in Fe concentration is almost 170% for the HCl preflush. The 9 wt% formic acid solution starts dissolving Fe at high temperature (300°F).

The dissolved Fe concentrations for NaGLDA and HCl main acid treatments (**Fig. 51 (b)**) show a decreasing trend as the temperature increases to 300ºF. Although there is no dissolution of Fe after the formic acid preflush and the main acid treatment at room temperature, the formic acid preflush and formic acid-HF solution start dissolving Fe at 300°F. KOH solution does not dissolve Fe at any temperature (77 and 300ºF).

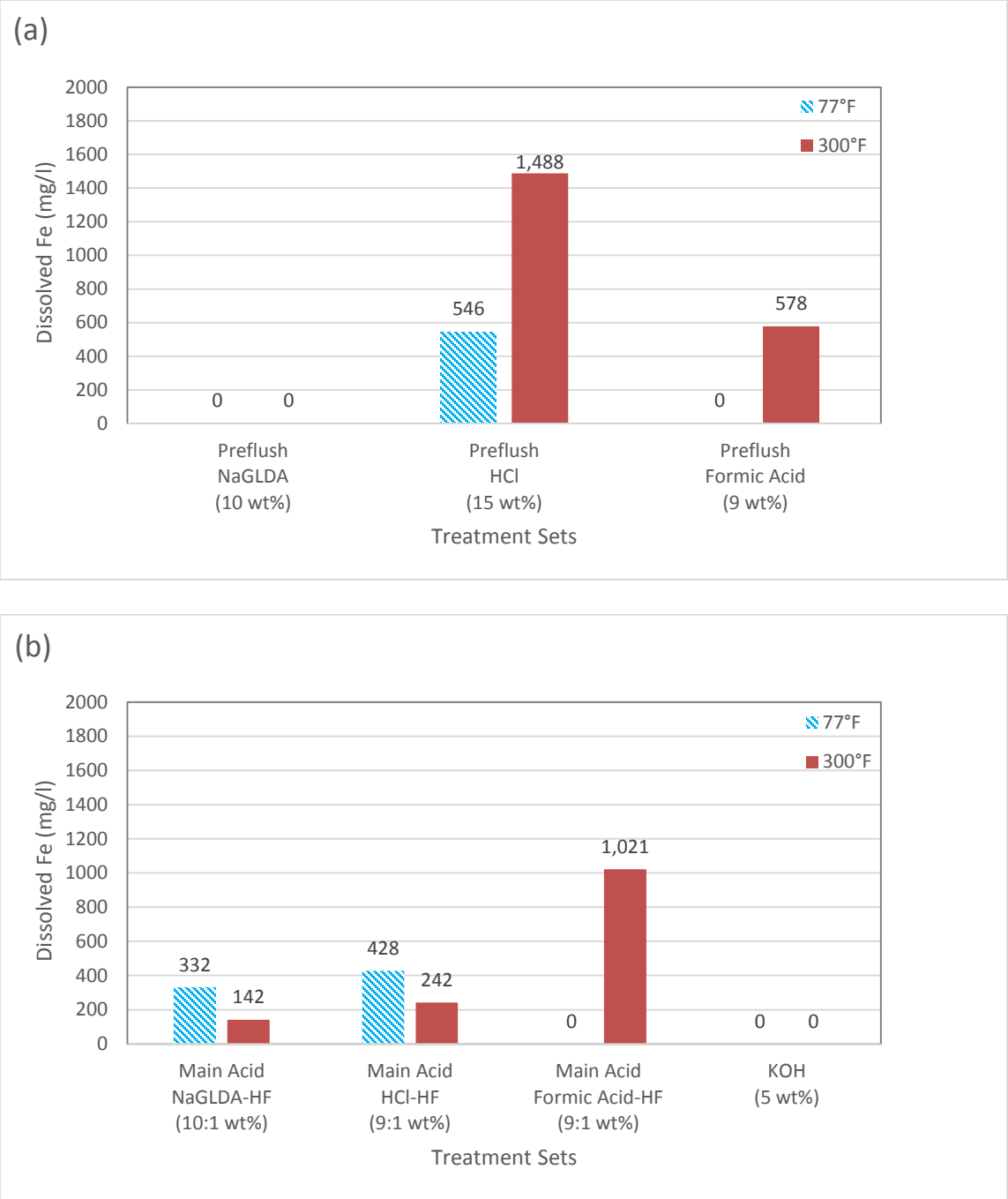


**Fig. 51—(a) Dissolved Fe concentration after preflush treatments for Scale #1. (b) Dissolved Fe concentration after main treatments for Scale #1.**

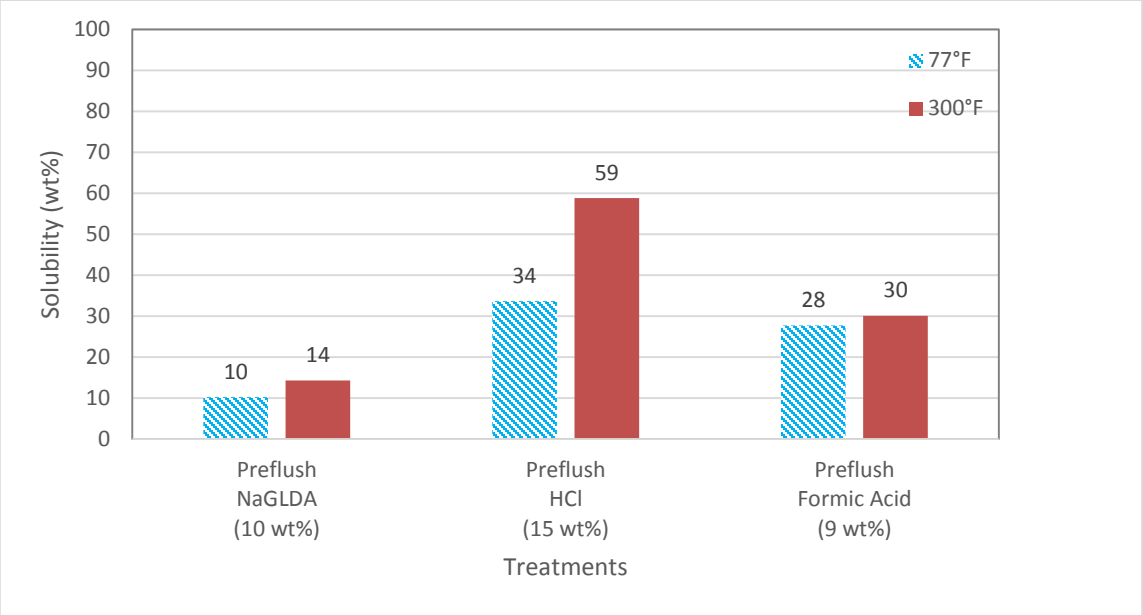


**Fig. 52—Solubility results for Scale #1 (preflush).**

Increase in temperature causes an increase in the solubility values for all the preflush stages (**Fig. 52**). The increase in solubility is almost 40% for the NaGLDA preflush, 75% for the HCl preflush, and 10% for the formic acid preflush. The HCl preflush results in the highest dissolution rates with the solubility values of 34 and 59 wt% at 77 and 300ºF, respectively. Increase in Ca concentrations (from 27,125 to 31,990 mg/l for the HCl preflush, from 4,481 to 7,615 mg/l for the NaGLDA preflush, and from 17,430 to 27,390 mg/l for the formic acid preflush) is consistent with increasing solubility values for the preflush stages.

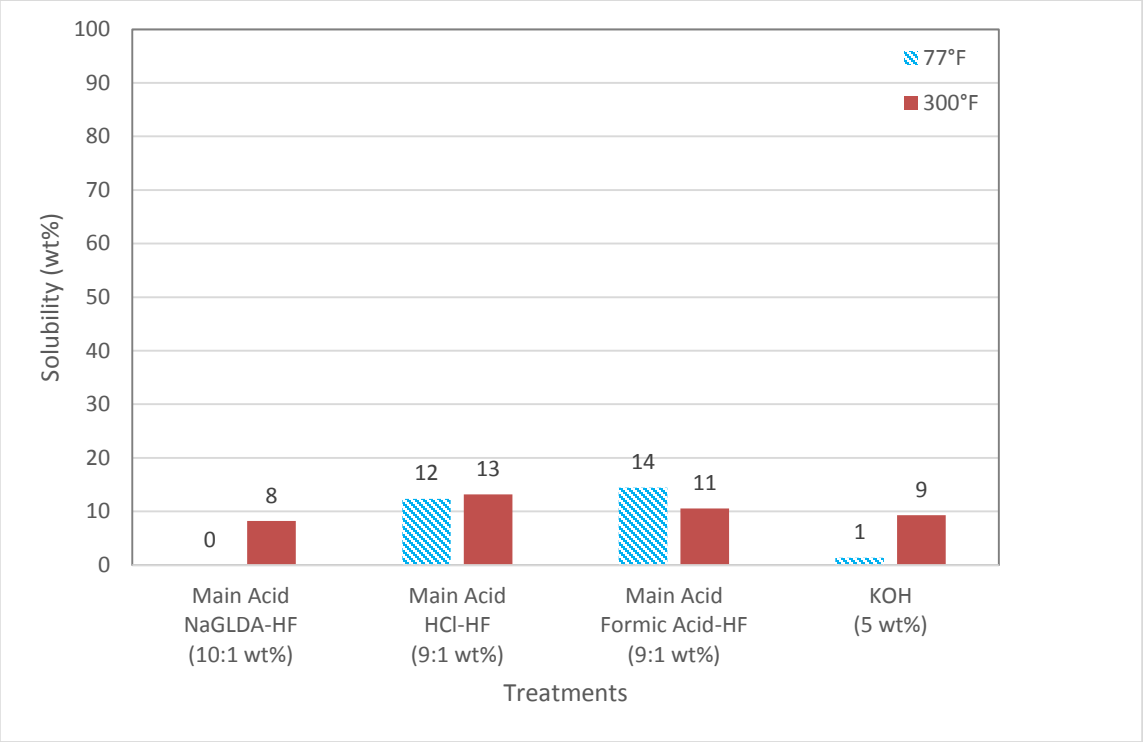


**Fig. 53—Solubility results for Scale #1 (main treatment).**

Increase in temperature shows an increase in solubility values for main acid treatments with NaGLDA-HF and HCl-HF solutions (**Fig. 53**). The increase in solubility is almost 10% with HCl-HF solution. When the temperature is increased to 300ºF, the solubility of Scale #1 decreases from 14 to 11 wt% after use of formic acid-HF solution. The HCl-HF main acid treatment results in the highest dissolution at 300ºF with the solubility value of 13 wt%. At room temperature, formic acid-HF solution is the most effective solution in terms of solubility value, which is 14 wt%. NaGLDA-HF solution does not dissolve Scale #1 at room temperature. Solubility of Scale #1 after the tests run with KOH solution increases from 1 wt% at 77ºF to 9 wt% at 300ºF.

### 3.1.2 Discussion for Scale #1

Scale #1 is mainly composed of the oxides of Na, Ca, Si, and Fe(III). The sample analyses before dissolution tests indicate that the minerals present in Scale #1 are pectolite, tremolite and anorthite which are the most common metal silicates in SAGD boilers.

As the main purpose of running a preflush stage is to reduce HF consumption by carbonates and to dissolve non-silica minerals to avoid the precipitation by HF in the main acid treatment, Si is dissolved slightly after all the preflush stages at any test temperature. Since HCl is the strongest acid among the tested solutions to be effective in the preflush stage, the highest dissolved Si concentration is obtained when the tests run with 9:1 wt% HCl-HF solution after 15wt% HCl preflush treatment compared to other treatment sets (10:1 wt% NaGLDA-HF treatment after 10 wt% NaGLDA and 9:1 wt% formic acid-HF solution after 9 wt% formic acid preflush). The main acid treatment stage is the most significant in terms of dissolving Si such that considerable amount of Si is dissolved at this stage for all treatment sets. Because HF and HF-based solutions decrease Si-O bond strength that results in higher dissolution rates (Ning et al. 2010).

The increase in temperature causes decrease in Si and Na concentrations for all treatment sets, while the dissolution of Fe and Ca is enhanced especially at preflush stages. This trend in Ca concentration is consistent with high solubility values of the HCl preflush. The high concentration of Ca after the formic acid-HF main acid treatment is an indication of high consumption of HF by Ca which might prevent to dissolve more Si concentrations and result in deposition of Si. Formic acid concentration in preflush stage might be increased to dissolve more Ca at preflush to avoid high consumption of HF by Ca which

results in calcium fluoride ($CaF_2$) (see Eq. 3.1) precipitation (Smith and Hendrickson 1965; Crowe 1986).

$$CaCO_3 + 2HF \rightarrow CaF_2\downarrow + H_2O + CO_2 \quad . \quad \ldots\ldots\ldots\ldots\ldots\ldots\ldots\ldots \quad (3.1)$$

Decrease in Si concentration with increasing temperature (from 77 to 300ºF) for all main acid treatments might be explained by secondary reactions of fluosilicic acid and silicon hexafluoride ($H_2SiF_6$ and $SiF_6$) (Ying-Hsiao and Fambrough 1998), which is reaction product of primary reactions (see Eq. 3.2).

$$SiO_2 + 6HF \rightarrow H_2SiF_6 + 2H_2O \quad . \quad \ldots\ldots\ldots\ldots\ldots\ldots\ldots\ldots\ldots \quad (3.2)$$

Secondary reactions of $SiF_6$ with $Na^+$ and $Ca^+$ causes precipitations of fluosilicates, such as calcium fluosilicate ($CaSiF_6$) and sodium fluosilicate ($Na_2SiF_6$) at temperatures above 125 ºF (Ying-Hsiao and Fambrough 1998) (see Eq. 3.3 and 3.4).

$$SiF_6^{2-} + 2Na^+ \rightarrow Na_2SiF_6\downarrow \quad . \quad \ldots\ldots\ldots\ldots\ldots\ldots\ldots\ldots \quad (3.3)$$

$$SiF_6^{2-} + Ca^+ \rightarrow CaSiF_6\downarrow \quad . \quad \ldots\ldots\ldots\ldots\ldots\ldots\ldots\ldots\ldots \quad (3.4)$$

$$H_2SiF_6 + 2Na^+ \rightarrow Na_2SiF_6\downarrow + 2H_2O \quad . \quad \ldots\ldots\ldots\ldots\ldots\ldots\ldots\ldots \quad (3.5)$$

Low solubility and dissolved ion concentrations indicate that KOH, as a strong alkali medium, is not effective to dissolve Scale #1.

The use of mud acid with HCl (9:1 wt% HCl-HF) after the preflush with strong acid solution (15 wt% HCl) at 77 and 300ºF seems to be the best solution to dissolve Scale #1 effectively in terms of solubility and total dissolved ion concentrations.

Increasing the concentration of HCl in the preflush stage, which is expected to dissolve most of Ca and Na in the scale, might be helpful to dissolve more Si in main acid treatment with mud acid at 77ºF by preventing possible $CaF_2$ precipitation in primary reactions.

## 3.2 Scale #2

### 3.2.1 Results for Scale #2

Dissolution tests for Scale #2 consist of four different treatment sets: HCl preflush followed by HCl-HF main acid, NaGLDA preflush followed by NaGLDA-HF main acid, formic acid preflush followed by formic acid -HF main acid, and KOH solution. These tests were performed dynamically at 77 and 300°F for three hours.

All the preflush stages (with NaGLDA, HCl, and formic acid) dissolves Si slightly which is expected, as the purpose of preflush stages are to dissolve Ca, Na, and Mg not Si (**Fig. 54 (a)**). The main acid treatment is the most significant stage in terms of dissolving considerable amounts of Si for all treatment sets (**Fig. 54 (b)**).

The increase in temperature from 77 to 300ºF causes a decrease in silica concentrations for all main acid treatments. The decrease in Si concentration is almost 55% for NaGLDA-HF, 15% for HCl-HF, 30% formic acid-HF, and 70% KOH main acid treatments. Dissolved Si concentration is the highest after the HCl-HF main acid treatment with the concentration values of 4,130 and 3,498 mg/l at 77 and 300ºF, respectively. 5 wt% KOH is the least effective solution with the lowest dissolved Si concentration at 77 and 300ºF (588 and 167 mg/l).

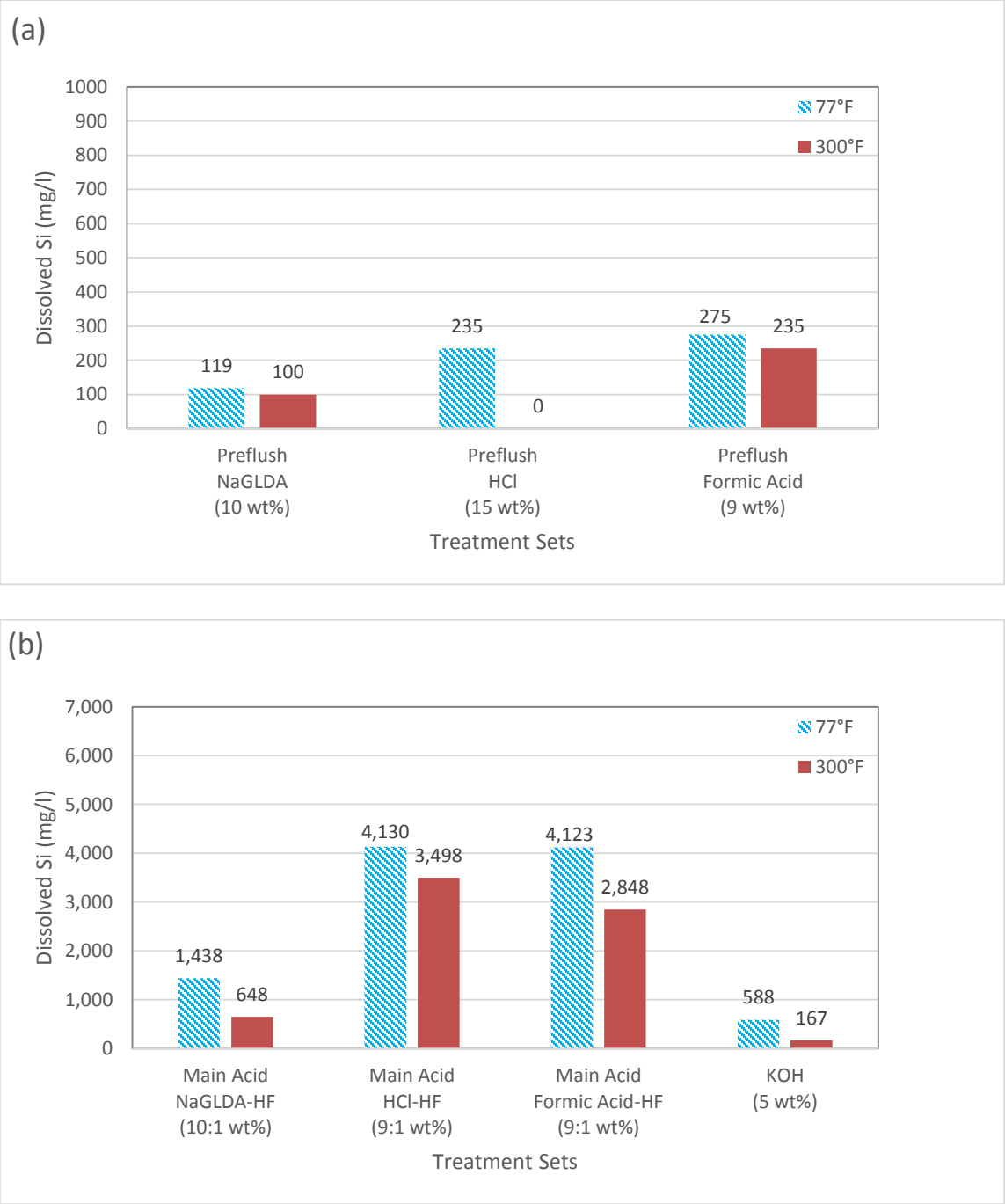


**Fig. 54—(a) Dissolved Si concentration after preflush treatments for Scale #2. (b) Dissolved Si concentration after main treatments for Scale #2.**

The preflush stage is the most significant in terms of dissolving considerable amounts of Ca for all treatment sets (**Fig. 55 (a)**). The increase in temperature from 77 to 300ºF causes an increase in Ca concentrations for all preflush stages except for the HCl preflush. The increase in Ca concentration is almost 340% for the NaGLDA preflush and 135% for the formic acid preflush. The preflush stages with HCl at 77 and formic acid at 300ºF are the most successful treatments in terms of dissolving Ca concentrations (11,445 and 10,625 mg/l, respectively) at preflush stage.

The dissolved Ca concentrations after main acid treatments (**Fig. 55 (b)**) are almost same for all solutions (NaGLDA-HF, HCl-HF, and formic acid-HF) with a concentration of almost 1,250 mg/l. Low Ca concentration after the preflush is desired, because the purpose of the preflush is to dissolve as much as Ca before the main acid stage to prevent precipitations with HF. It seems that the preflush stages are not effective to dissolve most of Ca which consumes more HF in the main acid treatment. It can be withdrawn that the concentrations of preflush solution should be increased to facilitate main acid treatment stages. KOH solution does not dissolve Ca at any test temperature.

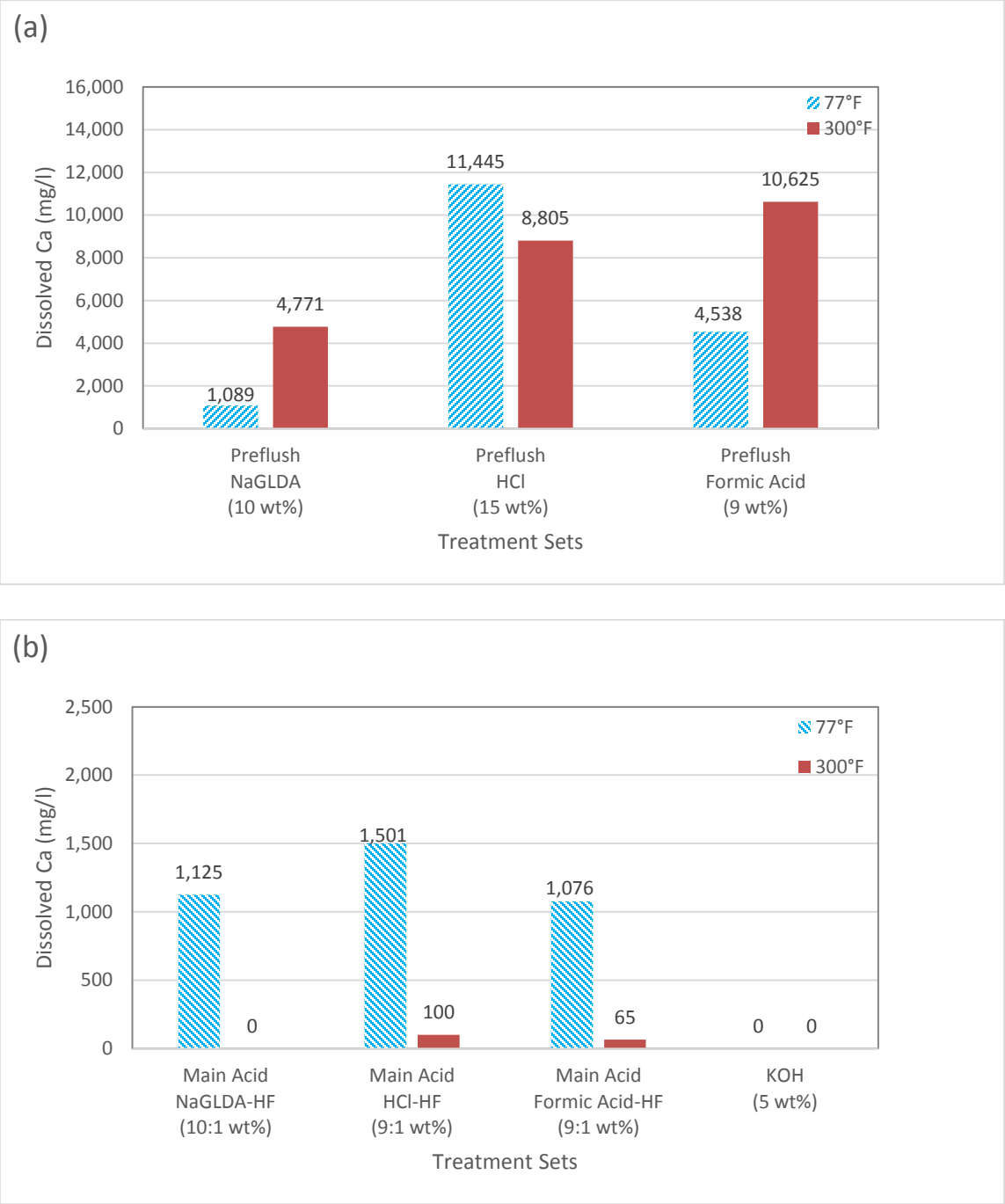


**Fig. 55— (a) Dissolved Ca concentration after preflush treatments for Scale #2. (b) Dissolved Ca concentration after main treatments for Scale #2.**

Dissolved Na concentration is the highest after the preflush and main acid treatment stages with NaGLDA (**Fig. 56 (a)** and **(b)**). These results can be explained by the Na content of NaGLDA itself; therefore, Na concentration obtained by ICP is misleading. Na concentrations in the filtrate solutions after the dissolution tests include Na coming from the scale and NaGLDA itself. Na concentration is almost 15,000 mg/l for 10 wt% NaGLDA solution and 12,000 mg/l for 10:1 wt% NaGLDA-HF solution. In the light of this information, it can be inferred from the results that dissolved Na concentration at room temperature (almost 8,000 mg/l) is still the highest in the case of NaGLDA preflush.

Although the increase in temperature from 77 to 300ºF causes a decrease in Na concentrations for all treatment sets, HCl-HF, formic acid-HF and KOH solutions are still able to dissolve Na at 300ºF. Increase in temperature results in negative Na concentration values (after subtraction of Na concentration which comes from NaGLDA solution itself) for preflush and main acid treatments with NaGLDA which is an indication of Na precipitation. Dissolved Na concentrations after main acid treatments are close to each other. Formic acid-HF solution at 300ºF is the most effective main treatment in terms of dissolving Na (1,805 mg/l).

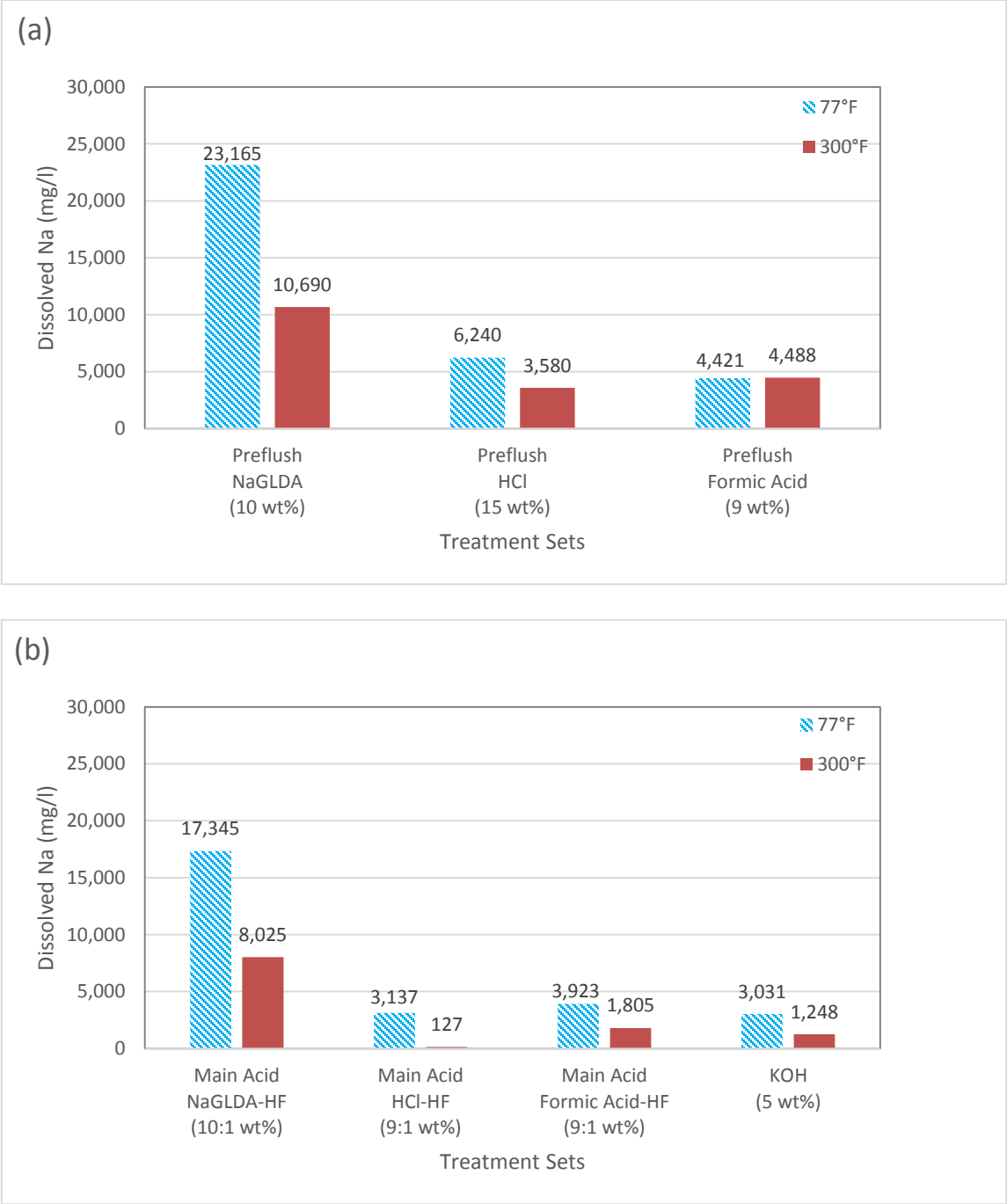


**Fig. 56—(a) Dissolved Na concentration after preflush treatments for Scale #2. (b) Dissolved Na concentration after main treatments for Scale #2.**

The preflush stage is supposed to dissolve most of Mg in Scale #2. The increase in temperature from 77 to 300ºF causes increase in Mg concentrations for all preflush stages (**Fig. 57 (a)**). The increase in Mg concentration is almost 185% for HCl preflush. The NaGLDA preflush, which is not capable of dissolving Mg at room temperature, starts dissolving Mg at 300°F. The preflush stages with HCl at 77 and formic acid at 300ºF are the most successful treatments in terms of dissolving Mg (633 and 1,803 mg/l, respectively) at preflush stage.

The dissolved Mg concentrations after main acid treatments (**Fig. 57 (b)**) show decreasing trend by increasing temperature. KOH solution does not dissolve Mg at any test temperature. Low Mg concentration after preflush is desired, because the purpose of preflush is to dissolve as much as Mg before main acid stage to prevent precipitations with HF. It seems that the preflush stages are not effective to dissolve most of Mg which consumes more HF in the main acid treatment. It can be withdrawn that the concentrations of preflush solution should be increased to facilitate main acid treatment stages.

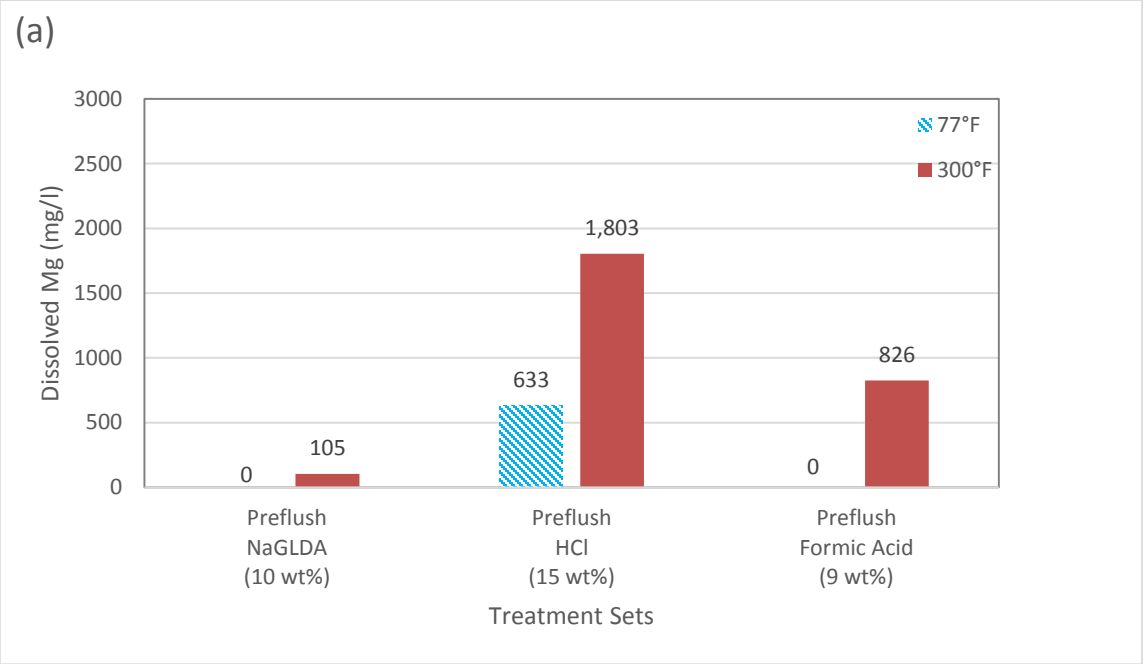


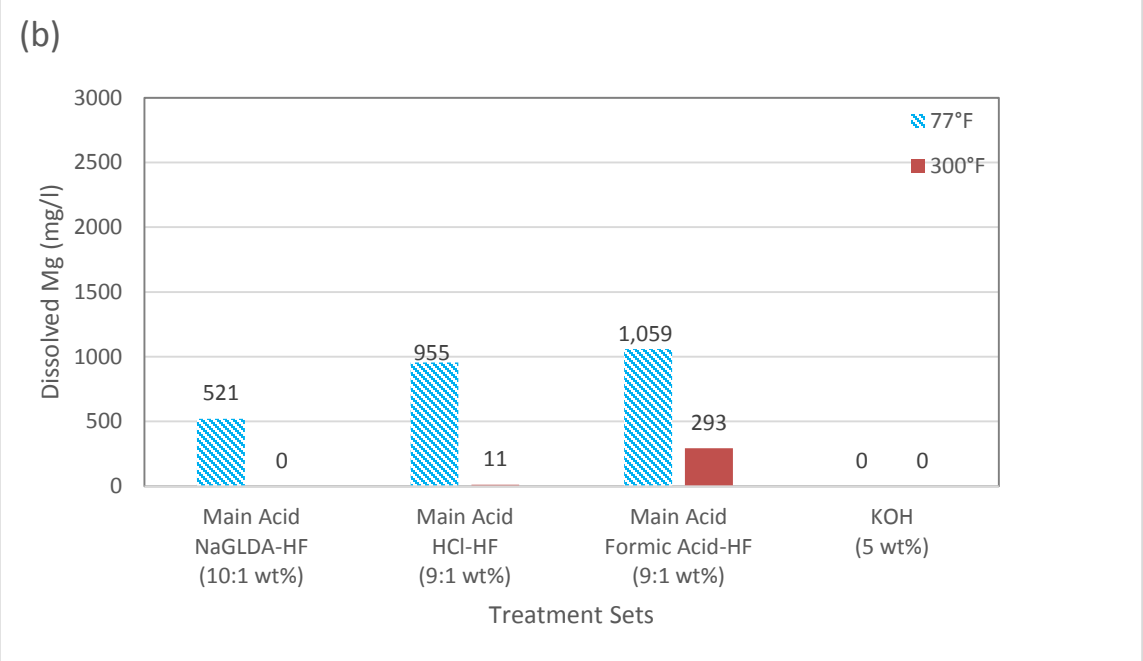


**Fig. 57—(a) Dissolved Mg concentration after preflush treatments for Scale #2. (b) Dissolved Mg concentration after main treatments for Scale #2.**

Dissolved Fe concentration is the highest after the preflush with 15 wt% HCl at 77 and 300ºF (**Fig. 58 (a)**). The increase in temperature from 77 to 300ºF causes increase in Fe concentrations for all preflush stages. The increase in Fe concentration is almost 300% for HCl preflush (1,794 mg/l at 300ºF). The NaGLDA and formic acid preflush, which are not capable of dissolving Fe at room temperature, start dissolving Fe at 300°F. The dissolved Fe concentrations after main acid treatments (**Fig. 58 (b)**) show an increasing trend as the temperature increases to 300ºF. KOH solution does not dissolve Fe at any test temperature (77 and 300ºF). The highest dissolved Fe concentrations are obtained after the main treatment with formic acid-HF solution at 77 and 300ºF (575 and 1,595 mg/l, respectively).

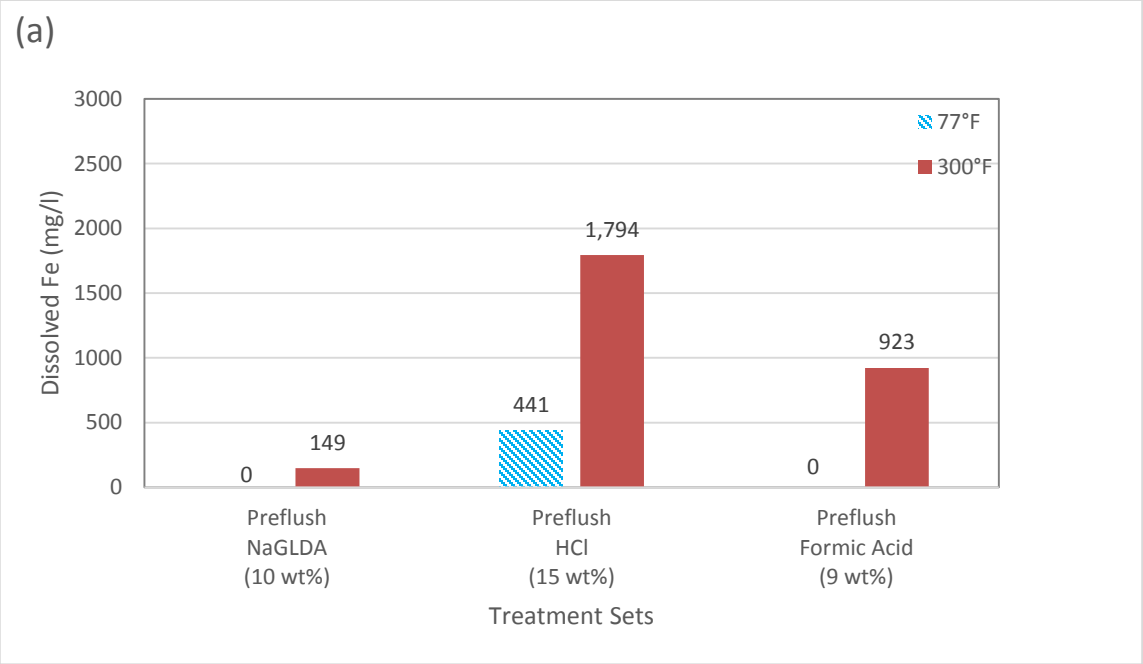


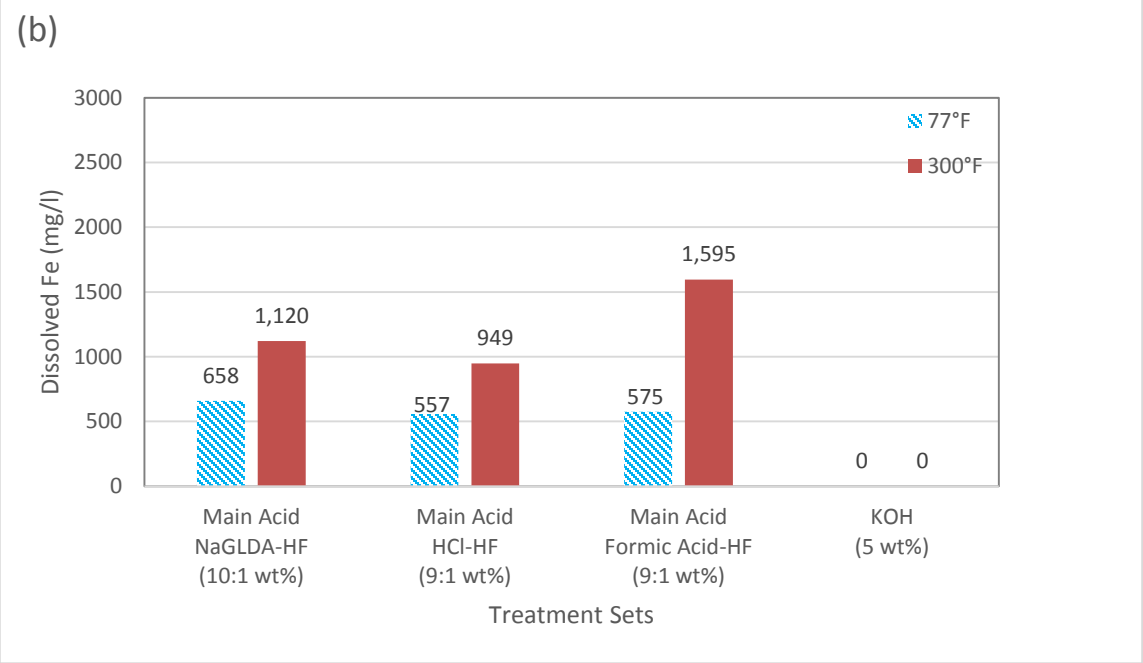


**Fig. 58—(a) Dissolved Fe concentration after preflush treatments for Scale #2. (b) Dissolved Fe concentration after main treatments for Scale #2.**

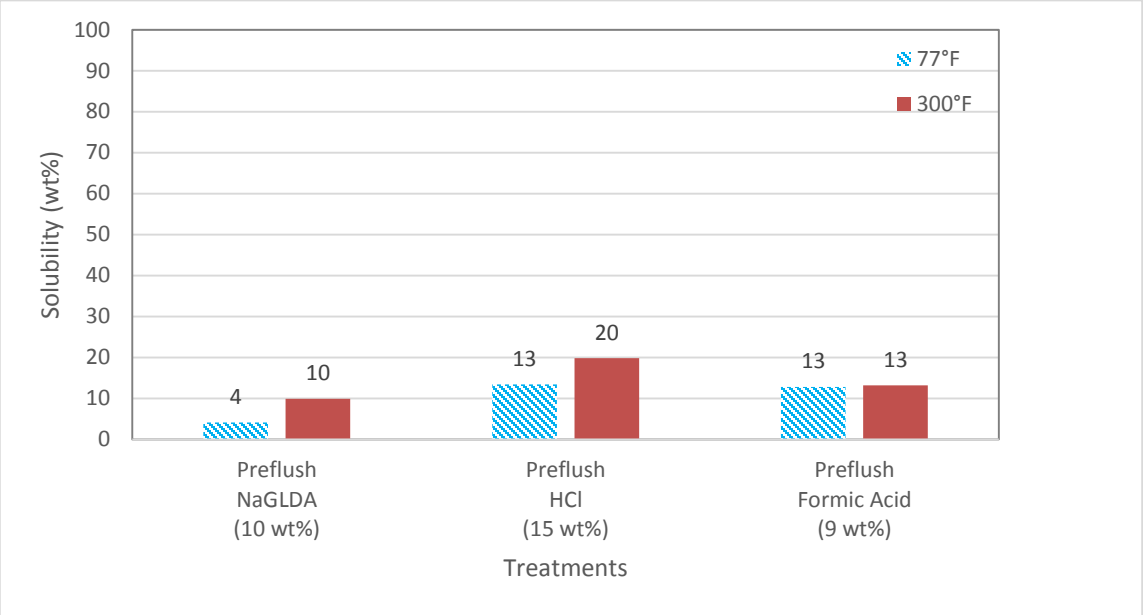


**Fig. 59—Solubility results for Scale #2 (preflush).**

Increase in temperature causes an increase in the solubility values for the preflush stages with NaGLDA and HCl (**Fig. 59**). The increase in solubility is almost 150% for the NaGLDA preflush and 55% for the HCl preflush. Shift in temperature does not affect the solubility value for the preflush stage run with formic acid (13 wt%). The HCl preflush results in the highest dissolution rates at 77 and 300ºF with the solubility values of 13 and 20 wt%, respectively.

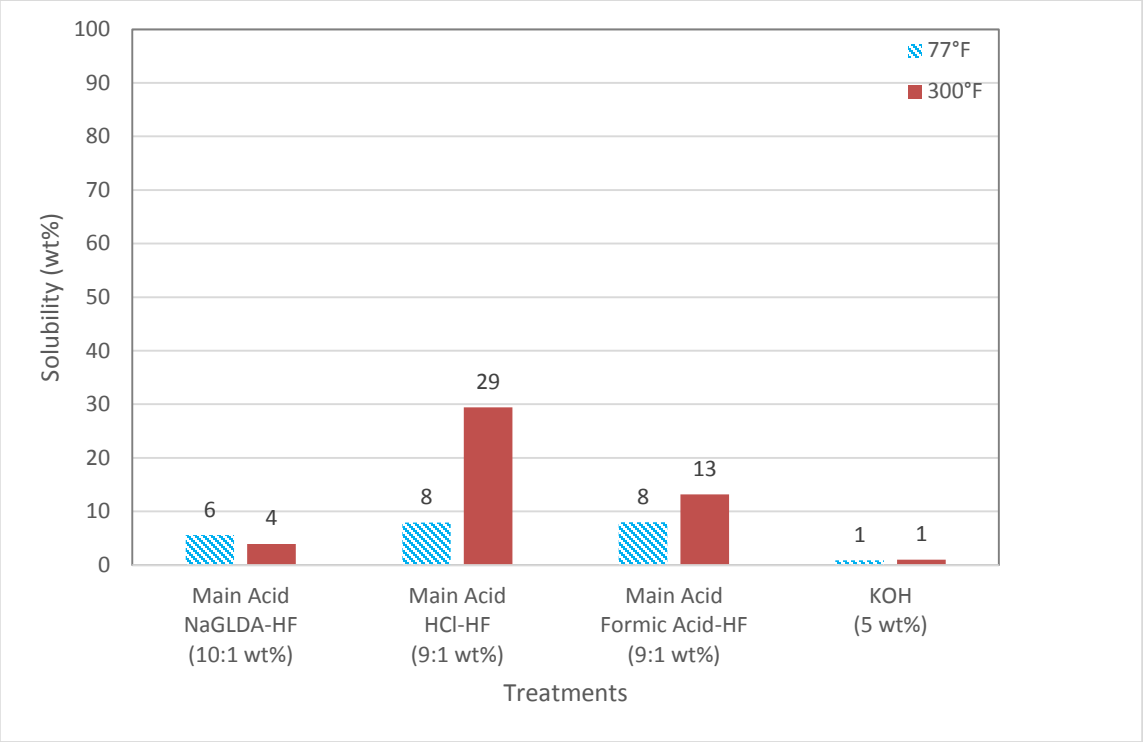


**Fig. 60—Solubility results for Scale #2 (main treatment).**

Increase in temperature shows an increase in solubility values for the main acid treatments with HCl-HF and formic acid-HF solutions (**Fig. 60**). The increase in solubility is almost 260% with HCl-HF solution and 60% with formic acid-HF solution. When the temperature is increased to 300ºF, the solubility of Scale #2 decreases from 6 to 4 wt% after use of NaGLDA-HF solution. At room temperature, formic acid-HF and HCl-HF solutions are the most effective solutions in terms of solubility value, which is 8 wt%. The HCl-HF main acid treatment results in the highest dissolution at 300ºF with the solubility value of 29 wt%. Solubility value for the tests run with KOH solution (1 wt% at 77ºF) does not show any change with increasing temperature.

### 3.2.2 Discussion for Scale #2

Scale #2 is mainly composed of the oxides of Si, Mg, Na, Fe (III), and Ca. The sample analyses before dissolution tests indicate that the minerals present in Scale #2 are pectolite, tremolite, fayalite, and anorthite which are the most common metal silicates in SAGD boilers.

The main acid treatment stage is the most significant stage in terms of dissolving Si such that considerable amount of Si is dissolved at this stage for all treatment sets. Because HF and HF-based solutions decrease Si-O bond strength that results in higher dissolution rates (Ning et al. 2010). The increase in temperature causes decrease in Si and Na concentrations for all treatment sets, while the dissolution of Fe and Mg is enhanced. The decrease in Si concentration is due to the precipitation of Si during the secondary reactions of fluosilicic acid ($H_2SiF_6$). Although Ca concentration decreases by temperature for the treatment sets with HCl and formic acid, the total dissolved Ca concentrations are still higher than the one after the treatment with NaGLDA. Increasing trend in Fe and Mg concentrations by increasing temperature is consistent with increasing solubility values of preflush stages for all treatment types.

KOH, as a strong alkali medium, is not effective to dissolve Scale #2 due to the low solubility and dissolved ion concentrations.

The use of mud acid (9:1 wt% HCl-HF) after preflush with strong acid solution (15 wt% HCl) especially at 300ºF seems to be the best solution to dissolve Scale #2 effectively in terms of solubility and total dissolved ion concentrations. Increasing the concentration of HCl in preflush stage, which is expected to dissolve more Ca, Na, and Mg in the scale, might be helpful to dissolve more Si in main acid treatment with mud acid at 77ºF by preventing possible precipitation of calcium fluoride ($CaF_2$), and magnesium fluoride ($MgF_2$) during the primary reactions (Eq. 3.1) and sodium fluosilicate ($Na_2SiF_6$). Treatment sets with both HCl and formic acid might be effective at room temperature based on their similar solubility values and dissolved ion concentrations.

## 3.3 Scale #3

### 3.3.1 Results for Scale #3

Dissolution tests for Scale #3 consist of four different treatment sets: HCl preflush followed by HCl-HF main acid, NaGLDA preflush followed by NaGLDA-HF main acid, formic acid preflush followed by formic acid-HF main acid, and KOH solution. These tests were performed dynamically at 77 and 300°F for three hours.

All the preflush stages (NaGLDA, HCl, and formic acid) dissolves Si slightly which is expected, as the purpose of preflush stages are to dissolve Ca, Na and Mg not Si (**Fig. 61 (a)**). The main acid treatment stage is the most significant stage in terms of dissolving considerable amounts of Si for all treatment sets (**Fig. 61 (b)**).

The increase in temperature from 77 to 300ºF causes a decrease in silica concentrations for all main acid treatments. The decrease in Si concentration is almost 80% for NaGLDA-HF, 45% for HCl-HF, 60% for formic acid-HF and 95% KOH main acid treatments. Dissolved Si concentration is the highest after the HCl-HF main acid treatment with the concentration values of 6,085 and 3,316 mg/l at 77 and 300ºF, respectively. KOH is the least effective solution with the lowest dissolved Si concentration at 77 and 300ºF (498 and 24 mg/l).

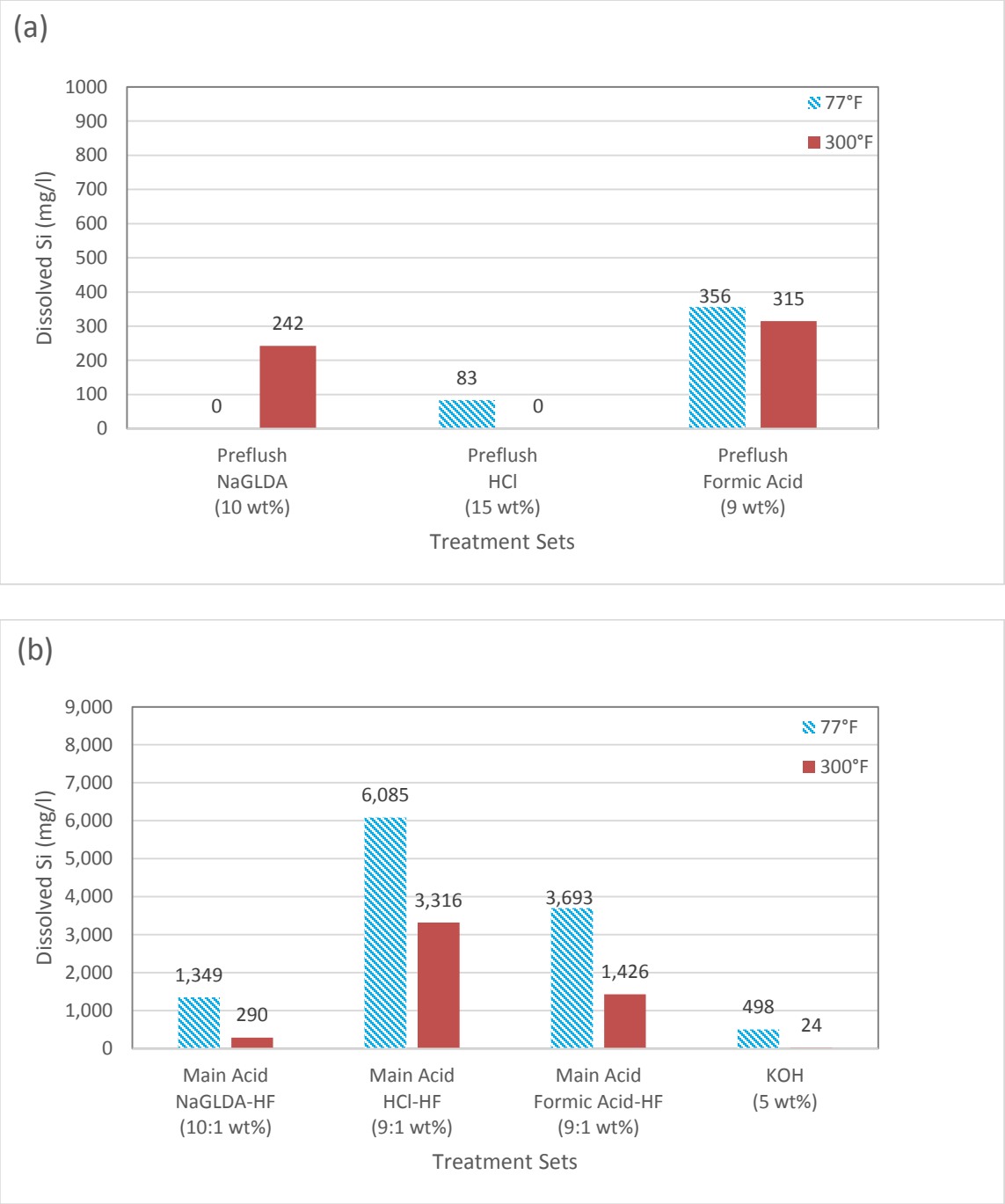


**Fig. 61—(a) Dissolved Si concentration after preflush treatments for Scale #3. (b) Dissolved Si concentration after main treatments for Scale #3.**

The preflush stage is the most significant stage in terms of dissolving considerable amounts of Ca for all treatment sets (**Fig. 62 (a)**). The increase in temperature from 77 to 300ºF causes increase in Ca concentrations for all preflush stages except for the HCl preflush. The increase in Ca concentration is almost 85% for the NaGLDA preflush and 40% for the formic acid preflush. The preflush stage with HCl at 77 is the most successful treatment in terms of dissolving Ca (2,120 mg/l) at preflush stage. The HCl and formic acid preflush stages dissolve almost same amount of Ca (1,000 mg/l) at 300 ºF.

KOH and NaGLDA-HF solutions are not able to dissolve Ca at any test temperature. Dissolved Ca concentrations are low after main acid treatments (**Fig. 62 (b)**) compared to the ones after preflush stages that might be an indication of low consumption of HF by Ca.

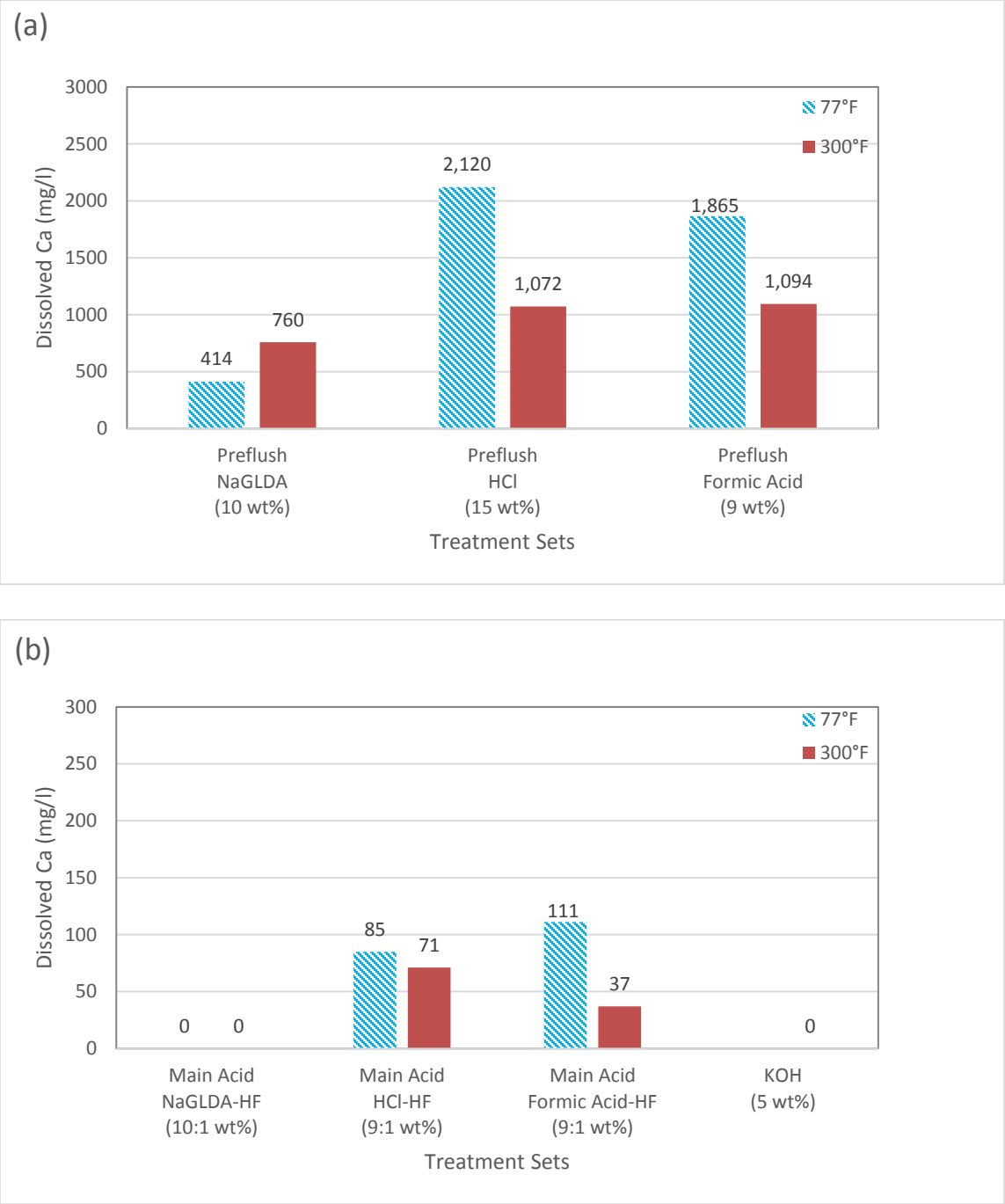


**Fig. 62—(a) Dissolved Ca concentration after preflush treatments for Scale #3. (b) Dissolved Ca concentration after main treatments for Scale #3.**

Dissolved Na concentration is the highest after the preflush and main acid treatment stages with NaGLDA (**Fig. 63 (a)** and **(b)**). These results can be explained by the Na content of NaGLDA itself; therefore, Na concentration obtained by ICP is misleading. Na concentrations in the filtrate solutions after the dissolution tests include Na coming from the scale and NaGLDA itself. Na concentration is almost 15,000 mg/l for 10 wt% NaGLDA solution and 12,000 mg/l for 10:1 wt% NaGLDA-HF solution. In the light of this information, it can be inferred from the results that dissolved Na concentration at room temperature (almost 6,500 mg/l) is still the highest in the case of NaGLDA preflush.

Although the increase in temperature from 77 to 300ºF causes decrease in Na concentrations for all treatment sets, formic acid-HF and KOH solutions are still able to dissolve Na at 300ºF. Increase in temperature results in negative Na concentration values (after subtraction of Na concentration which comes from NaGLDA solution itself) for preflush and main acid treatments with NaGLDA which is an indication of Na precipitation. The dissolved Na concentrations at 300ºF after the main acid treatments with formic acid-HF and KOH solutions are low, while HCl-HF is not able dissolve Na at 300ºF.

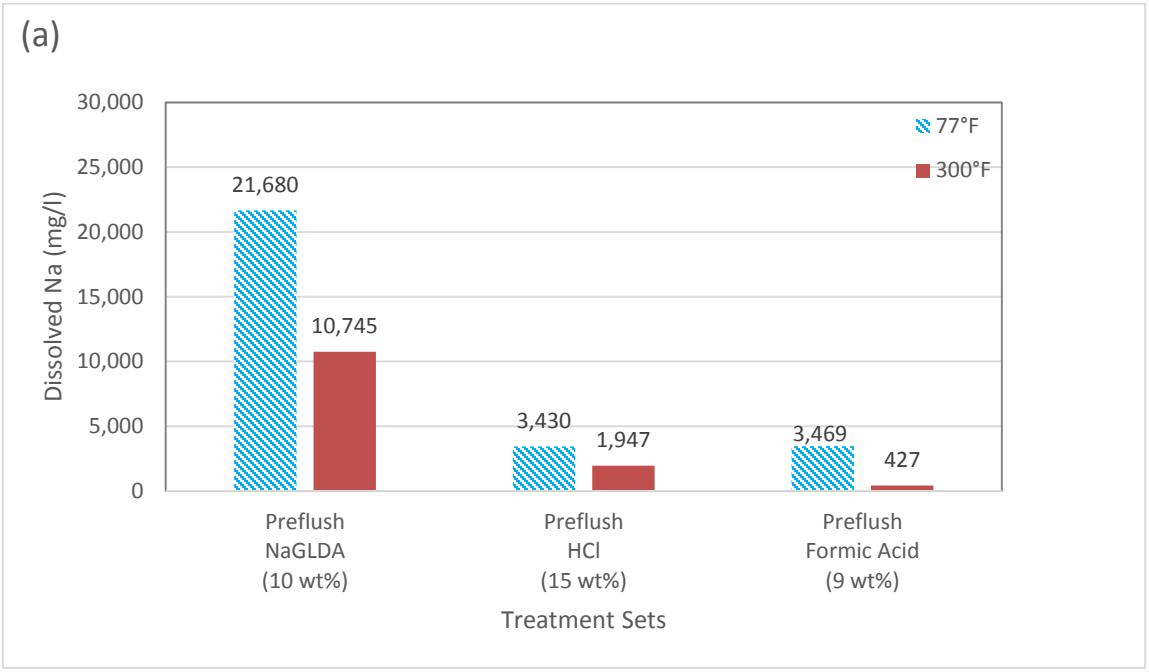


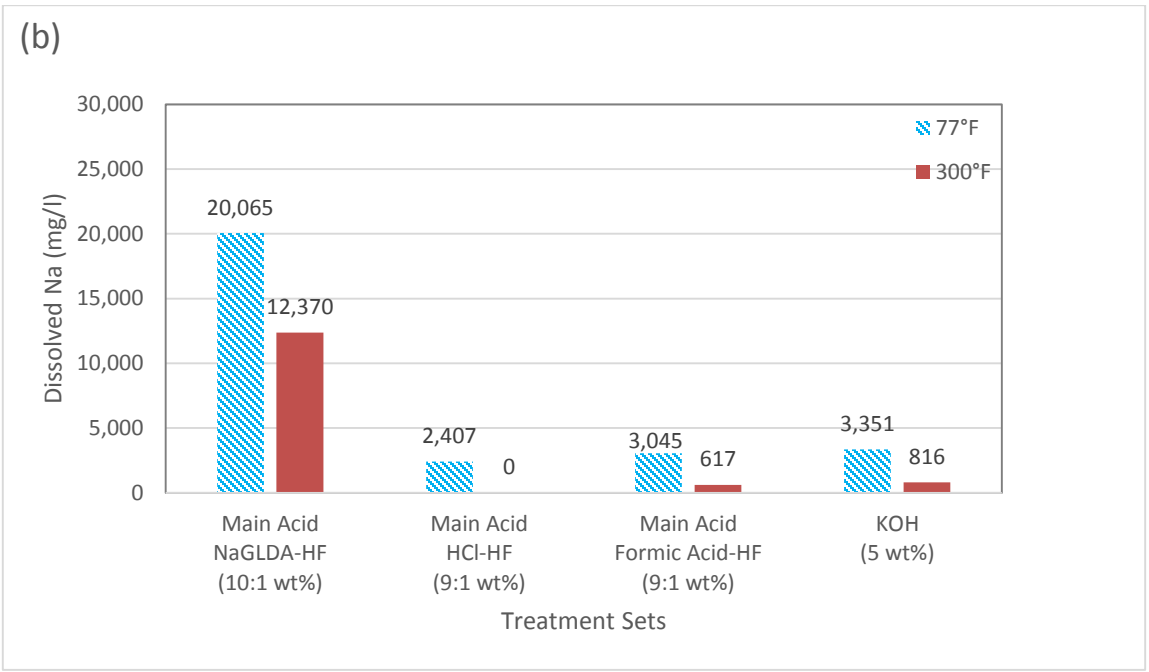


**Fig. 63—(a) Dissolved Na concentration after preflush treatments for Scale #3. (b) Dissolved Na concentration after main treatments for Scale #3.**

The preflush stage is supposed to dissolve most of Mg in Scale #3. The increase in temperature from 77 to 300ºF causes increase in Mg concentrations for all preflush stages except for HCl preflush (**Fig. 64 (a)**). The increase in Mg concentration is almost 235% for formic acid preflush by increasing temperature. The NaGLDA preflush, which is not capable of dissolving Mg at room temperature, starts dissolving Mg at 300°F. The preflush stages with HCl at 77 and 300ºF are the most successful treatments in terms of dissolving Mg (24,345 and 20,860 mg/l, respectively) at preflush stage.

The dissolved Mg concentrations after main acid treatments (**Fig. 64 (b)**) show decreasing trend by increasing temperature for all treatments except for formic acid-HF treatment. KOH solution becomes ineffective in terms of dissolving Mg when the temperature is increased to 300ºF. Low Mg concentration after preflush is desired, because the purpose of preflush is to dissolve as much as Mg before main acid stage to prevent precipitations with HF. As the preflush stage with NaGLDA does not dissolve Mg, dissolved Mg concentration is higher after NaGLDA-HF treatment. It can be withdrawn that the concentration of NaGLDA preflush solution should be increased to facilitate main acid treatment stage. The dissolved Mg concentrations after HCl-HF, formic acid-HF and KOH solution at room temperature are pretty much low when compared to the concentration after NaGLDA-HF treatment. Formic acid-HF treatment dissolves the highest Mg concentration at 300ºF. High dissolution of Mg at the main treatment stage is not preferable, as it might prevent further dissolution of Si.

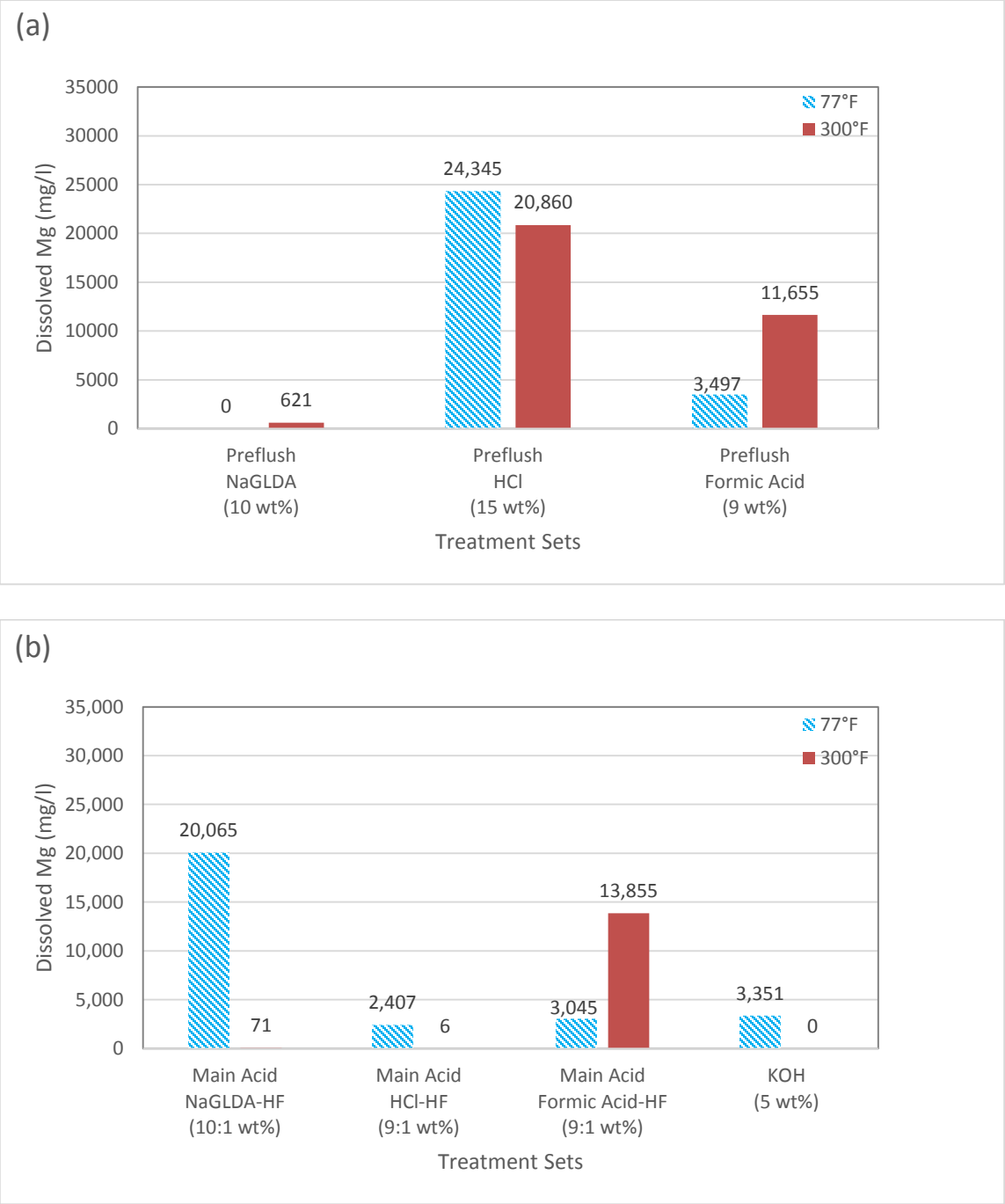


**Fig. 64—(a) Dissolved Mg concentration after preflush treatments for Scale #3. (b) Dissolved Mg concentration after main treatments for Scale #3.**

Dissolved Fe concentration is the highest after the preflush with 15 wt% HCl at 77 and 300ºF (**Fig. 65 (a)**). The increase in temperature from 77 to 300ºF causes increase in Fe concentrations for all preflush stages except for formic acid preflush. The increase in Fe concentration is almost 40% for 15 wt% HCl preflush (1,794 mg/l at 300ºF).

The dissolved Fe concentrations after main acid treatments (**Fig. 65 (b)**) show a decreasing trend as the temperature increases to 300ºF. KOH solution does not dissolve Fe at any test temperature (77 and 300ºF). The highest dissolved Fe concentrations are obtained after the main treatment with NaGLDA-HF solution at 77 and 300ºF (14,380 and 9,780 mg/l, respectively).

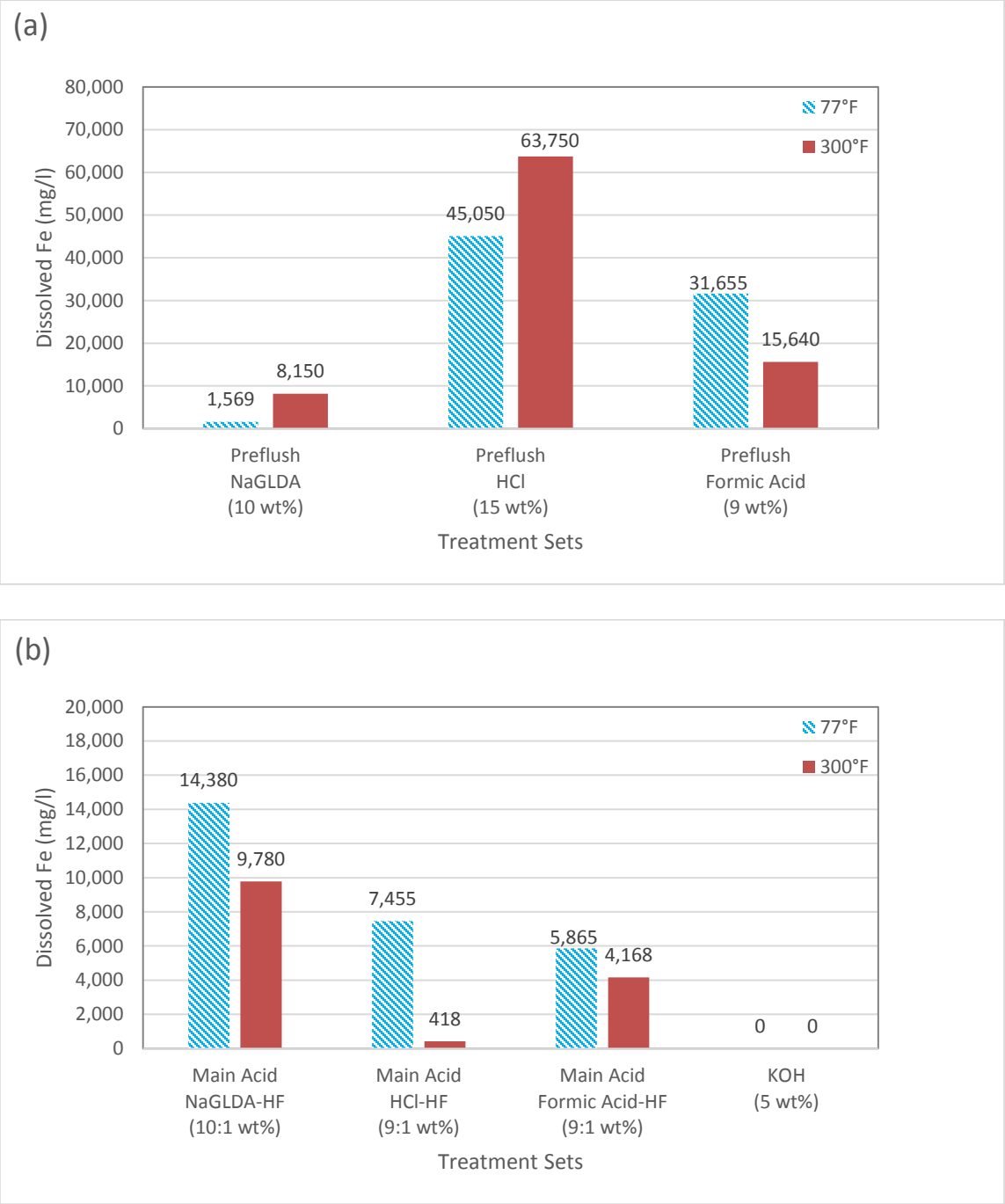


**Fig. 65—(a) Dissolved Fe concentration after preflush treatments for Scale #3. (b) Dissolved Fe concentration after main treatments for Scale #3.**

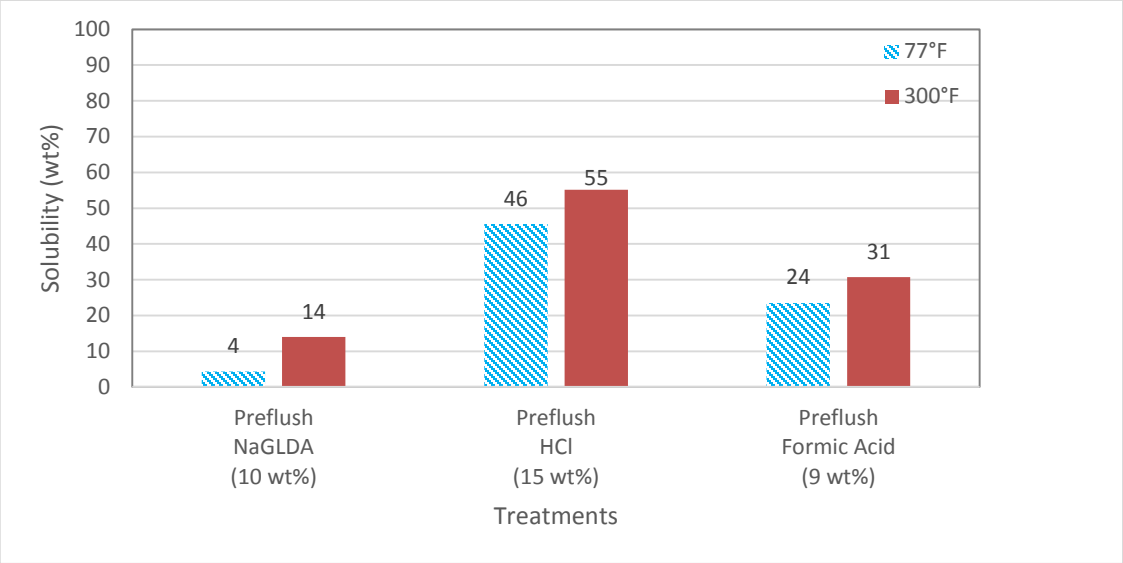


**Fig. 66—Solubility results for Scale #3 (preflush).**

Increase in temperature causes an increase in the solubility values for all the preflush stages (**Fig. 66**). The increase in solubility is almost 250% for the NaGLDA preflush, 20% for the HCl preflush, and 30% for the formic acid preflush. The HCl preflush results in the highest dissolution rates at 77 and 300ºF with the solubility values of 46 and 55 wt%, respectively.

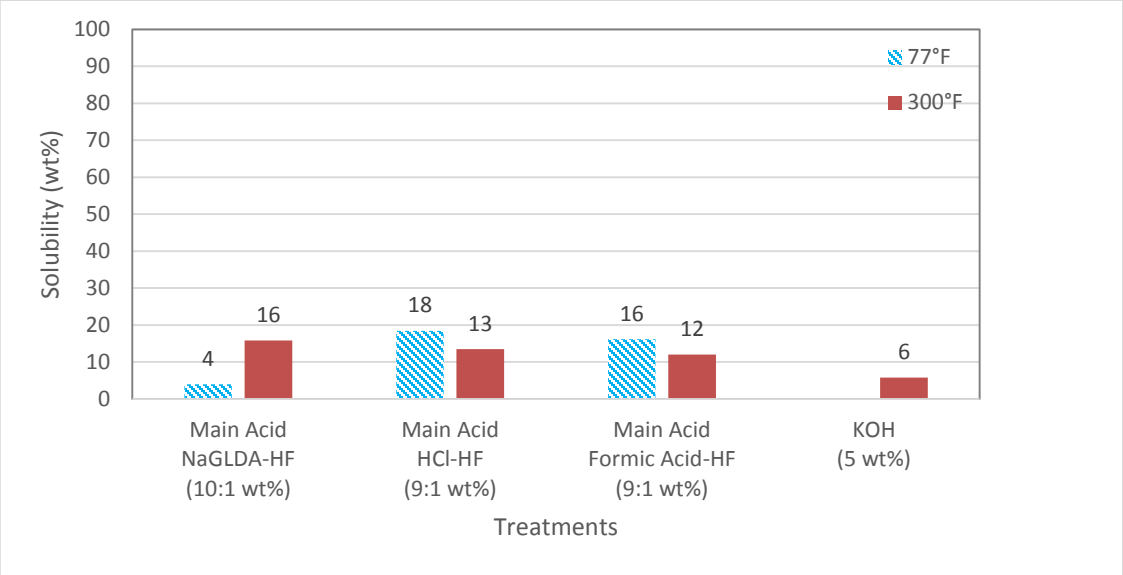


**Fig. 67—Solubility results for Scale #3 (main treatment).**

Increase in temperature shows a decrease in solubility values for main acid treatments with HCl and formic acid (**Fig. 67**). The decrease in solubility is almost 30% with HCl-HF solution and 25% with formic acid-HF solution. When the temperature is increased to 300ºF, the solubility of Scale #3 increases from 4 to 16 wt% after use of NaGLDA-HF solution. At room temperature, HCl-HF solutions is the most effective solution in terms of solubility value, which is 18 wt%. The NaGLDA-HF main acid treatment results in the highest dissolution at 300ºF with the solubility value of 16 wt%. Solubility of Scale #3 after the tests run with KOH solution is negative (-96 wt%) at 77ºF and 6 wt% at 300ºF.

As the dissolution tests with 5 wt% KOH showed negative solubility value for Scale #3, the sample after KOH treatment was analyzed by SEM, EDS, and XRF.

**Fig. 68—Scale #3 after 5 wt% KOH treatment at 77ºF (for XRF analysis).**

The whole sample (after 5 wt% KOH treatment) was ground by the help of mortar and pestle without damaging the crystal structure of sample to run XRF (**Fig. 68**).

| Formula | Concentration (wt%) |
|---|---|
| $SiO_2$ | 29.0 |
| $Fe_2O_3$ | 27.2 |
| MgO | 24.6 |
| $K_2O$ | 4.0 |
| CaO | 2.8 |

**Table 8—XRF Results for Scale #3 after KOH treatment.**

XRF results indicate that the sample is mostly composed of silicon dioxide, ferric oxide, and magnesium oxide with concentration values of 29.0, 27.2, and 24.6 wt%, respectively.

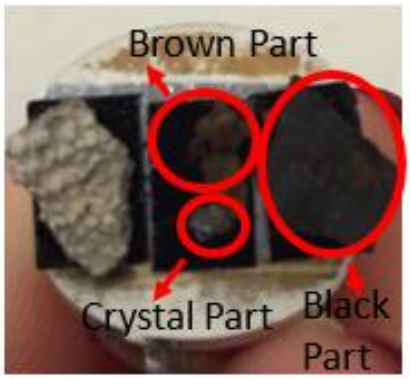


**Fig. 69—Sample #3 after KOH treatment - parts for SEM-EDS analysis.**

Scale #3 after 5 wt% KOH treatment had three different parts in terms of color, which are black, brown, and white (crystal) parts (**Fig. 69**). SEM-EDS were run for those parts separately.

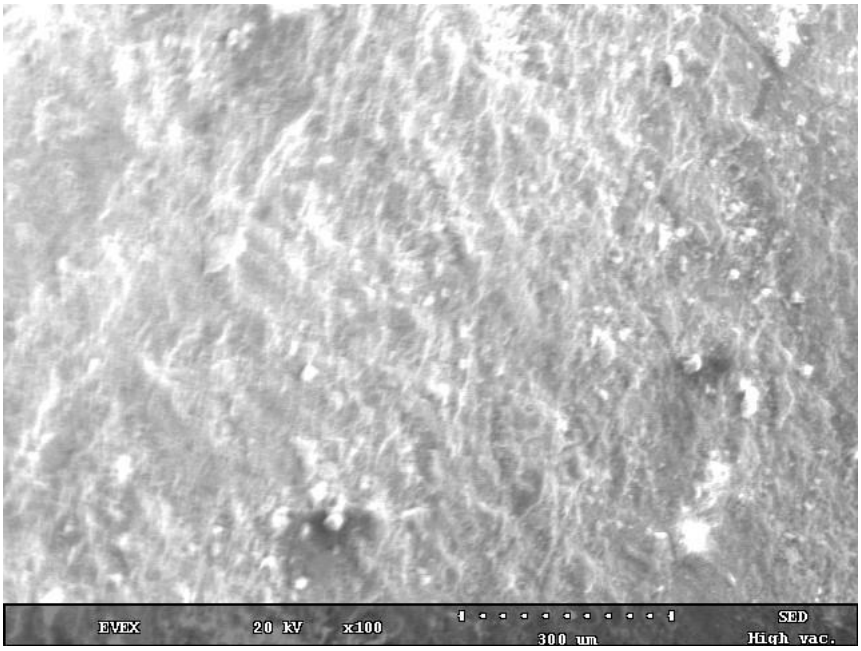


**Fig. 70—Scale #3 – After KOH treatment- black part- SEM image (magnification: 100X).**

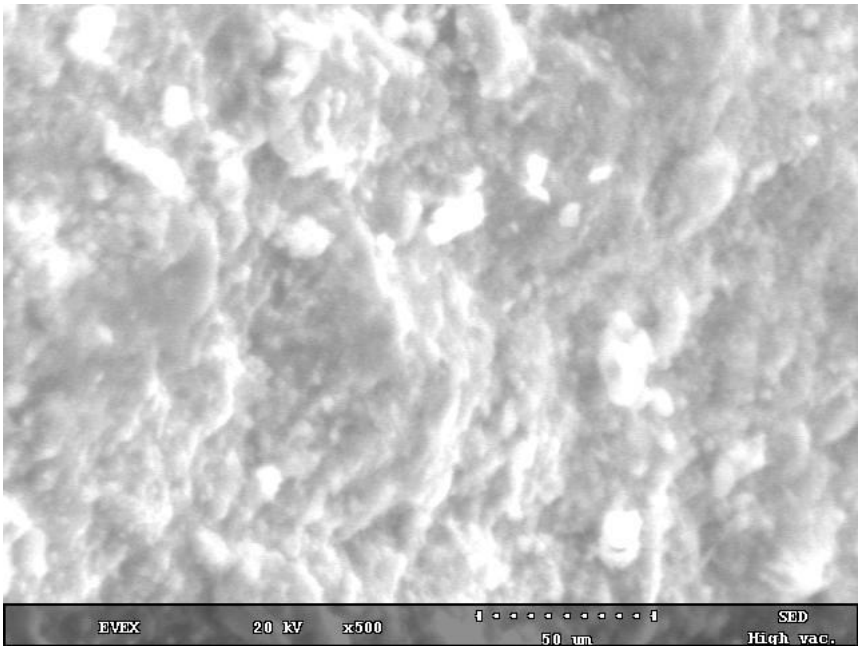


**Fig. 71—Scale #3 – After KOH treatment- black part- SEM image (magnification: 500X).**

**Fig. 70** and **Fig.71** are the electron microscope images with magnifications of 100 and 500X for Scale #3 after the KOH treatment (black part). **Fig. 72** represents the quantitative data about the chemical composition of Scale #3 after KOH treatment – black part. EDS result for this part of sample indicates that the sample is mostly composed of iron (~30 wt%), magnesium (~12 wt%), and silicon (~11 wt%). The KOH treatment alters the clear surface of Scale #3 and results in highly irregular shape, randomly distributed particles on the surface of scale. This composition strongly shows that the black part of Scale #3 after KOH treatment is mostly metal hydroxides, particularly iron and magnesium hydroxide. There are traces of phosphorus and calcium in this part of the sample with almost 1-3 wt%.

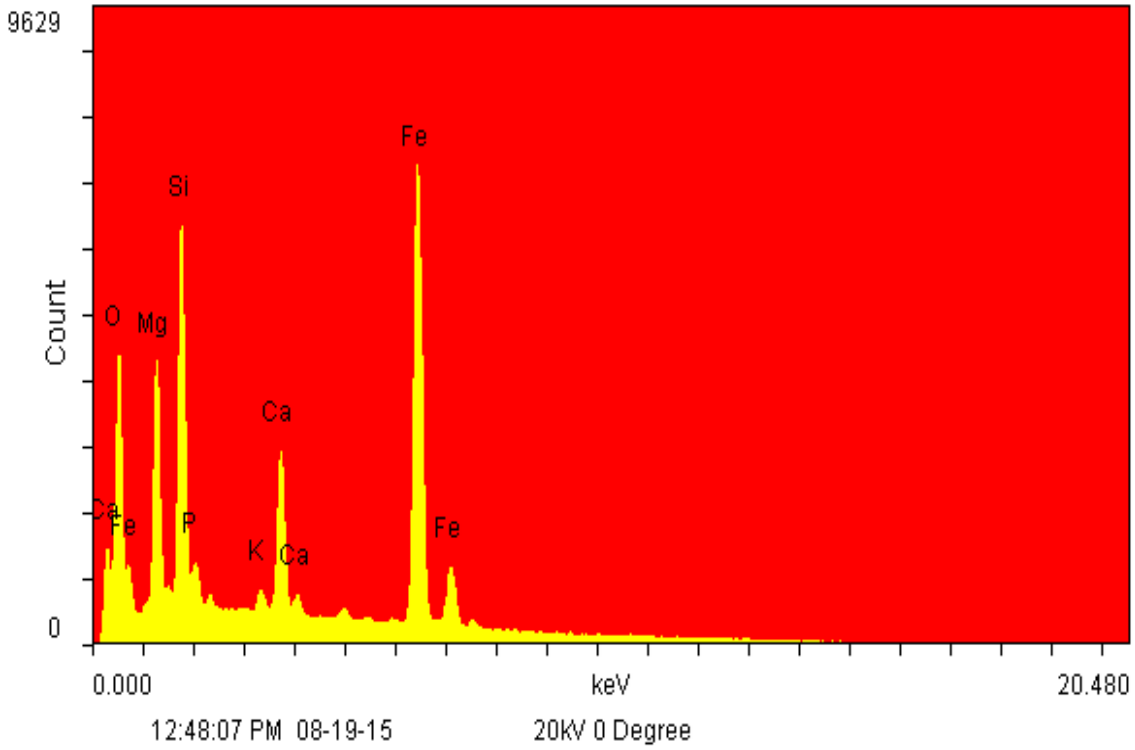


| Elements: | WT% | AT% | K_A | K_F | K_Z | Intensity | P/bkg |
|---|---|---|---|---|---|---|---|
| O K | 44.75 | 65.2 | 0.227 | 1 | 1.052 | 837.589 | 7.5 |
| FeL | 12.23 | 5.1 | 0.51 | 1 | 0.902 | 165.363 | 1.5 |
| MgK | 11.78 | 11.3 | 0.198 | 1.001 | 1.009 | 794.962 | 3.9 |
| SiK | 10.63 | 8.83 | 0.318 | 1.001 | 1.008 | 1374.18 | 6.4 |
| P K | 1.39 | 1.05 | 0.35 | 1.001 | 0.974 | 154.238 | 0.8 |
| K K | 0.24 | 0.14 | 0.778 | 1.009 | 0.958 | 55.051 | 0.3 |
| CaK | 2.85 | 1.66 | 0.845 | 1.009 | 0.981 | 657.99 | 3.2 |
| FeK | 16.14 | 6.74 | 1.012 | 1 | 0.892 | 2260.614 | 13.6 |

**Fig. 72—EDS data for Scale #3 after KOH treatment - black part.**


**Fig. 73—Scale #3 – After KOH treatment- brown part- SEM image (magnification: 100X).**

**Fig. 73** is the electron microscope image with magnification of 100X, and **Fig. 74** represents the quantitative data about the chemical composition for Scale #3 after KOH treatment – brown part. EDS results for this part of sample indicate that the sample is mostly composed of iron (~34 wt%), and silicon (~4 wt%). There are traces of aluminum and magnesium in this part of the sample with almost 3 wt%.

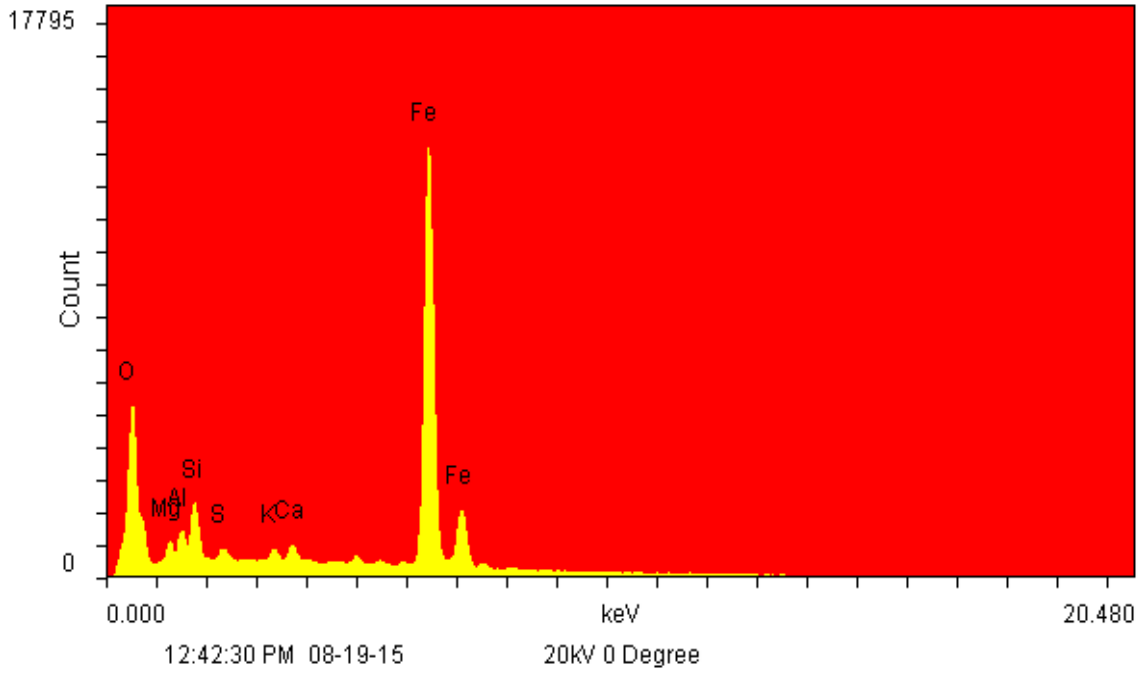


| Elements: | WT% | AT% | K_A | K_F | K_Z | Intensity | P/bkg |
|---|---|---|---|---|---|---|---|
| O K | 54.74 | 77.13 | 0.274 | 1 | 1.053 | 1320.85 | 10.7 |
| MgK | 2.75 | 2.55 | 0.173 | 1.001 | 1.01 | 173.441 | 1 |
| AlK | 2.79 | 2.33 | 0.239 | 1.001 | 0.981 | 265.281 | 1.4 |
| SiK | 4.02 | 3.22 | 0.312 | 1.001 | 1.009 | 544.4 | 2.5 |
| S K | 0.58 | 0.41 | 0.512 | 1.002 | 0.998 | 109.401 | 0.5 |
| K K | 0.46 | 0.27 | 0.826 | 1.008 | 0.959 | 121.129 | 0.6 |
| CaK | 0.63 | 0.36 | 0.882 | 1.013 | 0.982 | 163.047 | 0.8 |
| FeK | 34.03 | 13.74 | 1.03 | 1 | 0.893 | 5177.971 | 18.1 |

**Fig. 74—EDS data for Scale #3 after KOH treatment - brown part.**

**Fig. 75** is electron microscope image of Scale #3 after KOH treatment (crystal part) with magnification of 500X. **Fig. 76** represents the quantitative data about the chemical composition for Scale #3 after KOH treatment – crystal part. EDS result for this part of sample shows that the sample is composed of Si (26.48 wt%). This composition

strongly indicates that the crystal part of Scale #3 after KOH treatment is silicon dioxide. Quartz crystals are pretty much notable in SEM images for this part.

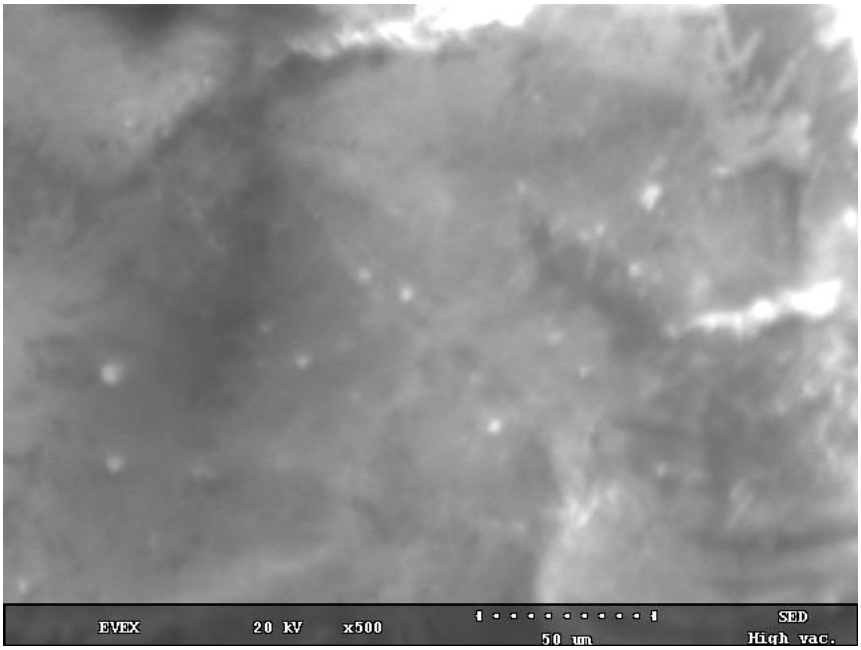


**Fig. 75—Scale #3 – After KOH treatment- crystal part- SEM image (magnification: 500X).**

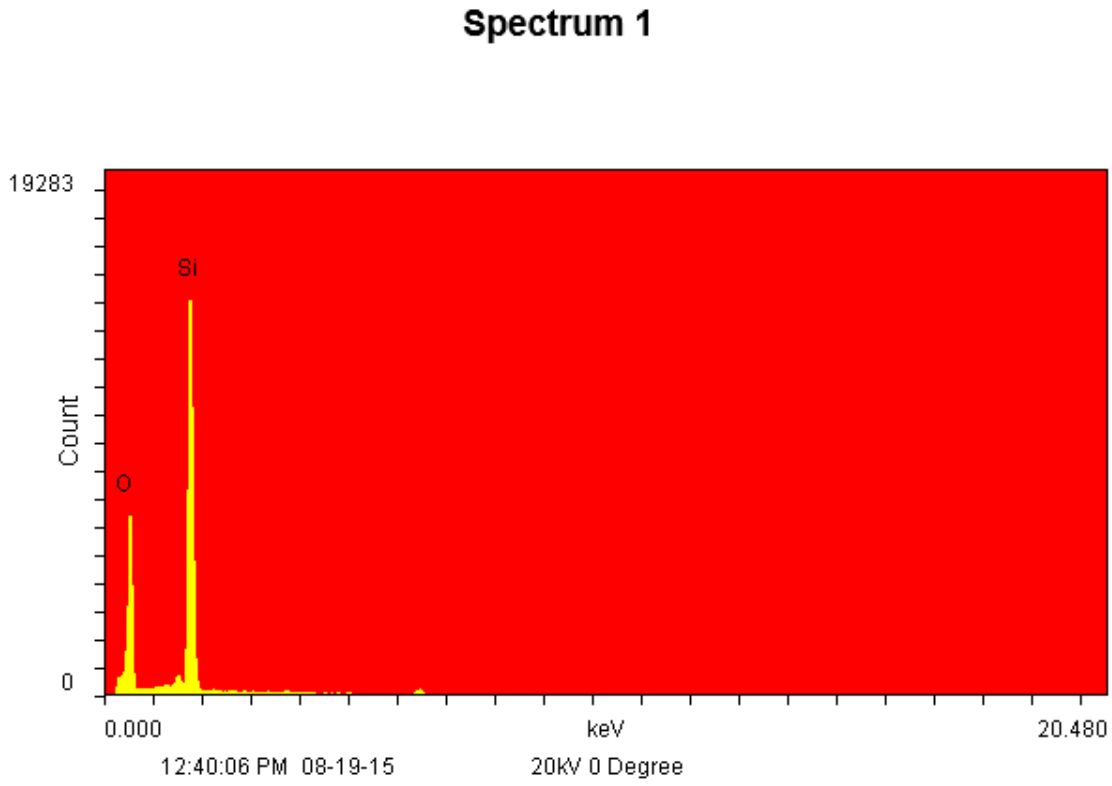


| Elements: | WT% | AT% | K_A | K_F | K_Z | Intensity | P/bkg |
|---|---|---|---|---|---|---|---|
| O K | 73.52 | 82.97 | 0.378 | 1 | 1.011 | 1546.077 | 20.3 |
| SiK | 26.48 | 17.03 | 0.598 | 1 | 0.969 | 4345.649 | 43.5 |

**Fig. 76—EDS data for Scale #3 after KOH treatment - crystal part.**

It can be concluded after those analysis (SEM-EDS and XRF) that 5 wt% KOH treatment causes extra precipitation for Scale #3. KOH treatment might deposit iron and magnesium hydroxides on the surface of Scale #3.

### 3.3.2 Discussion for Scale #3

Scale #3 is mainly composed of the oxides of Fe(III), Si, Mg, Ca, and Mg. The sample analyses before dissolution tests indicate that the minerals present in Scale #3 are pectolite, tremolite, greenalite, and anorthite which are the most common metal silicates in SAGD boilers.

The increase in temperature causes decrease in Si and Na concentrations for all treatment sets. The decrease in Si concentration is due to the precipitation of Si during the secondary reactions of fluosilicic acid ($H_2SiF_6$).

Preflush stage mitigates calcium and magnesium fluoride depositions by dissolving carbonate minerals and prevents consumption of hydrofluoric acid (HF) with those minerals (Williams et al. 1979; Da Motta et al. 1994; Hill et al. 1994). Although Ca concentration decreases by temperature for the treatment sets with HCl and formic acid, the total dissolved Ca concentrations are still higher than the one after the treatment with NaGLDA.

KOH, as a strong alkali medium, is not effective to dissolve Scale #3 due to negative solubility value and low dissolved ion concentrations. 5 wt% KOH solution causes extra precipitations in the form of $SiO_2$, $Fe(OH)_3$ and $Mg(OH)_2$. Ferric hydroxide forms in high pH solutions (5 wt% KOH in this case) (Ying-Hsiao and Fambrough 1998). High Mg concentration after treatment might be an indication of extra magnesium silicate deposition, as the presence of hydroxide ions in the fluid catalyzes the polymerization process (Amjad and Zuhl 2008).

The use of mud acid (9:1 wt% HCl-HF) after preflush with strong acid solution (15 wt% HCl) especially at 300ºF seems to be the best solution to dissolve Scale #3 effectively in terms of solubility and total dissolved ion concentrations. Increasing the concentration of HCl in preflush stage, which is expected to dissolve most of Mg and Na in the scale, might be helpful to dissolve more Si in main acid treatment with mud acid at 77ºF by preventing possible precipitation of magnesium fluoride ($MgF_2$) and sodium fluosilicate ($Na_2SiF_6$). Treatment sets with both HCl and formic acid might be effective based on their similar solubility values and dissolved ion concentrations.

## 3.4 Scale #4

### 3.4.1 Results for Scale #4

Dissolution tests for Scale #4 consist of four different treatment sets: HCl preflush followed by HCl-HF main acid, NaGLDA preflush followed by NaGLDA-HF main acid, formic acid preflush followed by formic acid-HF main acid, and KOH solution. These tests were performed dynamically at 77 and 300°F for three hours.

Si is dissolved slightly after all the preflush stages with NaGLDA, HCl, and formic acid (**Fig. 77 (a)**). The main acid treatment stage is the most significant stage in terms of dissolving considerable amounts of Si for all treatment sets (**Fig. 77 (b)**). The increase in temperature from 77 to 300ºF causes decrease in silica concentrations for all main acid treatments except for the formic acid-HF main acid treatment. The decrease in Si concentration is almost 55% for NaGLDA-HF, 40% for HCl-HF, and 35% for formic acid-HF main acid treatments. Dissolved Si concentration is the highest after the HCl- HF main acid treatment with the concentration values of 6,125 and 3,774 mg/l at 77 and 300ºF, respectively. KOH is the least effective solution with the lowest dissolved Si concentration (316 mg/l) at 77ºF and stops dissolving Si at 300ºF.

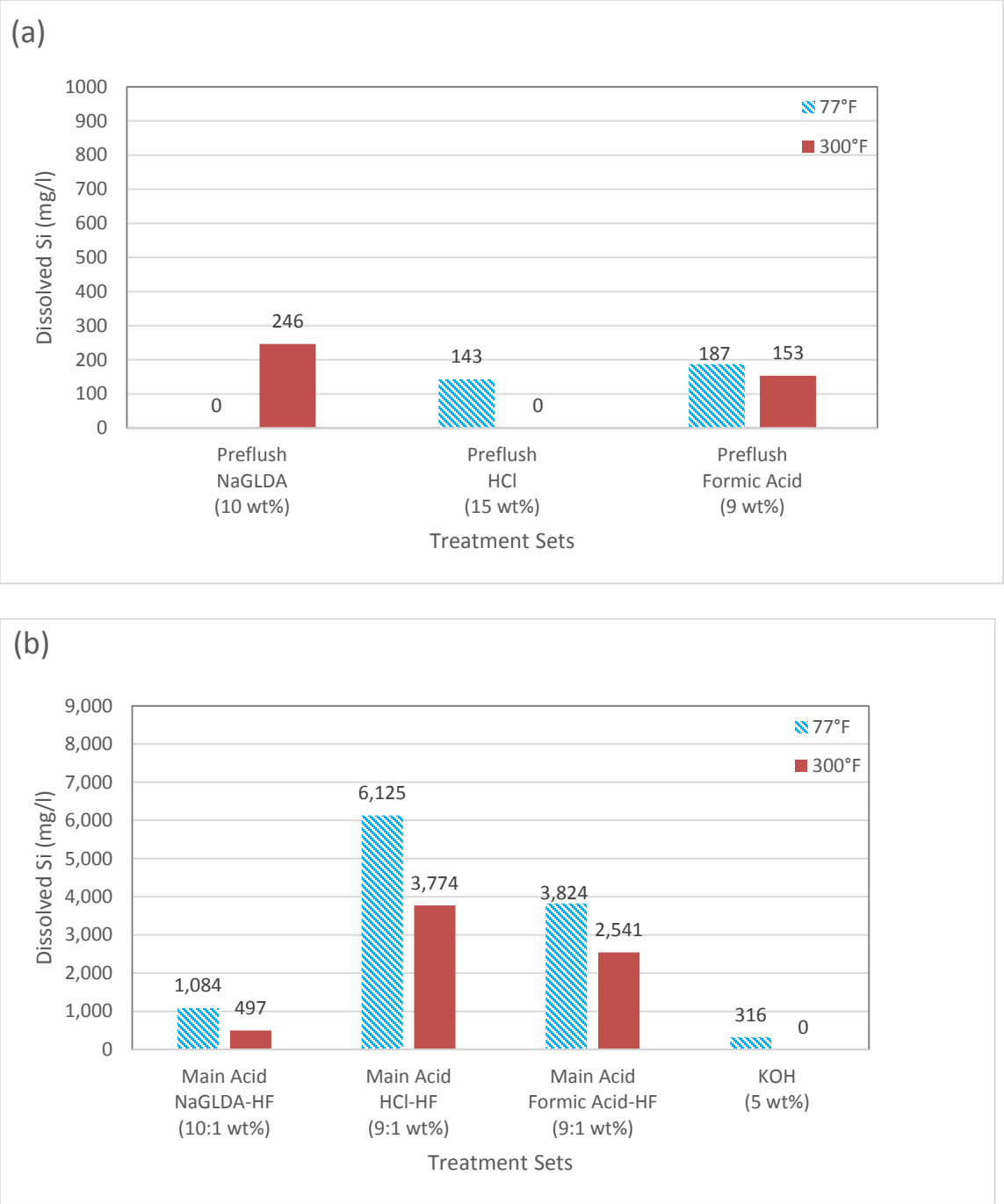


**Fig. 77—(a) Dissolved Si concentration after preflush treatments for Scale #4. (b) Dissolved Si concentration after main treatments for Scale #4.**

The preflush stage is the most significant stage in terms of dissolving considerable amounts of Ca for all treatment sets (**Fig. 78 (a)**). The increase in temperature from 77 to 300ºF does not result in any change in Ca concentrations for the preflush stages with NaGLDA and formic acid. Although the decrease in Ca concentration is almost 25% for HCl preflush when the temperature is increased to 300ºF, the preflush treatments with HCl at 77 and 300ºF are the most successful treatments in terms of dissolving Ca. Dissolved Ca concentration is the highest after 15 wt% HCl preflush with the concentration values of 1,259 and 958 mg/l at 77 and 300ºF, respectively.

KOH and NaGLDA-HF solutions do not dissolve Ca at any test temperature. The dissolved Ca concentrations for HCl and formic acid main acid treatments (**Fig. 78 (b)**) are not as high as the ones after preflush stages. The low Ca concentration after main acid treatments is desired, because the purpose of preflush is to dissolve as much as Ca before main acid stage to prevent precipitations with HF.

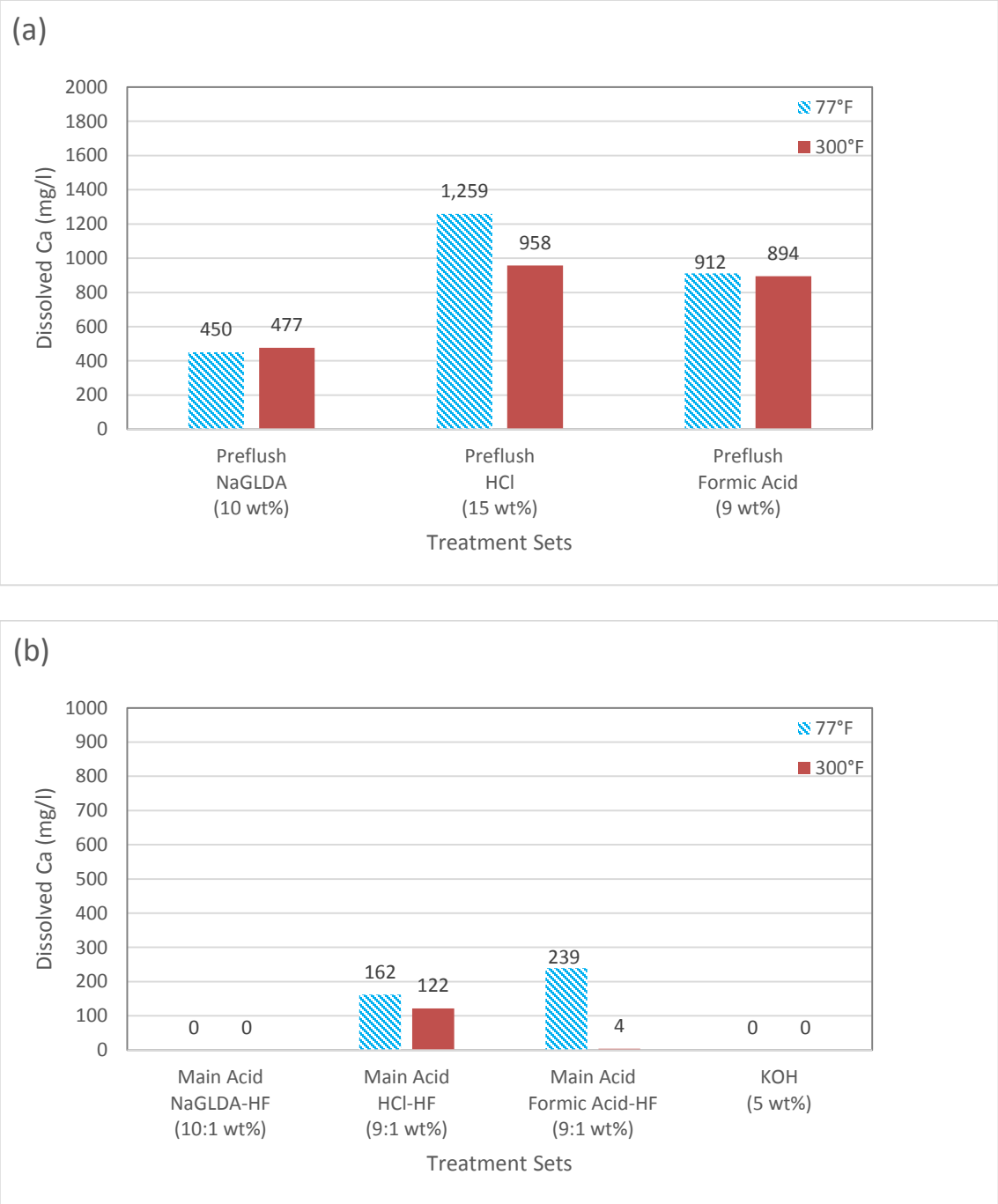


**Fig. 78—(a) Dissolved Ca concentration after preflush treatments for Scale #4. (b) Dissolved Ca concentration after main treatments for Scale #4.**

Dissolved Na concentration is the highest after the preflush and main acid treatment stages with NaGLDA (**Fig. 79 (a)** and **(b)**). These results can be explained by the Na content of NaGLDA itself; therefore, Na concentration obtained by ICP is misleading. Na concentrations in the filtrate solutions after the dissolution tests include Na coming from the scale and NaGLDA itself. Na concentration is almost 15,000 mg/l for 10 wt% NaGLDA solution and 12,000 mg/l for 10:1 wt% NaGLDA-HF solution. In the light of this information, it can be inferred from the results such that dissolved Na concentration (almost 7,000 mg/l) is still the highest in the case of NaGLDA preflush at room temperature.

The increase in temperature from 77 to 300ºF causes decrease in Na concentrations for all treatment sets (preflush and main treatments). Increase in temperature results in negative Na concentration values (after subtraction of Na concentration which comes from NaGLDA solution itself) for preflush and main acid treatments with NaGLDA. The highest dissolved NA concentrations among the main treatments are 4,028 mg/l after HCl-HF main treatment at 77ºF and 2,042 mg/l after formic acid-HF main treatment at 300ºF.

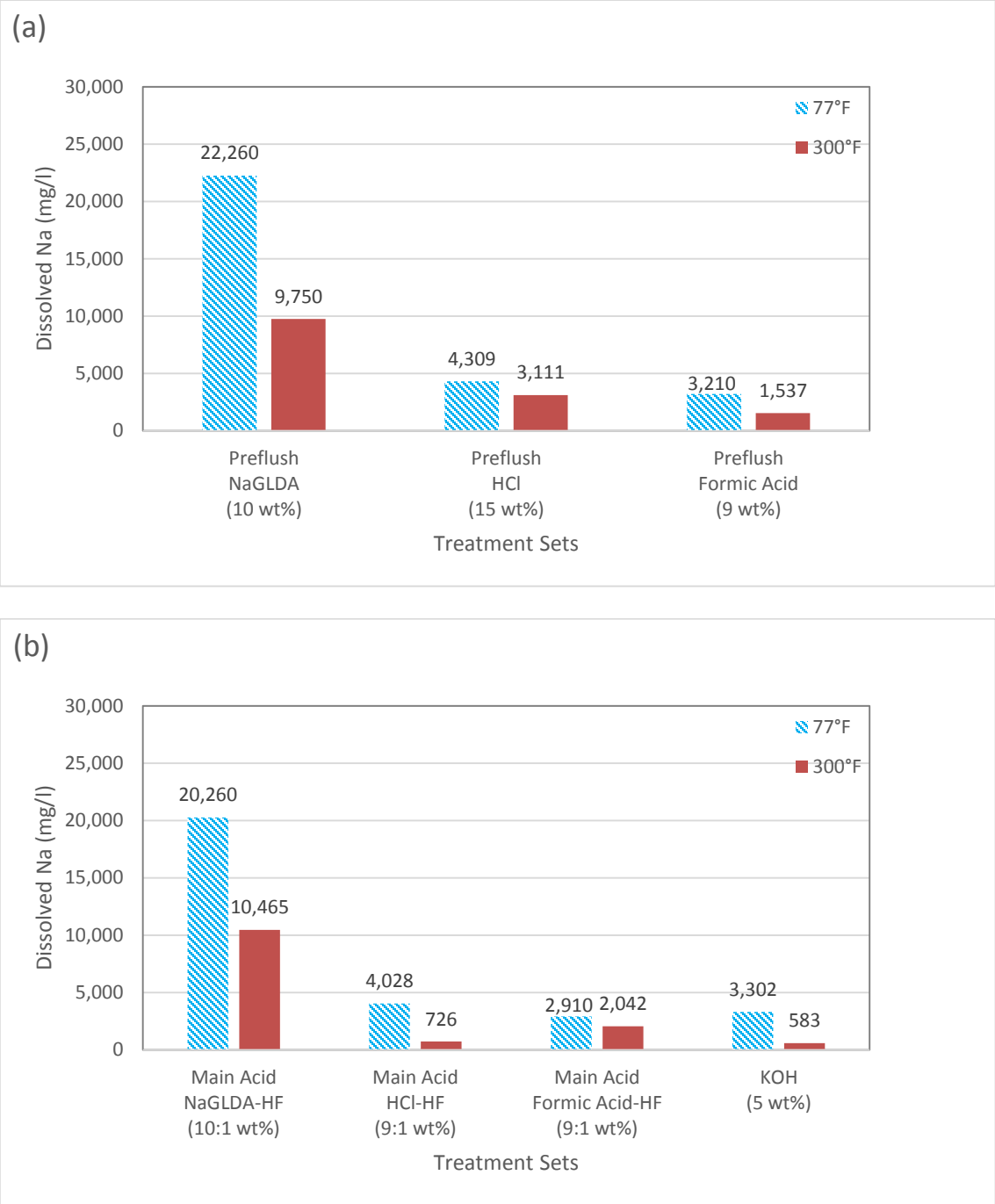


**Fig. 79—(a) Dissolved Na concentration after preflush treatments for Scale #4. (b) Dissolved Na concentration after main treatments for Scale #4.**

The preflush stage is supposed to dissolve most of Mg in Scale #4. The increase in temperature from 77 to 300ºF causes increase in Mg concentrations for all preflush stages (**Fig. 80 (a)**). The NaGLDA preflush, which is not capable of dissolving Mg at room temperature, starts dissolving Mg at 300°F. The preflush stages with HCl at 77 and 300ºF are the most successful treatments in terms of dissolving Mg (1,857 and 6000 mg/l, respectively).The dissolved Mg concentrations after main acid treatments (**Fig. 80 (b)**) show decreasing trend by increasing temperature. KOH and NaGLDA solutions do not dissolve Mg at any test temperature. Low Mg concentration after preflush is desired, because the purpose of preflush is to dissolve as much as Mg before main acid stage to prevent precipitations with HF. It seems that the preflush stages are not effective to dissolve most of Mg which consumes more HF in the main acid treatment. It can be withdrawn that the concentrations of preflush solution should be increased to facilitate main acid treatment stages.

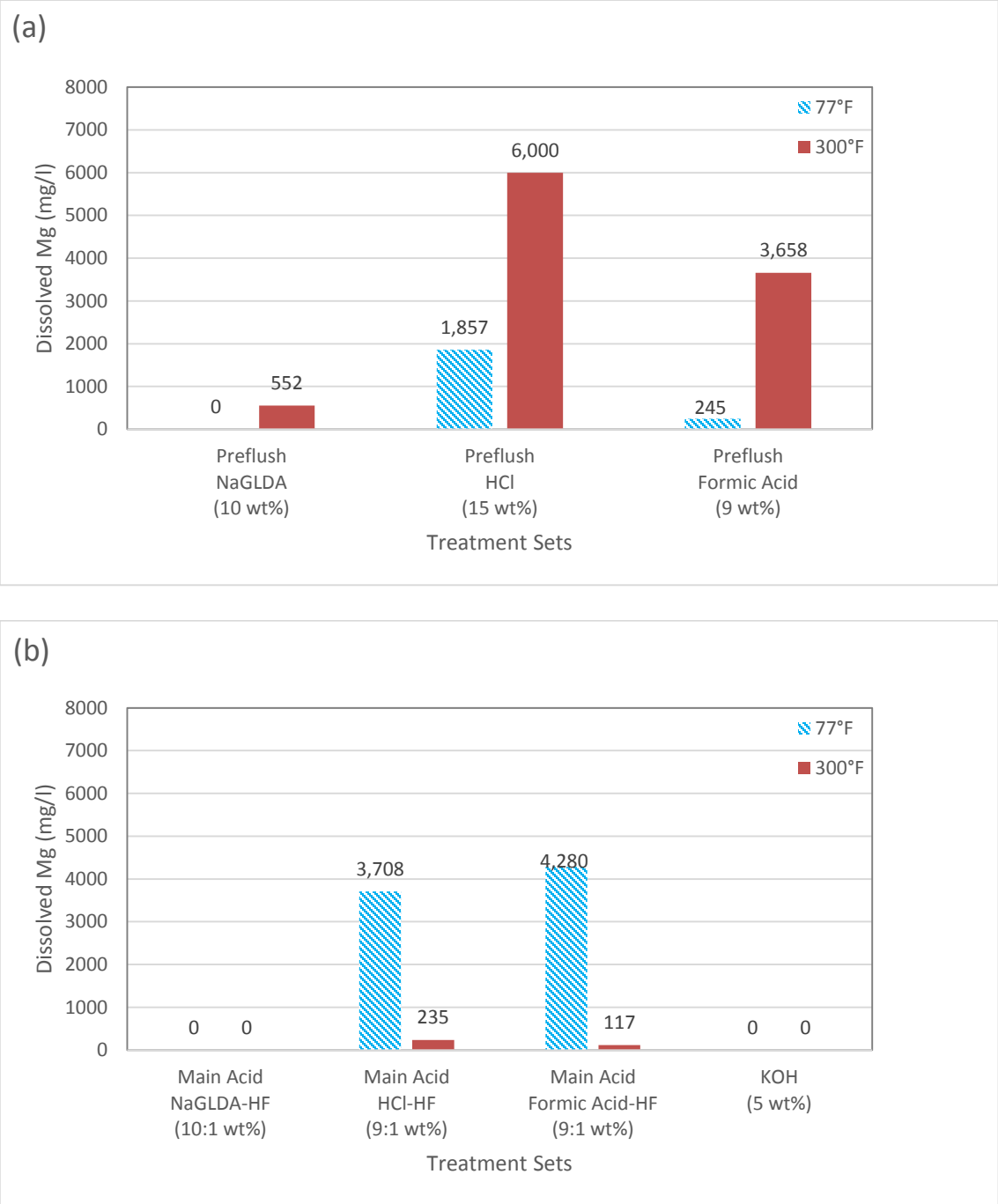


**Fig. 80—(a) Dissolved Mg concentration after preflush treatments for Scale #4. (b) Dissolved Mg concentration after main treatments for Scale #4.**

Dissolved Fe concentrations (**Fig. 81 (a)**) are the highest after the preflush with 15 wt% HCl at 77 and 300ºF (21,650 and 48,415 mg/l, respectively). The increase in temperature from 77 to 300ºF causes increase in Fe concentrations for all the preflush stages.

The dissolved Fe concentrations after main acid treatments (**Fig. 81 (b)**) show an increasing trend as the temperature increases to 300ºF except for the HCl-HF main treatment. KOH solution does not dissolve Fe at any test temperature (77 and 300ºF). The highest dissolved Fe concentrations are obtained after the main treatment with the formic acid-HF solution at 77 and 300ºF (9,635 and 13,990 mg/l, respectively).

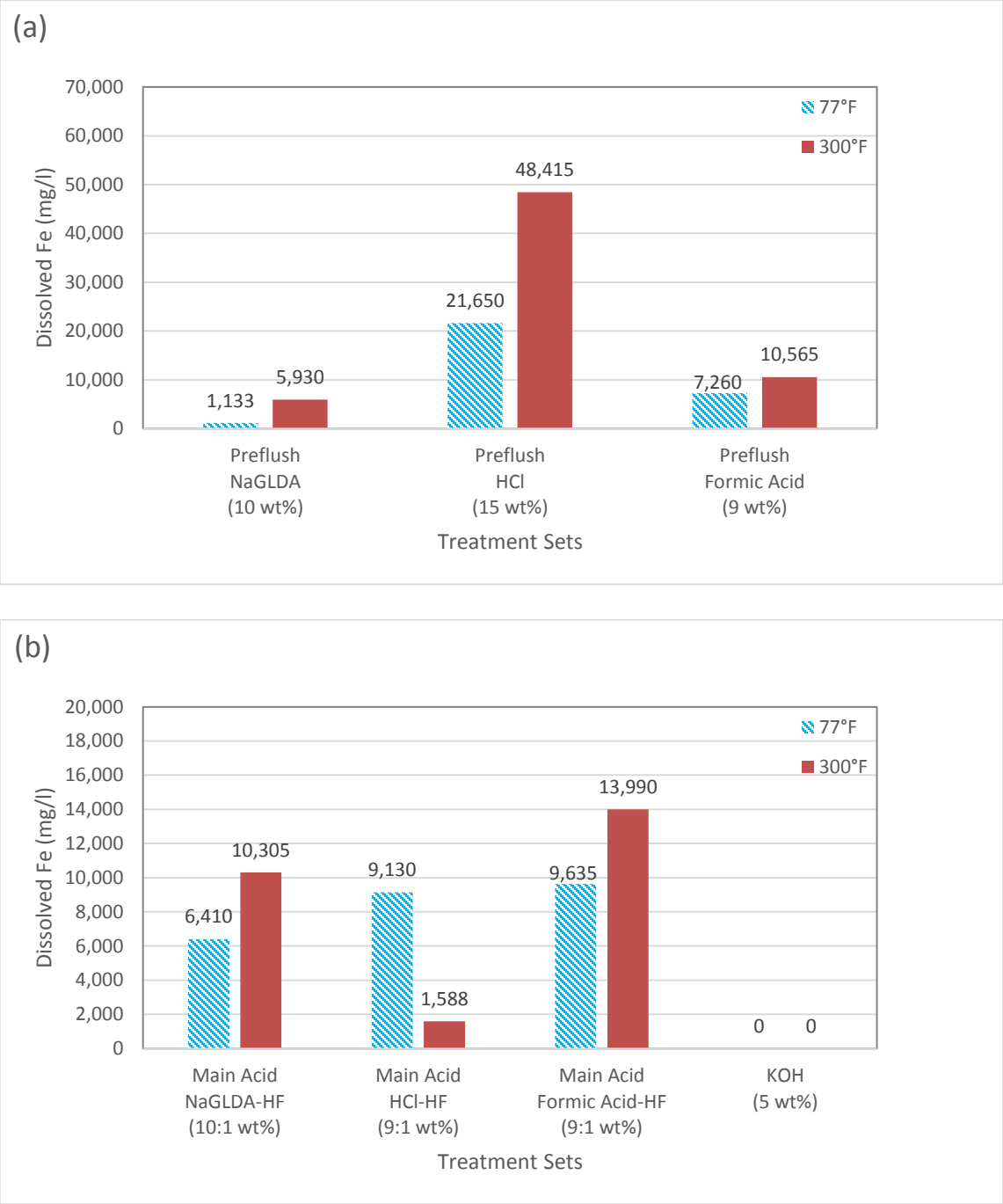


**Fig. 81—(a) Dissolved Fe concentration after preflush treatments for Scale #4. (b) Dissolved Fe concentration after main treatments for Scale #4.**

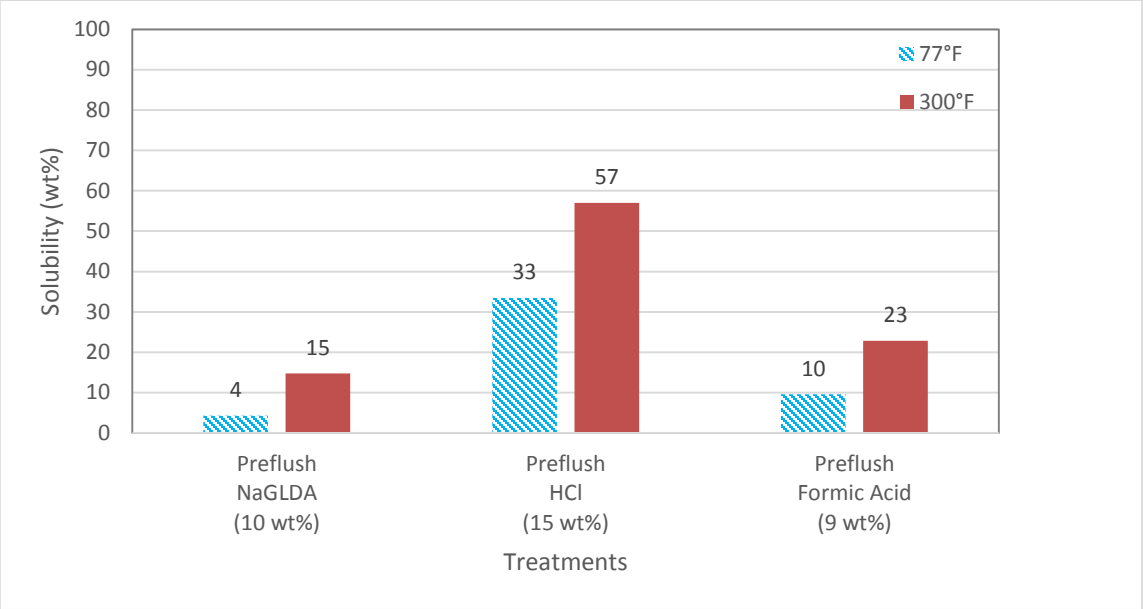


**Fig. 82—Solubility results for Scale #4 (preflush).**

Increase in temperature causes an increase in solubility values for all the preflush stages (**Fig. 82**). The increase in solubility is almost 275% for the NaGLDA preflush, 70% for the HCl preflush, and 130% for the formic acid preflush. The HCl preflush results in the highest dissolution rates with the solubility values of 33 and 57 wt% at 77 and 300ºF, respectively.

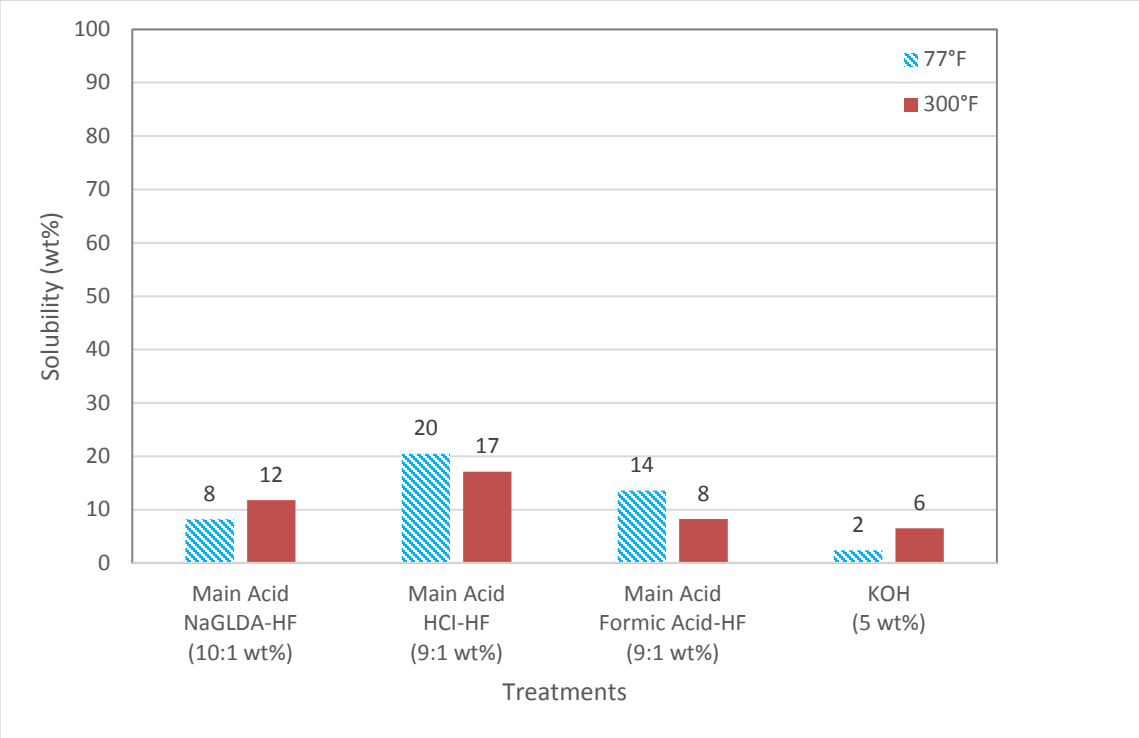


**Fig. 83—Solubility results for Scale #4 (main treatment).**

Increase in temperature shows a decrease in solubility values for the main acid treatments with HCl-HF and formic acid-HF solutions (**Fig. 83**). The decrease in solubility is almost 15% with HCl-HF solution and 40% with formic acid-HF solution. When the temperature is increased to 300ºF, the solubility of Scale #4 increases from 8 to 12 wt% after use of NaGLDA-HF solution. At room temperature, HCl-HF solution is the most effective solution in terms of solubility value, which is 20 wt%. The HCl-HF main acid treatment results in the highest dissolution at 300ºF with the solubility value of 17 wt%. Solubility of Scale #4 after the tests run with KOH solution is 2 wt% at 77ºF and 6 wt% at 300ºF.

### 3.4.2 Discussion for Scale #4

Scale #4 is mainly composed of the oxides of Ca, Si, and Fe(III). The sample analyses before dissolution tests indicate that the minerals present in Scale #4 are pectolite, tremolite, and chlorite which are the most common metal silicates in SAGD boilers.

The increase in temperature causes decrease in Si and Na concentrations for all treatment sets, while the dissolution of Fe and Mg is enhanced. The decrease in Si concentration is due to the precipitation of Si during the secondary reactions of fluosilicic acid ($H_2SiF_6$). Although Ca concentration decreases by temperature for the treatment sets with HCl and formic acid, the total dissolve Ca concentrations are still higher than the one after the treatment with NaGLDA.

KOH, as a strong alkali medium, is not effective to dissolve Scale #4 due to negative solubility value and low dissolved ion concentrations.

The use of mud acid (9:1 wt% HCl-HF) after preflush with strong acid solution (15 wt% HCl) especially at 300ºF seems to be the best solution to dissolve Scale #4 effectively in terms of high solubility values and high total dissolved ion concentrations.

# 4. CONCLUSIONS AND RECOMMENDATIONS

## 4.1 Conclusions

In this study four different scale samples (named as Scale #1, #2, #3, and #4) from different SAGD boilers were analyzed to determine an effective treatment to dissolve them. HCl, NaGLDA, and formic acid preflush treatments were applied to each scale sample separately. The preflush stages were followed by the main acid treatment stages with HCl-HF, NaGLDA-HF, and formic acid-HF, respectively. KOH solution was also tested on scale samples. The tests were performed at both 77 and 300ºF. Conclusions drawn from this research and its contribution to industry will be covered below:

- Analyses before application of any treatment on scale samples show that they are mostly composed of metal silicates and silica-based minerals (pectolite, tremolite, greenalite, anorthite, and fayalite) according to the composition and quantity of metal ions and silicon dioxide ($SiO_2$) in their structures.
- The treatments show that the most effective way to dissolve scale samples is 9 wt% HCl preflush followed by 9:1 wt% HCl-HF main acid treatment at both 77 and 300ºF.
- The concentration of HCl at the preflush stage might be increased based on the concentrations of Ca, Na, and Mg in the scale samples to prevent possible precipitations during primary ($CaF_2$ and $MgF_2$) and secondary ($CaSiF_6$ and $Na_2SiF_6$) reactions.
- Although dissolved Si concentration decreases by increasing temperature due to precipitations of $CaSiF_6$ and $Na_2SiF_6$ at high temperature, the proposed treatment set

with HCl still provides the highest dissolved Si concentration and solubility values at 300ºF.

- The low solubility results and dissolved ion concentrations show that 5 wt% KOH solution, as selected to test the effect of strong alkali mediums on solubility of silica-based scales, is not able to dissolve any scale samples at any tested temperature (77 and 300ºF).
- Although increasing temperature enhances the solubility of scale samples by KOH solution, KOH as a representative for strong alkali medium is the least effective solution.
- 5 wt% KOH solution even causes extra precipitations ($Fe(OH)_3$ and $Mg(OH)_2$) on Scale #3 with negative solubility value. High Mg concentration after treatment might be an indication of extra magnesium silicate deposition, as the presence of hydroxide ions in the fluid catalyzes the polymerization process (Amjad and Zuhl 2008).
- On the contrary to Demadis et al. 2007, the study shows that the presence of cations might aid the precipitation in alkaline solutions (high pH) as in the case of Scale #3 (Gill 1998).
- The main focuses of previous studies were the removal of silica and the inhibition of silica scale to prevent any operational problems. This work, however, is a case study which provides both analysis and removal of silica scales in SAGD boilers. The steps followed in this research to design an effective treatment method to remove silica-based scale samples might be applied to similar cases.

## 4.2 Recommendations

- Material of boiler tubes should be analyzed to evaluate the applicability of suggested solutions to boiler tubes.
- Disposal of suggested solutions should be studied to handle with environmental concerns and storage issues.
- Further analyses should be carried out on feed-water and blowdown water to figure out the effect of the composition of these water types on scaling and removal process.
- It is also suggested to compare the cost effectiveness of use of proposed solutions over piggling method.

# REFERENCES


Amjad, Z., and Zuhl, R. W. 2008. An Evaluation of Silica Scale Control Additives for Industrial Water Systems. Presented at NACE International Corrosion Conference and Expo, New Orleans, Louisiana, 16-20 March. NACE-08368.

Bremere, I., Kennedy, M., and Mhyio, S. 2000. Prevention of Silica Scale in Membrane Systems: Removal of Monomer and Polymer Silica. *Desalination* **132** (1): 89-100. http://dx.doi.org/10.1016/S0011-9164(00)00138-7.

Butler, R. M. and Stephens, D. J. 1981. The Gravity Drainage of Steam-Heated Heavy Oil to Parallel Horizontal Wells. *J Can Pet Technol* **20** (2): 90-96. PETSOC-81-02-07. http://dx.doi.org/10.2118/81-02-07.

Butler, N. M., Mcnab, G. S., and Lo, H. Y. 1981. Theoretical Studies on the Gravity Drainage of Heavy Oil During In-Situ Steam Heating. *Canadian Journal of Chemical Engineering* **59** (4): 455-460. http://dx.doi.org/10.1002/cjce.5450590407.

Campopiano, A., Olori, A., and Cannizzaro, A. 2015. Quantification of Tremolite in Friable Material Coming from Calabrian Ophiolitic Deposits by Infrared Spectroscopy. *Journal of Spectroscopy* **2015**: 1-9. http://dx.doi.org/doi:10.1155/2015/974902.

Chan, S. H. 1989. A Review on Solubility and Polymerization of Silica. *Geothermics* **18** (1): 49-56.

Clark, L. M. 1948. The Identification of Minerals in Boiler Deposits: Examples of Hydrothermal Synthesis in Boilers. *Mineralogical Magazine* **28** (202): 359-366.

Crabtree, M., Eslinger, D., and Fletcher, P. 1999. Fighting Scale-Removal and Prevention. *Schlumberger Oilfield Review* **11** (3): 30-45.

Crowe, C. W. 1986. Precipitation of Hydrated Silica From Spent Hydrofluoric Acid: How Much of a Problem Is It?. *J Pet Technol* **38** (11): 1234-1240. SPE-13083-PA. http://dx.doi.org/10.2118/13083-PA.

Da Motta, E. P., Plavnik, B., and Schechter. 1993. Accounting for Silica Precipitation in the Design of Sandstone Acidizing. *SPE Prod & Fac* **8** (2): 138–144. SPE-23802-PA. http://dx.doi.org/10.2118/23802-PA.

Demadis, K., Stathoulopoulou, A., and Ketsetzi, A. 2007. Inhibition and Control of Colloidal Silica: Can Chemical Additives Untie the Knot of Scale Formation?. Presented at the NACE International Corrosion Conference & Expo, Nashville, Tennessee, 11-15 March. NACE-07058.

Demadis, K. D. 2010. Recent Developments in Controlling Silica and Magnesium Silicate Foulants in Industrial Water Systems. In *The Science and Technology of Industrial Water Treatment.* Chapt. 10, 179-203. Boca Raton, Florida: Taylor and Francis, LLC.

Frenier, W. W. and Ziauddin, M. 2008. *Formation, Removal, and Inhibition of Inorganic Scale in the Oilfield Environment*. Richardson, Texas: Textbook Series, SPE.

Gill, J. S. 1993. Inhibition of Silica-Silicate Deposit in Industrial Waters. *Colloids and Surfaces* **74** (1): 101-106.

Gill, J. S. 1998. Silica Scale Control. Presented at the NACE International Corrosion Conference and Expo, San Diego, California, 22-27 March. NACE-98226.

Heins, W.F. 2010. Is a Paradigm Shift in Produced Water Treatment Technology Occurring at SAGD Facilities?. *J Can Pet Technol* **49** (1): 10-15. SPE-132804-PA. http://dx.doi.org/10.2118/132804-PA.

Hill, A. D., Sepehrnoori, K., and Wu, P. Y. 1994. Design of the HCl Preflush in Sandstone Acidizing. *SPE Prod & Fac* **9** (2): 115–120. SPE-21720-PA. http://dx.doi.org/10.2118/21720-PA.

Iler, R. K. 1979. *The Chemistry of Silica: Solubility, Polymerization, Colloid and Surface Properties, and Biochemistry*. New York: Wiley.

Meyers, P. 1999. Behavior of Silica in Ion Exchange and Other Systems. Presented at the International Water Conference, Pittsburgh, Pennsylvania, 18-20 October.

Milne, N. A., O'Reilly, T., and Sanciolo, P. 2014. Chemistry of Silica Scale Mitigation for RO Desalination with Particular Reference to Remote Operations. Water Research 65: 107-133. http://dx.doi.org/10.1016/j.watres.2014.07.010.

Myszczyszyn, M. M. 2010. To Scale or Not to Scale in 2500 Psig Once Through Steam Generators. Presented at the Annual Meeting of International Association for the Properties of Water and Steam, Helmholtz Award Lecture.

Ning, R. Y. 2003. Discussion of Silica Speciation, Fouling, Control and Maximum Reduction. *Desalination* **151** (1): 67-73. http://dx.doi.org/10.1016/S0011-9164(02)00973-6.

Ning, R. Y., Tarquin, A., and Balliew, J. E. 2010. Seawater RO Treatment of RO Concentrate to Extreme Silica Concentrations. *Desalination and Water Treatment* **22** (1): 286-291. http://dx.doi.org/10/5004/dwt.2010.1877.

Pedenaud, P., Goulay, C., and Pottier, F. 2004. Silica Scale Inhibition for Steam Generation in OTSG Boiler. Presented at the SPE International Thermal Operations and Heavy Oil Symposium and Western Regional Meeting, Bakersfield, California, 16-18 March. SPE-86934-MS. http://dx.doi.org/10.2118/86934-MS.

Pedenaud, P., Goulay, C., and Michaud, P. 2005. Oily Water Treatment Schemes for Steam Generation in SAGD Heavy Oil Developments. Presented at the SPE International Thermal Operations and Heavy Oil Symposium, Calgary, Canada, 1-3 November. SPE-97750-MS. http://dx.doi.org/10.2118/97750-MS.

Pedenaud, P., Goulay, C., Pottier, F. et al. 2006. Silica Scale Inhibition for Steam Generation in OTSG Boiler. *SPE Prod & Oper* **21** (1): 26-32. SPE-86934-PA. http://dx.doi.org/10.2118/86934-PA.

Sahachaiyunta, P., Koo, T., and Sheikholeslami, R. 2002. Effect of Several Inorganic Species on Silica Fouling in RO Membranes. *Desalination* **144** (1): 373-378. http://dx.doi.org/10.1016/S0011-9164(02)00346-6.

Sheikholeslami, R., Al-Mutaz, I. S., and Koo, T. 2001. Pretreatment And The Effect Of Cations and Anions on Prevention Of Silica Fouling. *Desalination* **139** (1): 83-95. http://dx.doi.org/10.1016/S0011-9164(01)00297-1.

Sheikholeslami, R. and Bright, J. 2002. Silica and Metals Removal by Pretreatment to Prevent Fouling of Reverse Osmosis Membranes. *Desalination* **143** (3): 255-267. http://dx.doi.org/10.1016/S0011-9164(02)00264-3.

Sheikholeslami, R., Al-Mutaz, I. S., and Tan, S. 2002. Some Aspects of Silica Polymerization and Fouling and its Pretreatment by Sodium Aluminate, Lime and Soda Ash. *Desalination* **150** (1): 85-92. http://dx.doi.org/10.1016/S0011-9164(02)00932-3.

Smith, C. F. and Hendrickson, A. R. 1965. Hydrofluoric Acid Stimulation of Sandstone Reservoirs. *J Pet Technol* **17** (2). SPE-980-PA. http://dx.doi.org/10.2118/980-PA.

Thimm, H. F. 2008. Understanding the Generation of Dissolved Silica in Thermal Projects: Theoretical Progress. *J Can Pet Technol* **47** (1): 22-25. PETSOC-08-01-22-TN. http://dx.doi.org/10.2118/08-01-22-TN.

Todd, D. K. 1980. *Groundwater Hydrology*, second edition. New York: Wiley.

Tokoro, C., Suzuki, S., Haraguchi, D. et al. 2014. Silicate Removal in Aluminum Hydroxide Co-Precipitation Process. *Materials* **7** (2): 1084-1096. http://dx.doi.org/10.3390/ma7021084.

Ueda, A., Kato, K., and Mogi, K. 2003. Silica Removal from Mokai, New Zealand, Geothermal Brine by Treatment with Lime and a Cationic Precipitant. *Geothermics* **32** (1): 47-61. http://dx.doi.org/10.1016/S0375-6505(02)00050-0.

Vassenden, F., Gustavsen, O., and Nielsen, F. 2005. Why Didn't All the Wells at Smorbukk Scale In?. Presented at the SPE International Symposium on Oilfield Scale, Aberdeen, United Kingdom, 11-12 May. SPE-94578-MS. http://dx.doi.org/10.2118/94578-MS.

Wahl, E. F. 1977. *Geothermal Energy Utilization.* New York: Wiley. http://dx.doi.org/10.2118/98-04-05.

Williams, B. B., Gidley, J. L., and Schechter, R. S. 1979. *Acidizing Fundamentals*. Dallas, Texas: Monograph Series, SPE.

Ying-Hsiao, L. and Fambrough, J. D. 1998. Mathematical Modeling of Secondary Precipitation from Sandstone Acidizing. Presented at the SPE Formation Damage Control Conference, Lafayette, Louisiana, 18-19 February. SPE-39420-MS. http://dx.doi.org/http://dx.doi.org/10.2118/39420-MS.

Zeng, Y., Yang, C., Pu, W. et al. 2007. Removal of Silica from Heavy Oil Wastewater to Be Reused in a Boiler by Combining Magnesium and Zinc Compounds with Coagulation. *Desalination* **216** (1-3): 147-159. http://dx.doi.org/10.1016/j.desal.2007.01.005.